Sentinel-6 MF validation and cross calibration activities

2023 Annual Report

Reference : SALP-RP-MA-EA-23648-CLS
Issue : 1/ 2
Date : April 7, 2025

EUMETSAT
Eumetsat-Allee 1, D-64295 Darmstadt, Germany
Tel: +49 6151 807-7
Fax: +49 6151 807 555
http://www.eumetsat.int

Document Reference:	SALP-RP-MA-EA-23648-CLS
Date:	April 7, 2025
Issue	1.2

Project:	MISSION PERFORMANCE SERVICE FOR SENTINEL-6 MISSION	
Title:	Sentinel-6 MF validation and cross calibration activities 2023 Annual Report	
	Name	**Company**
Author(s):	B. Courcol E. Cadier	CLS CLS
Approved by:	F. Bignalet-Cazalet	CNES
Application authorized by :	C. Martin-Puig	EUMETSAT

Change Log

Version	Date	Changes
1.0	21/03/2024	First Draft
1.1	27/03/2024	CNES review taken into account
1.2	28/03/2025	Eumetsat review taken into account

Acronyms

AMR	Advanced Microwave Radiometer
CLS	Collecte Localisation Satellites
CMEMS	Copernicus Marine Service
CNES	Centre National d'Etudes Spatiales
DUACS	Data Unification and Altimeter Combination System
DV	Default Value
ECMWF	European Centre for Medium-range Weather Forecasting
EUMETSAT	European Organisation for the Exploitation of Meteorological Satellites
ESA	European Space Agency
GIM	Global Ionosphere Maps
GDR	Geophysical Data Record
GMSL	Global Mean Sea Level
HR	High Resolution Mode, also called Synthetic Aperture Radar (SAR) or Delay Doppler Altimetry (DDA)
HRMR	High Resolution Microwave Radiometer
LR	Low Resolution Mode (=LRM)
MLE	Maximum Likelihood Estimator
MQE	Mean Quadratic Error
MSS	Mean Sea Surface
NASA	National Aeronautics and Space Administration
NOAA	National Oceanic and Atmospheric Administration
NTC	Non Time Critical
PB	Processing Baseline
RMC	Range Migration Correction
SSH	Sea Surface Height
SSHA	Sea Surface Height Anomaly(=SLA)
SLA	Sea Level Anomaly(=SSHA)
SSB	Sea State Bias
STD	Standard Deviation
SWH	Significant Wave Height
WTC	Wet troposphere Correction

Table of Content

List of Figures

List of Tables

1 Introduction

Sentinel-6 is a collaborative Copernicus mission, implemented and co-funded by the European Commission, ESA, EUMETSAT and the USA through NASA and NOAA.

EUMETSAT is responsible for the Sentinel-6 operations as part of the Copernicus component of the EU Space Programme. The Sentinel-6 Quality Assessment reports are generated by CNES in the frame of a EUMETSAT CNES agreement in the context of Copernicus.

This document presents the synthesis report concerning validation activities of Sentinel-6 data for the year 2023.

1.1. History

Sentinel-6 MF satellite was successfully launched on the 21th of November 2020. On November 30th, its Poseidon-4 altimeter was switched on, and since December 17th 2020, Sentinel-6 MF is on its operational orbit to continue the long term climate data record on the primary TOPEX, Jason-1, Jason-2 and Jason-3 ground track.

In order to calibrate both altimeters, POS4 was switched to its redundant side (POS4-B) on the 14th of September 2021. It remains in this configuration from this date onwards.

Until April 7th, 2022, Sentinel-6 MF and Jason-3 were in tandem flight, with only a 30 seconds delay, before Jason-3 was moved to the same interleaved orbit that was used by TOPEX from 2002 to 2005, Jason-1 from 2009 to 2012 and Jason-2 from 2016 to 2017.

After the tandem phase with Jason-3, Sentinel-6 MF has become the reference mission in DUACS system.

Over 2023, the main events for Sentinel-6 MF are :

- Processing baseline update to F08 (see section 3.4.), deployed on 2023/03/09. This baseline was used to perform a full mission reprocessing, available to all users since July 2023 (see related Eumetsat news). In particular, this baseline introduced a new Numerical Retracking (NR) in LR mode.
- Processing baseline patch on F08 (see section 3.4.), deployed on 2023/11/01. NTC products are processed with the patched F08 from 2023/10/05 sensing time.

Since the beginning of the mission, Sentinel-6 data have been analysed and monitored in order to assess the products quality. Cycle per cycle reports summarizing mission performance are generated and made available through Eumetsat website. Please note that analyses are done over ocean only, no assessment is done over hydrological targets. This encompasses several points, which are either part of Cal/Val routine activities or following mission events:

- mono-mission validation and monitoring,
- accuracy and stability of SLA measurements check,

- specific studies and investigations.

1.2. Overview

The present document assesses Sentinel-6 MF data quality and performance over ocean. After an executive summary in the next page, dedicated sections of this report deal with:

- description of data processing,
- data coverage / availability,
- monitoring of rejected spurious data,
- analysis of relevant parameters derived from instrumental measurements and geophysical corrections,
- system performance via analyses at crossover points,
- system performance via along-track Sea Level Anomalies monitoring,
- GMSL analysis,
- compliance with system requirements.

Over all these parts, the document also presents some Sentinel-6 MF/Jason-3 cross-calibrations. However, the full tandem flight phase (November 21st 2020 to April 7th 2022) analysis can be found in the PB F08 reprocessing CalVal assessment.

2 Executive Summary

By succeeding to TOPEX/Poseidon, Jason-1, Jason-2 and Jason-3 on their primary ground track, Sentinel-6 MF has extended the high-precision ocean altimetry data record.

Sentinel-6 MF was launched on November 21st 2020. Its onboard altimeter (POS4) operates simultaneously in two acquisition modes in a so-called **interleaved mode**. These modes are:

- Low Resolution Mode, hereafter "LR", which is the historical mode used by previous altimeters in the Topex/Jason satellites.
- High Resolution Mode, hereafter "HR", a.k.a. Synthetic Aperture Radar (SAR) or Delay Doppler Altimetry (DDA), already used on Cryosat-2 and on the Sentinel-3 satellites.

HR data can be telemetered on ground either on RAW mode, i.e. with the full range window of the HR waveform, or in RMC mode, that transmits a truncated waveform thanks to on-board processing, to cut data volume in half. More information on the different telemetry configurations can be found in the L1 Product Generation Specification[1].
Sentinel-6 MF POS4 operates in LR plus HR-RMC mode globally since cycle 32 (2021/09/21). This configuration is called LRMC. Before 2021/09/21, several configurations have been tested via predefined mode masks, mainly in order to validate to HR-RMC performance versus HR-RAW.

During Sentinel-6 MF tandem phase with Jason-3 (2020/12/17 to 2022/04/07), both satellites were on the same ground-track (with only 30 seconds delay), which was a unique opportunity to precisely assess parameter discrepancies between both missions and detect geographically correlated biases, jumps or drifts. In order to calibrate both altimeters, POS4 was switched to its redundant side (POS4-B) on 2021/09/14. It remains in this configuration from this date onwards.
Thanks to this tandem phase, Sentinel-6 MF has been precisely calibrated leading to a seamless transition between Jason-3 and Sentinel-6 MF LR as reference mission in the DUACS system.

In July 2023, the **PB F08 full mission reprocessing for Sentinel-6 MF** was distributed for both LR and HR products. F08 LR products include a **new Numerical Retracking** (NR)for Ku-band in addition to MLE4 retracking. Numerical retracking allows accounting for the PTR shape evolution thanks to the use of in-flight PTRs. An anomaly on LR NR SWH was raised following the pre-operational validation of F08 data (AR 2620), and corrected in a patched version of PB F08 from 2023-10-05 sensing time. The anomaly will be retroactively corrected during the next reprocessing campaign.

During each cycle, missing measurements were monitored, spurious data were edited, and relevant parameters derived from instrumental measurements and geophysical corrections were analysed. Please note that analysis are done **over ocean** only, no assessment is done over hydrological targets.

[1] https://www.eumetsat.int/media/48261

1/ Data availability

Data availability over ocean is excellent for Sentinel-6 MF LR products, with 99.7 % of available data over the complete mission lifetime. It is only impacted by few events, occurring during Sentinel-6 MF commissioning phase, represented with grey lines on figure 8 and listed below.

Sentinel-6 MF HR requirements on data availability are met, with a slightly reduced percentage of available data compared to LR at 98.5 %. From cycle 4 to 31 (i.e. from 2021/02/05 to 2021/09/21, in red on the figure), different mode masks were activated on POS-4. Over these cycles, HR data were not always available globally. From cycle 32, the average percentage of available HR data is of 99.4 %, which is still lower than LR.

The following events impact data availability in both LR and HR products:

- POS4 restart on 2021/01/26
- POS4 restart on 2021/02/25
- POS4 restart on 2021/04/22
- Satellite switch off for satellite software patch from 2021/04/27 03:35 to 2021/04/28 17:07
- POS4 restart on 2021/08/26
- Switch from POS4-A to POS4-B on 2021/09/14.

No important event occurred over 2023.

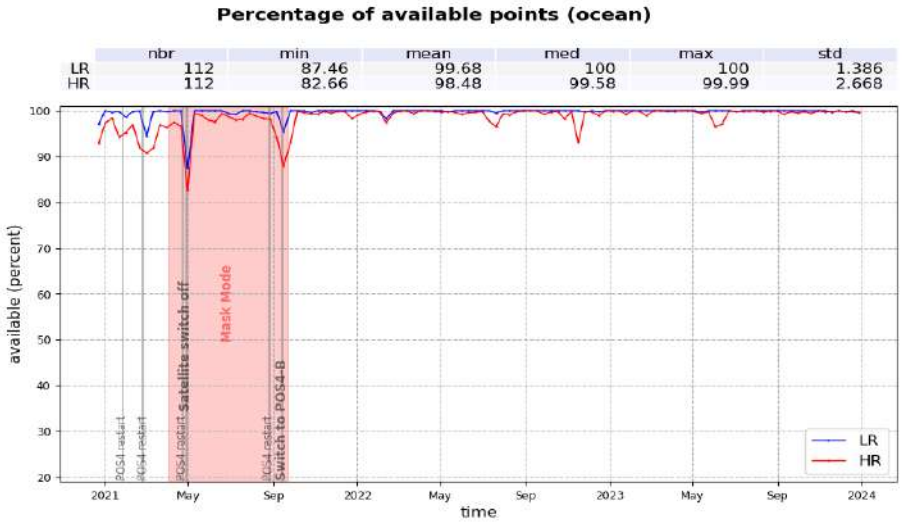

Figure 1: Percentage of available data over ocean for NTC Sentinel-6 MF LR (blue) and HR (red) per cycle.

2/ Sea Level Anomalies

Sentinel-6 MF and Jason-3 SSHA follow identical seasonal cycles and variations (cf figure 2), with mean value of 4.9 cm for Sentinel-6 MF LR MLE4, 4.2 cm for Sentinel-6 MF LR NR, 3.8 cm for Sentinel-6 MF HR and 3.6 cm for Jason-3. Excluding the Caspian Sea, Sentinel-6 MF SSHA cyclic standard deviation is similar between all datasets. The spike in HR on April 28th, 2021, visible on both mean and standard deviation, is caused by a higher number of missing passes on that day.

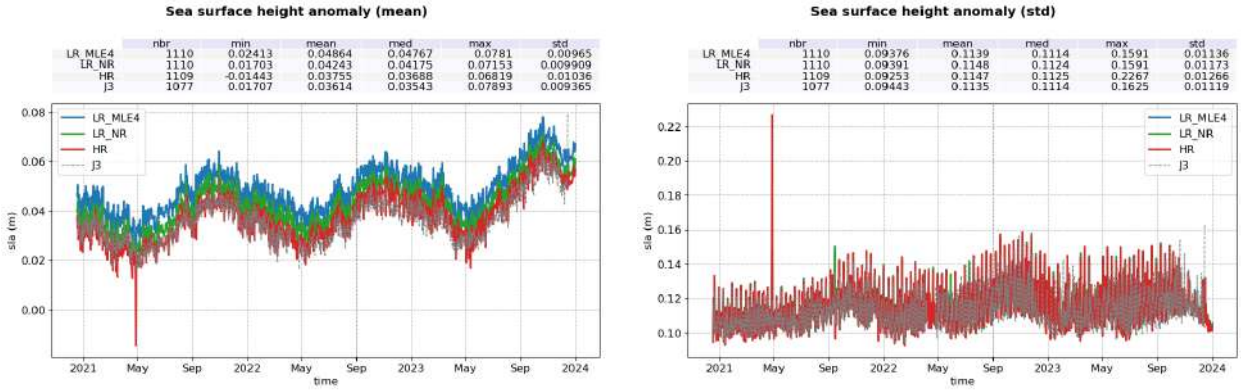

Figure 2: Mean (left) and standard deviation (right) SSHA by day for LR MLE4 (red), LR NR (green), HR (blue) and Jason-3 (black).

The NR - MLE4 SSHA differences monitoring on figure 3 shows an about 1.5mm jump at side B switch, resulting from range and ionosphere correction behaviours. The corresponding map highlights a significant SWH correlation, with about -1.5 cm decrease between 0.5 and 8m-SWH. This behaviour is expected and is part of the improvement brought by the numerical retracker. Indeed, contrary to MLE4, numerical retracker outputs are not corrected by instrumental LUTs, which are applied as function of SWH values. Numerical retracker retrievals are then less sensitive to any approximation in the LUT estimation.

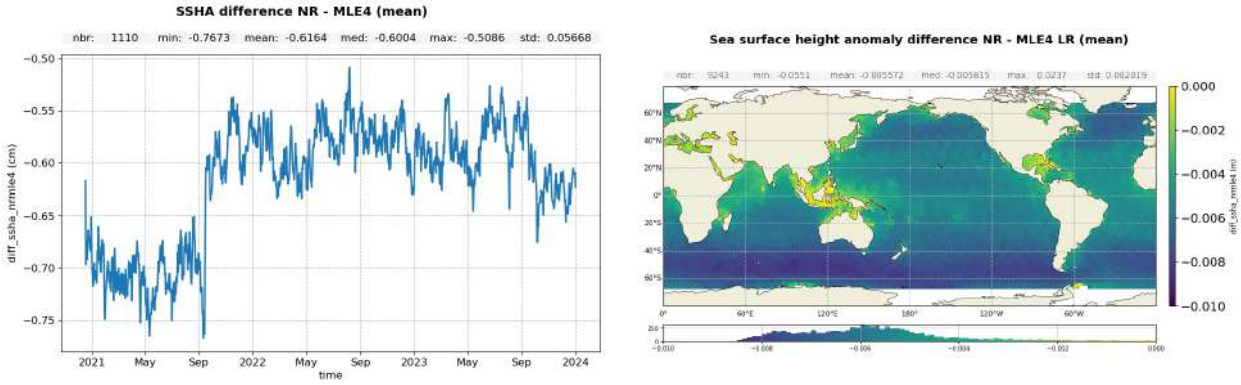

Figure 3: Left : Time monitoring per day of Sentinel-6 MF NR - MLE4 SSHA in meters, without the Caspian Sea. Right : gridded map computed over 2023.

3/ Performance at crossover points

Looking at SSH difference at mono-mission crossovers, mean values are well centred around 0 for LR MLE4, LR NR and HR data (figure 4 left panel). A small 120-day signal similar to Jason-3 is visible with amplitude below 1.5 cm. This signal disappear with the use of JPL orbits instead of CNES POE-F (cf Cadier et al. 2024, under review [5]). Further investigations are required to fully understand this behavior.
Concerning SSH error at mono-mission crossovers ($STD\ /\ \sqrt{2}$), Sentinel-6 MF shows very good and stable performance with an error of 3.3 cm for Sentinel-6 MF LR MLE4, LR NR and Jason-3 (figure 4 right panel). The error for Sentinel-6 MF HR SSH is slightly lower (3.2 cm).

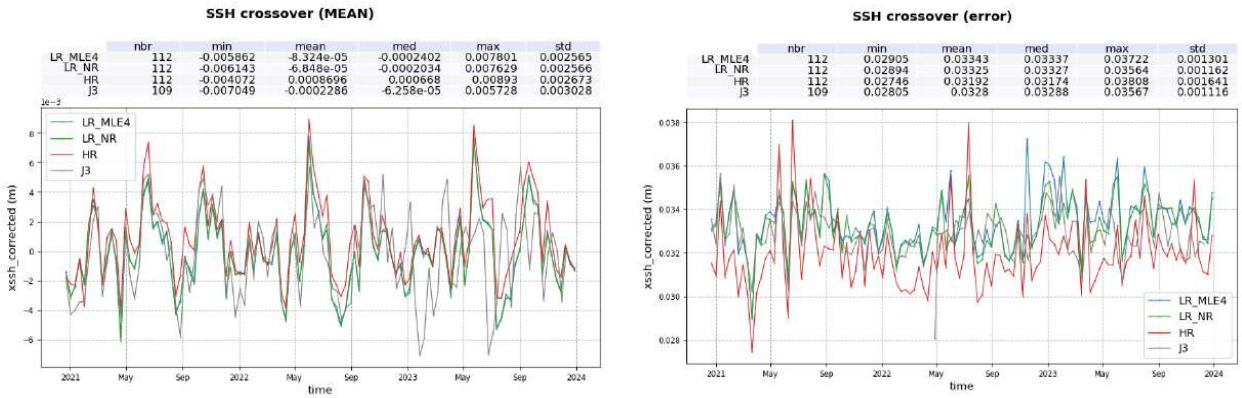

Figure 4: Monitoring of SSH difference at mono-mission crossover for Sentinel-6 MF LR MLE4 (blue), LR NR (green), Sentinel-6 MF HR (red) and Jason-3 (black), mean (left) and error (right) per cycle. Only data with |latitude| < 50 °, bathymetry < -1000 m and low oceanic variability were selected.

The mean SSH differences at Sentinel-6 MF/Jason-3 crossovers is following the same variations for LR MLE4, LR NR and HR, with means of -1.7 cm, -1.1 cm and 0.1 cm respectively (figure 5 top panel). On all curves, a jump of about -3 mm is visible at the end of April 2021, concomitant with a Sentinel-6 MF restart on April 27-28th, 2021. Then, on both S6-MF LR NR/J3 and S6-MF HR/J3 datasets, a downward drift is visible until approximately the end of the tandem phase in April 2022. These drifts might be caused by the evolution of the Jason-3 PTR shape in the first case, that would not be compensated by a similar effect in Sentinel-6 MF LR NR due to the use of the in-flight PTR, and by the range walk effect impacting HR data in the second case.

No significant regional pattern can be seen in the Sentinel-6 MF LR/Jason-3 SSH crossovers differences for both MLE4 and NR (figure 5 bottom panels). The map of Sentinel-6 MF HR/Jason-3 SSH differences at crossover highlights the absence of skewness parameter in the HR processing, leading to correlation to sea state conditions in the comparison to Jason-3.

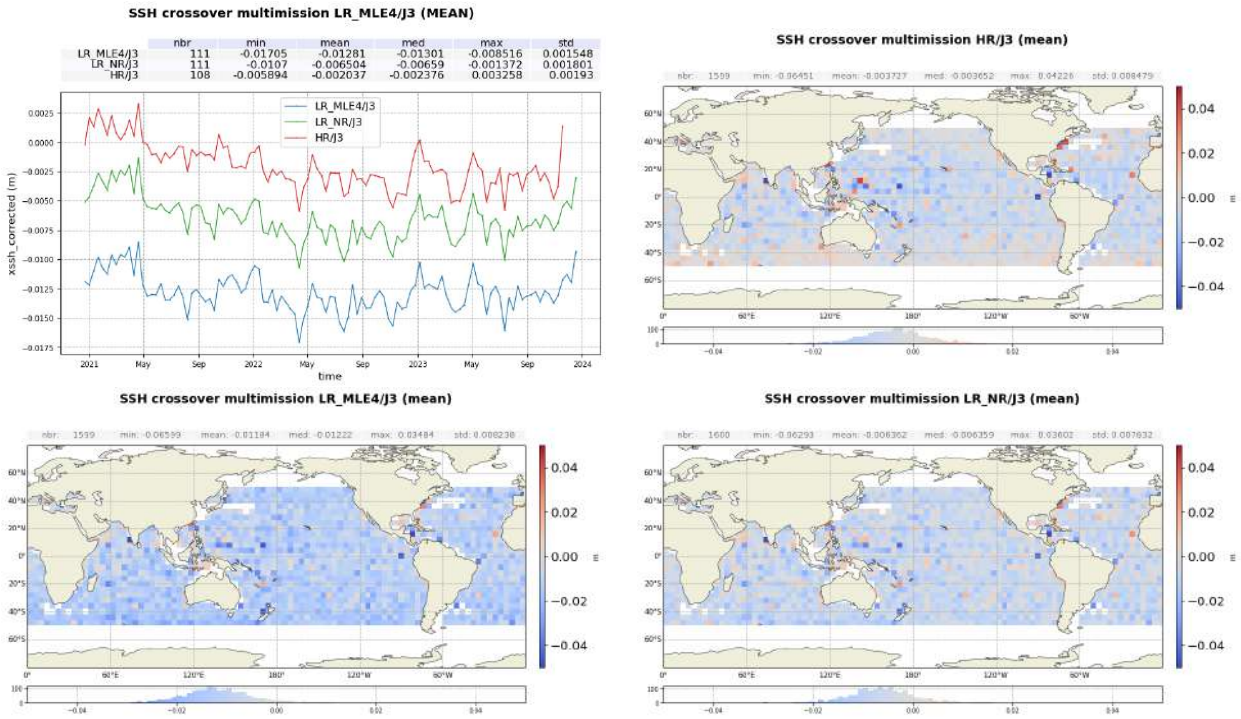

Figure 5: Cyclic monitoring of Sentinel-6 MF - Jason-3 SSH crossover differences mean (top left) and maps over year 2023 for HR (top right), LR MLE4 (bottom left) and LR NR (bottom right). Only data with |latitude| < 50 °, bathymetry < -1000 m and low oceanic variability were selected.

4/ Contribution to Global Mean Sea Level

Since April 2022 (Sentinel-6 MF cycle 52), Sentinel-6 MF is the reference altimetry mission to estimate the Global Mean Sea Level (GMSL), replacing Jason-3. Regional and global biases between missions have to be precisely estimated in order to ensure the quality of the reference GMSL series as seen on Figure 6. For more clarifications, see the dedicated section on AVISO+ website[2].

Sentinel-6 MF GMSL are impacted by two known effects:

- the evolution of the PTR shape in the range direction. It impacts range and SWH estimates both in LR MLE4 and HR SAMOSA. Numerical retracker allows accounting for the PTR shape evolution thanks to the use of in-flight PTRs. HR NR is implemented in the PB F09 deployed in February 2024.
- the evolution of the PTR shape in the azimuth direction, impacting the range variations within a burst, in HR only. It is corrected thanks to the range walk correction, that is available in PB F09.

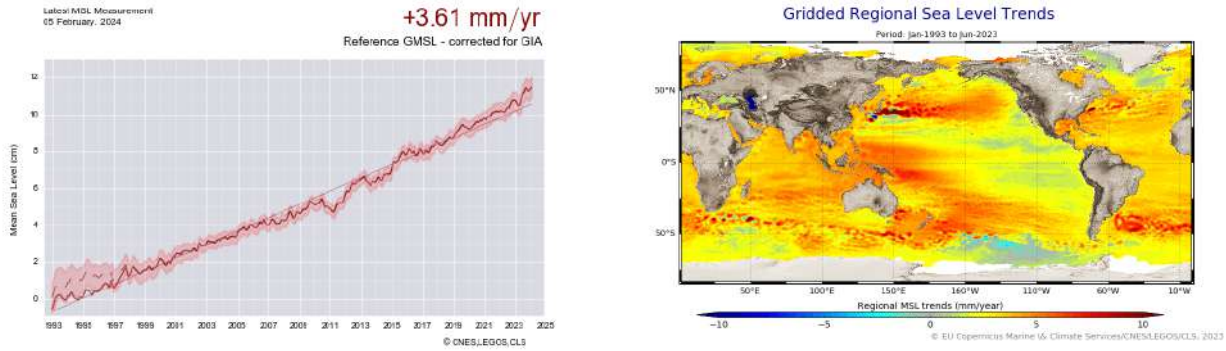

Figure 6: Global (left) and regional (right) MSL trends from 1993 onwards.

[2] https://www.aviso.altimetry.fr/en/data/products/ocean-indicators-products/mean-sea-level.html

3 Processing Status

3.1. Data used

Sentinel-6 MF
Metrics provided in this document are based on Sentinel-6 MF dataset from cycle 4 pass 14 to cycle 115 for L2 NTC 1Hz products (corresponding to December 17th 2020 to December 31st 2023). Data before cycle 4 pass 14 are not included as Sentinel-6 MF was not yet on its definitive orbit.

From 2020/12/17 to 2023/10/05 (corresponding to cycle 107 pass 7), Sentinel-6 MF data were processed with the original Processing Baseline (PB) F08. No data with PB anterior to F08 is present in this report thanks to the 2023 F08 reprocessing. Data after 2023/10/05 were processed with the patched PB F08. See section 3.4. for more details on the processing baselines.

"Ocean" retrackers were used, being MLE4 and NR for LR mode and SAMOSA for HR mode. A detailed description of the products can be found in the Sentinel-6 MF user handbook [1].

Jason-3
Comparison with Jason-3 uses L2 1 Hz GDR-F products with MLE4 retracking on the same period as Sentinel-6.

Sentinel-6 MF F08 and Jason-3 GDR-F share the same standard in terms of geophysical corrections: same tide models, same mean surface height, etc. In particular :

- for the wind speed, Collard algorithm is used on both mission
- for the sea state bias, Sentinel-6 MF processing uses sea state bias parametrization derived from Jason-3 GDR-F data, both in LR and in HR.

Note that after the end of the tandem phase on 07-04-2022, and until Jason-3 reached its current interleaved orbit on 25-04-2022, no data are available. Furthermore, cycles before and after the transition (cycles number 227 and 300) are truncated, lasting only 5h30 and 4 days respectively instead of the standard 10 days. This can lead to artefacts in cyclic monitoring involving Jason-3.

3.2. List of events

The following table shows the major events that occurred over Sentinel-6 MF lifetime.

Date start	Date end	Cycle	System	Event
30/11/2020	N/A	1	POSEIDON	POS4 switch on
17/12/2020 19:38	N/A	4		Sentinel-6 MF on its final orbit
18/01/2021	N/A	7	STR	On-board star-tracker update
25/01/2021 19:45	25/01/2021 19:45	7	AMR-C	AMR deep sky calibration
26/01/2021 12:17	N/A	8	POSEIDON	POS4 restart
04/02/2021 23:59	N/A	9	POSEIDON	POS4 mode mask activated

25/02/2021	N/A	11	POSEIDON	POS4 restart
27/02/2021 00:43	27/02/2021 00:43	11	AMR-C	AMR deep sky calibration
11/03/2021 05:00	11/03/2021 05:00	12	AMR-C	AMR-C Deep-sky Calibration Over Land-Ocean Boundary
16/03/2021 21:53	16/03/2021 21:530	13	AMR-C	AMR-C Deep sky calibration over Ocean
17/03/2021 09:36	18/03/2021 09:38	13	AMR-C	24h Warm target Calibration
23/03/2021 15:12	23/03/2021 15:27	13	AMR-C	Deep Sky Calibration over the Ocean/Land Boundary
15/04/2021 00:36	15/04/2021 00:36	15	Platform	(+0.4) POS-4 Roll bias
15/04/2021 12:56	15/04/2021 12:56	16	Platform	(-0.4) POS-4 Roll Bias
22/04/2021 13:24	N/A	16	POSEIDON	POS4 restart
25/04/2021 01:31	25/04/2021 01:31	16	AMR-C	AMR deep sky calibration
27/04/2021 03:35	28/04/2021 17:07	17	Platform	Satellite switched off for satellite software patch.
21/05/2021 20:20	21/05/2021 20:36	19	AMR-C	AMR deep sky calibration
24/05/2021 16:30	24/05/2021 16:30	19	Platform	-0.4deg Roll
25/05/2021 04:50	25/05/2021 04:50	20	Platform	+0.4deg Roll
18/06/2021 06:46	18/06/2021 06:46	22	AMR-C	AMR deep sky calibration
01/07/2021 13:08	01/07/2021 13:12	23	Platform	Yaw flip maneuver
05/07/2021 12:56	05/07/2021 13:00	24	Platform	Yaw flip maneuver
19/07/2021 19:59	19/07/2021 19:59	25	AMR-C	AMR deep sky calibration
18/08/2021 01:40	18/08/2021 01:40	28	AMR-C	AMR deep sky calibration
26/08/2021 10:00	26/08/2021	29	POSEIDON	POS4 restart: POS4-A Application Software (ASW) 2.4 uplo and activation
01/09/2021 04:44	01/09/2021 05:18	29	Platform	Yaw flip maneuver
05/09/2021 06:11	05/09/2021 06:46	30	Platform	Yaw flip maneuver
14/09/2021 09:00	15/09/2021 09:00	31	POSEIDON	Switch from POS-A to POS-B
17/09/2021 20:02	17/09/2021 20:02	31	AMR-C	AMR deep sky calibration
21/09/2021 01:25:37	N/A	32	POSEIDON	End of POS4 mode mask. LRMC-OL acquisition mode activat globally from cycle 32 onwards.
20/10/2021 00:58	20/10/2021 00:58	34	AMR-C	AMR deep sky calibration
05/11/2021 16:26	05/11/2021 16:26	36	Platform	Yaw flip maneuver
09/11/2021 17:29	09/11/2021 17:29	37	Platform	Yaw flip maneuver
16/11/2021 14:37	16/11/2021 14:37	37	AMR-C	AMR deep sky calibration
19/11/2021 03:45:52	19/11/2021 03:45:52	37	Platform	Yaw slew +90deg
19/11/2021 04:03:45	19/11/2021 04:03:45	37	Platform	Roll -0.4 deg
19/11/2021 04:27:45	19/11/2021 04:27:45	37	Platform	Roll +0.4 deg
19/11/2021 04:38:20	19/11/2021 04:38:20	37	Platform	Yaw slew -90deg
19/11/2021 16:13:21	19/11/2021 16:13:21	38	Platform	Yaw slew +90deg
19/11/2021 16:24:25	19/11/2021 16:24:25	38	Platform	Roll +0.4 deg
19/11/2021 16:48:25	19/11/2021 16:48:25	38	Platform	Roll -0.4 deg
19/11/2021 16:59:00	19/11/2021 16:59:00	38	Platform	Yaw slew -90deg
19/11/2021 17:38:00	19/11/2021 17:38:00	38	AMR-C	AMR deep sky calibration
16/12/2021 01:42:00	16/12/2021 01:42:00	40	AMR-C	AMR deep sky calibration
17/07/2022 15:42:57	17/07/2022 15:42:57	62	Platform	Yaw Slew +90deg
17/07/2022 16:18:55	17/07/2022 16:18:55	62	Platform	Yaw Back Slew -90deg
18/01/2022 04:03:34	18/01/2022 04:03:34	44	Platform	Yaw Slew -90deg
18/01/2022 04:39:32	18/01/2022 04:39:32	44	Platform	Yaw Back Slew +90deg
12/02/2022 01:03:00	12/02/2022 01:03:00	46	AMR-C	AMR deep sky calibration
27/02/2022 15:54:35	27/02/2022 16:03:24	48	Platform	Yaw flip maneuver
03/03/2022 17:12:32	03/03/2022 17:21:21	48	Platform	Yaw flip maneuver
13/03/2022 15:30:00	13/03/2022 15:30:00	49	AMR-C	AMR deep sky calibration
11/04/2022 02:12:00	11/04/2022 02:12:00	52	AMR-C	AMR deep sky calibration
25/04/2022 16:45:10	25/04/2022 16:53:58	53	Platform	Slew 180deg

29/04/2022 16:36:20	29/04/2022 16:45:08	54	Platform	Back Slew 180deg
10/05/2022 20:16:00	10/05/2022 20:16:00	55	AMR-C	AMR deep sky calibration
07/07/2022 19:29:00	07/07/2022 19:29:00	61	AMR-C	AMR deep sky calibration
08/07/2022 01:38:00	08/07/2022 01:38:00	61	AMR-C	AMR deep sky calibration
05/12/2022 10:25:05	05/12/2022 10:33:52	76	Platform	Slew 180deg
05/12/2022 10:44:46	05/12/2022 10:45:26	76	Platform	Back Slew 180deg
07/12/2022 00:28:00	07/12/2022 00:28:00	76	AMR-C	AMR deep sky calibration
02/01/2023 19:23:00	02/01/2023 19:23:00	79	AMR-C	AMR deep sky calibration
17/01/2023 13:14:59	17/01/2023 13:15:01	80	Platform	station keeping maneuver
01/02/2023 01:00:00	01/02/2023 01:00:00	82	AMR-C	AMR deep sky calibration
03/03/2023 15:45:38	03/03/2023 15:45:38	85	AMR-C	AMR deep sky calibration
01/04/2023 19:16:00	01/04/2023 19:16:00	88	AMR-C	AMR deep sky calibration
28/04/2023 19:48:24	28/04/2023 19:48:24	90	AMR-C	AMR deep sky calibration
25/05/2023 06:04:59	25/05/2023 06:05:01	93	Platform	Station keeping maneuver
31/05/2023 00:40:53	31/05/2023 00:40:53	94	AMR-C	AMR deep sky calibration
26/06/2023 19:25:00	26/06/2023 19:25:00	96	AMR-C	AMR deep sky calibration
27/07/2023 19:29:00	27/07/2023 19:29:00	99	AMR-C	AMR deep sky calibration
03/08/2023 07:02:09	03/08/2023 07:02:11	100	Platform	Station keeping maneuver
25/08/2023 19:29:00	25/08/2023 19:29:00	102	AMR-C	AMR deep sky calibration
24/09/2023 01:12:00	24/09/2023 01:12:00	105	AMR-C	AMR deep sky calibration
18/10/2023 08:35	18/10/2023 08:40	108	POSEIDON	POS-4B restart
24/10/2023 15:59:00	24/10/2023 15:59:00	109	AMR-C	AMR deep sky calibration
21/11/2023 19:05:00	21/11/2023 19:05:00	111	AMR-C	AMR deep sky calibration
29/11/2023 08:24:59	29/11/2023 08:25:01	112 Platform	Station keeping maneuver	
21/12/2023 18:23:00	21/12/2023 18:23:00	114	AMR-C	AMR deep sky calibration

Table 1: Events on Sentinel-6 MF.

3.3. Tracking and acquisition mode

Sentinel-6 MF altimeter, Poseidon-4, always operates in interleaved mode, which enables simultaneous measurements in :

- Low Resolution Mode, hereafter "LR", which is the historical mode used by previous altimeters in the Topex/Jason satellites. Please note that while Topex/Jason altimeters were acquiring data with a 2kHz PRF, Sentinel-6 LR mode uses a 9kHz PRF.
- High Resolution Mode, hereafter "HR", commonly called Synthetic Aperture Radar (SAR) or Delay Doppler Altimetry (DDA), already used on Cryosat-2 and on the Sentinel-3 satellites.

HR mode can be downlinked in two ways :

- HR-RAW, which contains the entire waveform. This mode cannot be activated globally, as the volume of data is too large to be downlinked.
- HR-RMC (Range Migration Correction), which only transmits to the ground a lighter, truncated waveform computed after on-board RMC compensation. This mode enables global coverage, as the volume of data is only half of HR-RAW's.

Table 2 summarizes the acquisition modes under which POS-4 can operate. All these modes have been activated during Sentinel-6 MF Phase-E1.

Acquisition mode	Open Loop	Closed Loop	Data telemetered
LRM	X	X	Only LR data
LX	X	X	LR + HR-RAW data
LX2		X	LR + HR-RAW + HR-RMC data
LRMC	X	X	LR + HR-RMC data
TRANSPONDER			LR + HR-RAW + HR-RMC data (fixed Gain and H0)

Table 2: POS-4 acquisition modes

In order to validate HR-RMC versus HR-RAW modes, a masking mode has been activated on the 05/02/2021 (start of cycle 9) and lasted until the 21/09/2021 (end of cycle 31). Over this period, POS-4 operated :

- in LRM only over land,
- in LX over coastal areas
- in LRMC over open ocean except over the masks where it operates in LX.

Several masks have been used, covering different areas of interest (ocean with strong geoid slopes or dynamic regions, ice zones, Amazon for hydrology, etc.).
Switching from LRMC to LX over open ocean allows to verify the continuity between HR-RMC and HR-RAW data. Furthermore, an on-ground convertor allowed converting HR-RAW data to HR-RMC. It enables direct comparison between the two retrievals.
After the complete validation of the HR-RMC mode, POS4 mode mask test phase ended and the acquisition mode has been set to LRMC-OL globally from cycle 32 (21/09/2021).

The LR and HR modes use separate retrackers (MLE4/NR and SAMOSA respectively) and the resulting data are available in distinct products.
Please note that while LR products contain both Ku and C bands, because of data volume constrains, the telemetry of HR does not include C band data, and therefore HR products contain only the Ku band.

3.4. Processing versions

Thanks to the 2023 reprocessing campaign, PB prior to F08 are no longer present in the datasets.

The main change to this new F08 baseline is the **addition of numerical retracker (NR) retrievals in LR products for Ku band**. Numerical retracking allows accounting for the PTR shape evolution thanks to the use of in-flight PTRs. Please note that this new set of parameters does not replace but complement MLE4-derived parameters: NR and MLE4 retrievals are both included in LR products.

Other changes in PB F08 include :

- The update of the antenna aperture angle from 1.33 degrees to 1.34 degrees[3].
- The update of the total electron content (TEC) computation with a more appropriate scaling factor (0.881 instead of 0.925) to align the altimeter-derived TEC with the GPS-derived JPL GIM model.

An anomaly on NR SWH was raised following the pre-operational validation of F08 data (AR 2620). Due to an implementation error, LR NR SWH 1Hz compression was done using sigma-composite whereas it

[3] In-flight operations have been conducted to better characterize the antenna aperture.

should have been done by direct averaging. The main impact of this error is that negative measurements of SWH are mapped to their absolute value at 20Hz and mixed to actual positive SWH during compression. This was corrected in a patched version of the PB F08, which was deployed on 2023-11-01. NTC products are processed with the patched F08 from 2023-10-05 sensing time. The anomaly will be retroactively corrected during the next reprocessing campaign.

More details on the PB F08 can be found in the associated product notice [3].

The F08 reprocessing Cal/Val assessment is available online [4].

4 Data coverage and edited measurements

4.1. Missing measurements

4.1.1. Over land and ocean

Determination of missing measurements relative to the theoretically expected orbit ground pattern is an essential tool to detect missing telemetry or satellite events.

Figure 7 shows the percentage of available measurements for Sentinel-6 MF LR and HR modes for all surfaces observed. In average LR mode provides 98.8% of measurements over 111 cycles.

HR mode provides in average less measurements (93.6%) on the same time-period. From cycle 4 to 31 (in red on the figure), different mode masks were activated on POS-4. Over these cycles, HR data were not always available globally. It was the case only on cycles where the LRMC acquisition mode is activated everywhere (cycles 14, 22, 28 and from cycle 32 onwards).
From cycle 32, the average percentage of available HR data is of 98.6%, which is barely lower than LR.

Other events, such as POS4 restarts or the switch from POS4A to POS4B, impact data availability during Sentinel-6 MF first year (see grey lines on the figure).

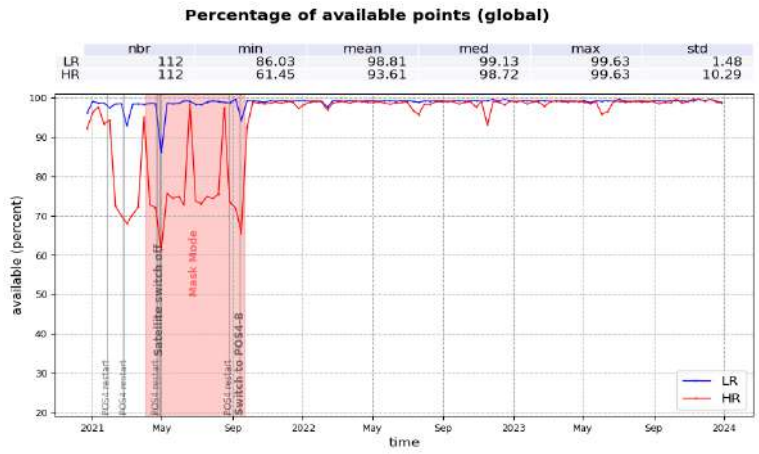

Figure 7: Percentage of available data over all surfaces for both LR (blue) and HR (red) per cycle.

Table 3 and 4 give the list of fully missing passes for LR and HR respectively, along with related events.

Cycle	Pass	Date	Comment
4	88	2020-12-20 19:25:52 to 2020-12-20 21:21:40	
	152	2020-12-23 07:25:51 to 2020-12-23 09:22:07	
	216	2020-12-25 19:22:58 to 2020-12-25 21:18:53	POS4 restart
8	126 to 128	2021-01-30 23:04:03 to 2021-01-31 02:49:31	

10	1	2021-02-24 19:56:33 to 2021-02-24 20:52:47	
17	52 to 79 83 to 86	2021-04-27 07:28:16 to 2021-04-28 09:56:12 2021-04-28 11:43:02 to 2021-04-28 17:07:49	Satellite switched off for satellite software patch
23	230	2021-07-02 18:06:02 to 2021-07-02 20:01:59	
24	230	2021-07-12 16:04:34 to 2021-07-12 18:00:31	
31	84 to 85 88 to 90 110 112 to 114	2021-09-14 08:58:51 to 2021-09-14 11:45:01 2021-09-14 12:42:06 to 2021-09-14 16:39:47 2021-09-15 09:18:54 to 2021-09-15 11:13:23 2021-09-15 11:13:35 to 2021-09-15 15:07:45	Switch from POS4-A to POS4-B
46	22 98	2022-02-07 16:31:06 to 2022-02-07 18:26:45 2022-02-10 15:43:12 to 2022-02-10 17:38:39	
74	68	2022-11-14 03:10:04 to 2022-11-14 04:06:17	
92	237	2023-05-18 05:03:46 to 2023-05-18 06:00:00	

Table 3: List of missing passes in LR

Date	Cycle	Pass	Comment
4	82 to 84 88 152 198 216 226 249	2020-12-20 13:37:34 to 2020-12-20 17:19:22 2020-12-20 19:25:52 to 2020-12-20 21:21:40 2020-12-23 07:25:51 to 2020-12-23 09:22:07 2020-12-25 02:23:06 to 2020-12-25 04:19:34 2020-12-25 19:15:12 to 2020-12-25 21:18:53 2020-12-26 04:41:52 to 2020-12-26 06:37:48 2020-12-27 02:28:08 to 2020-12-27 03:24:22	POS4 restart
5	32 76 78 226	2020-12-28 12:16:13 to 2020-12-28 14:09:25 2020-12-30 06:12:27 to 2020-12-30 07:52:28 2020-12-30 08:08:40 to 2020-12-30 09:58:41 2021-01-05 02:40:24 to 2021-01-05 04:36:20	
6	224 232	2021-01-14 22:45:17 to 2021-01-15 00:38:57 2021-01-15 06:27:01 to 2021-01-15 07:32:58	
7	104 126 150 154 176 204 206 226 229 to 230 234	2021-01-20 04:32:35 to 2021-01-20 05:28:49 2021-01-21 01:09:18 to 2021-01-21 02:05:32 2021-01-21 23:38:28 to 2021-01-22 00:34:41 2021-01-22 03:23:19 to 2021-01-22 04:19:33 2021-01-23 00:00:03 to 2021-01-23 00:56:16 2021-01-24 02:14:03 to 2021-01-24 03:10:17 2021-01-24 04:06:29 to 2021-01-24 05:02:43 2021-01-24 22:37:27 to 2021-01-25 00:33:23 2021-01-25 00:53:22 to 2021-01-25 03:47:04 2021-01-25 06:03:49 to 2021-01-25 07:33:31	
8	22 24 30 46 126 to 129 226	2021-01-26 21:41:30 to 2021-01-26 22:37:44 2021-01-26 23:33:56 to 2021-01-27 00:30:10 2021-01-27 04:18:50 to 2021-01-27 06:11:57 2021-01-27 19:56:11 to 2021-01-27 21:49:31 2021-01-30 22:57:13 to 2021-01-31 02:52:42 2021-02-03 20:35:58 to 2021-02-03 22:31:54	
9	102 to 103 178 to 179 204 to 205	2021-02-08 22:27:28 to 2021-02-09 00:30:02 2021-02-11 21:36:30 to 2021-02-11 23:41:59 2021-02-12 21:59:32 to 2021-02-13 00:04:35	

	254	2021-02-14 20:51:49 to 2021-02-14 22:55:02	
10	42	2021-02-16 12:19:05 to 2021-02-16 14:11:54	
	98	2021-02-18 16:34:04 to 2021-02-18 18:29:51	
	128 to 129	2021-02-19 20:46:54 to 2021-02-19 22:51:07	
	150	2021-02-20 17:13:47 to 2021-02-20 19:17:01	
	178 to 179	2021-02-21 19:33:41 to 2021-02-21 21:40:30	
	226	2021-02-23 16:16:48 to 2021-02-23 18:28:56	
	252 to 254	2021-02-24 16:47:09 to 2021-02-24 20:52:26	
11	16	2021-02-25 09:59:47 to 2021-02-25 10:56:00	
	26 to 27	2021-02-25 19:12:30 to 2021-02-25 21:15:05	
	102 to 103	2021-02-28 18:25:12 to 2021-02-28 20:27:05	
	128 to 129	2021-03-01 18:48:34 to 2021-03-01 20:49:39	
	178 to 179	2021-03-03 17:33:58 to 2021-03-03 19:39:02	
	207 to 221	2021-03-04 20:47:14 to 2021-03-05 11:13:52	
12	26 to 27	2021-03-07 17:11:56 to 2021-03-07 19:13:37	
	48	2021-03-08 13:27:54 to 2021-03-08 15:39:02	
	64	2021-03-09 04:56:37 to 2021-03-09 05:52:50	
	124	2021-03-11 12:42:51 to 2021-03-11 14:44:38	
	128 to 129	2021-03-11 16:46:24 to 2021-03-11 18:48:11	
	156	2021-03-12 18:59:31 to 2021-03-12 20:04:36	
	178 to 180	2021-03-13 15:33:46 to 2021-03-13 18:33:45	
	204 to 206	2021-03-14 15:54:47 to 2021-03-14 18:55:20	
	226	2021-03-15 12:21:13 to 2021-03-15 14:26:00	
	232	2021-03-15 18:00:07 to 2021-03-15 19:16:55	
	254	2021-03-16 14:48:36 to 2021-03-16 16:49:30	
13	26 to 27	2021-03-17 15:08:14 to 2021-03-17 17:12:08	
	70	2021-03-19 08:16:37 to 2021-03-19 10:10:15	
	178 to 179	2021-03-23 13:32:15 to 2021-03-23 15:36:05	
	254	2021-03-26 12:47:06 to 2021-03-26 14:43:27	
14	48	2021-03-28 09:40:38 to 2021-03-28 11:36:28	
	118	2021-03-31 03:25:12 to 2021-03-31 05:11:13	
	146	2021-04-01 05:30:01 to 2021-04-01 07:21:09	
	226	2021-04-04 08:27:07 to 2021-04-04 10:23:03	
15	172	2021-04-12 03:39:20 to 2021-04-12 05:41:18	
16	120	2021-04-20 01:18:27 to 2021-04-20 02:14:58	
	200 to 205	2021-04-23 04:01:49 to 2021-04-23 09:54:15	
17	48 to 86	2021-04-27 03:36:11 to 2021-04-28 17:07:49	Satellite switched off for satellite software patch
	88 to 90	2021-04-28 17:08:30 to 2021-04-28 20:39:36	
21	166 to 168	2021-06-10 10:08:36 to 2021-06-10 13:59:58	
22	120	2021-06-18 13:09:54 to 2021-06-18 14:06:08	
23	230 to 231	2021-07-02 18:05:56 to 2021-07-02 20:06:31	
24	230 to 231	2021-07-12 16:04:28 to 2021-07-12 18:05:03	
25	153	2021-07-19 14:00:34 to 2021-07-19 15:16:50	
28	33 to 34	2021-08-13 15:29:57 to 2021-08-13 17:37:04	
	170	2021-08-18 23:51:46 to 2021-08-19 00:48:00	
29	78	2021-08-25 07:32:27 to 2021-08-25 08:48:32	
	106	2021-08-26 09:30:54 to 2021-08-26 11:10:31	POS4 restart
	251	2021-09-01 01:43:41 to 2021-09-01 02:39:55	
30	196 to 207	2021-09-08 20:09:12 to 2021-09-09 07:29:39	
	222	2021-09-09 20:28:35 to 2021-09-09 22:00:52	

31	82 to 86	2021-09-14 07:01:41 to 2021-09-14 12:05:01	Switch from POS4-A to POS4-B
	88 to 95	2021-09-14 12:42:06 to 2021-09-14 21:10:01	
	98 to 114	2021-09-14 21:47:06 to 2021-09-15 15:07:45	
32	62 to 72	2021-09-23 10:22:49 to 2021-09-23 21:36:32	
	120	2021-09-25 16:55:09 to 2021-09-25 17:51:23	
	224	2021-09-29 17:33:33 to 2021-09-29 20:00:36	
34	170	2021-10-17 11:42:56 to 2021-10-17 12:39:09	
35	120	2021-10-25 10:50:43 to 2021-10-25 11:46:57	
36	170	2021-11-06 07:39:57 to 2021-11-06 08:36:12	
38	120	2021-11-24 04:46:17 to 2021-11-24 05:42:31	
41	2	2021-12-19 08:03:51 to 2021-12-19 09:59:27	
	64	2021-12-21 18:04:25 to 2021-12-21 20:00:28	
42	162	2022-01-04 11:30:49 to 2022-01-04 13:40:22	
46	21 to 23	2022-02-07 15:49:15 to 2022-02-07 18:37:54	
	97 to 99	2022-02-10 15:01:33 to 2022-02-10 17:50:13	
59	170	2022-06-22 09:06:02 to 2022-06-22 10:02:15	
61	36	2022-07-06 22:51:34 to 2022-07-07 01:01:04	Ground segment anomaly (UNS 8401)
	92	2022-07-09 03:53:10 to 2022-07-09 05:48:47	Ground segment anomaly (UNS 8420)
	246	2022-07-15 04:12:47 to 2022-07-15 05:44:02	Ground segment anomaly (UNS 8449)
62	20	2022-07-16 06:11:54 to 2022-07-16 08:07:30	Ground segment anomaly (UNS 8451)
	114	2022-07-19 22:13:23 to 2022-07-20 00:18:31	Ground segment anomaly (UNS 8463)
	120	2022-07-20 04:10:54 to 2022-07-20 05:07:08	
	160	2022-07-21 17:02:52 to 2022-07-21 19:03:37	Ground segment anomaly (UNS 8487)
	202	2022-07-23 08:49:45 to 2022-07-23 10:46:04	Ground segment anomaly (UNS 8492)
	254	2022-07-25 09:34:45 to 2022-07-25 11:31:20	Ground segment anomaly (UNS 8495)
63	120	2022-07-30 02:09:26 to 2022-07-30 03:05:39	Ground segment anomaly (UNS 8602)
64	124	2022-08-09 03:38:55 to 2022-08-09 05:34:53	Ground segment anomaly (UNS 8546)
69	144	2022-09-28 12:26:27 to 2022-09-28 14:08:05	Ground segment anomaly (UNS 8718)
72	45	2022-10-24 09:40:03 to 2022-10-24 10:36:16	Ground segment anomaly (UNS 8803)
	47 to 49	2022-10-24 11:32:29 to 2022-10-24 14:21:07	
74	19 to 22	2022-11-12 05:15:33 to 2022-11-12 09:00:24	Ground segment anomaly (UNS 9059)
	35	2022-11-12 20:14:59 to 2022-11-12 21:11:12	
	68	2022-11-14 03:10:04 to 2022-11-14 04:06:17	
	147 to 148	2022-11-17 05:00:48 to 2022-11-17 07:46:36	
	154	2022-11-17 10:52:57 to 2022-11-17 12:49:05	
	156	2022-11-17 13:34:47 to 2022-11-17 15:09:59	
	202	2022-11-19 08:42:05 to 2022-11-19 10:28:24	
77	148	2022-12-16 23:28:30.44 to 2022-12-17 01:42:11	Ground segment anomaly (UNS 9117)
81	140	2023-01-25 08:17:20 to 10:13:151	Ground segment anomaly (UNS 9203)
84	234	2023-02-27 from 18:09:47 to 19:40:37	Ground segment anomaly (UNS 9339)
92	237	2023-05-18 05:03:46 to 2023-05-18 06:00:00	
94	150 to 156	2023-06-03 15:17:05 to 2023-06-03 22:40:29	Ground segment anomaly (UNS 9649)
95	148 to 152	2023-06-13 11:20:51 to 2023-06-13 17:08:07	
107	136	2023-10-09 23:22:51 to 2023-10-10 01:32:16	Ground segment anomaly (UNS 10073)

Table 4: List of missing passes in HR

4.1.2. Over ocean

Figure 8 shows the percentage of available measurements for Sentinel-6 MF LR and HR modes for ocean only. In average LR mode provides 99.7% of measurements over 111 cycles.

As expected, HR mode provides in average less measurements (98.5%) on the same time-period. From cycle 32 onwards, in LRMC mode only, the average percentage of available HR data is of 99.4%.

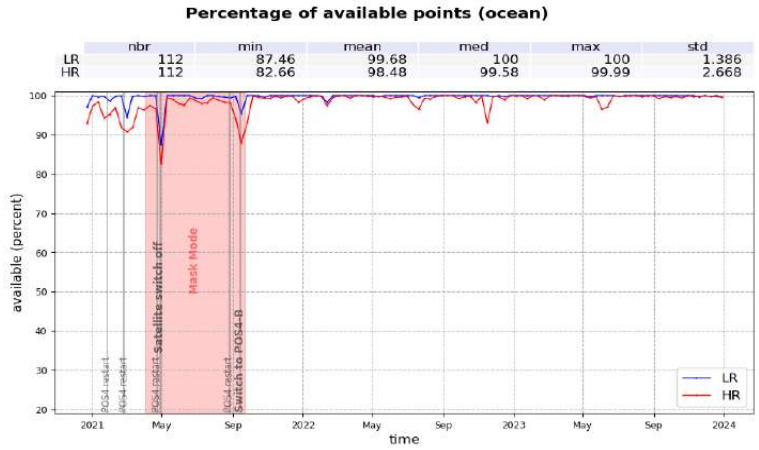

Figure 8: Percentage of available data over ocean for both LR (blue) and HR (red) per cycle.

4.2. Edited measurements

4.2.1. Overview

The outlier detection or editing step of the Cal/Val process is applied to remove any measurement that is considered erroneous. Thus, it helps to refine the various metrics which are provided in the specific sections dedicated to the performance over the ocean. The definition of an erroneous measurement, and of the accepted error level on the final sea level anomaly is of course a trade-off between accuracy and data coverage. The monitoring of the percentage of valid and edited measurements also provides relevant information about the mission performance.

A series of editing criteria are used to detect outliers over ocean. This process is divided into 3 main parts:

- removal of all measurements affected by sea-ice,
- removal of all measurements which exceed defined thresholds on different parameters,
- further checks on along-track SLA consistency.

For each step of the process, the number of outliers is routinely monitored at Cal/Val level. The number of removed data is used to detect processing anomalies which could be due to instrumental, geophysical or algorithmic changes. The process performed here is dedicated to ocean applications. Data over land are removed using a land/water mask prior to the analysis described in this section.

The percentage of edited data per day for HR and LR datasets over ocean is monitored on figure 9. In average, slightly fewer data is edited in HR mode (10.3%) compared to LR (11.8% in MLE4 and 11.6% in NR). The main spikes observed are :

- Cycle 8, track 12 to 60 (26/01/21 21:19 to 28-01-2021 10:14): Range anomaly (-9 m) following a POS-4 restart, for HR only (see "Sea level anomaly" paragraph in section 4.2.3.2.).
- Cycle 13, track 20 to 45 (17/03/21 09:36 to 18/03/21 09:38): AMR-C 24h warm target calibration (see section 4.2.2.).

Before 21-09-2022 (cycle 32) and the switch to full LRMC-OL mode (section 3.3.), a higher percentage of data is edited in HR compared to LR, with additional spikes. This is due to less overall measurements being available in HR with the use of masks (see figure 8).

An annual signal is visible : the total percentage of edited data is lower during March/April/May (5-7%), then increasing during May to July and remains around 14-17%, and start to slowly decrease in mid-September. This expected behaviour is related to sea ice coverage (see dedicated part 4.2.2.), and was already observed on previous altimetry missions such as Jason-3.

The maps of figure 10 represent the percentage of edited data for LR MLE4, LR NR and HR, over the year 2023. Equatorial wet zones or zones with sea ice appear on the maps as regions with less valid data, as it is also the case for other altimeters: measurements are corrupted by rain or sea ice. They were therefore removed by editing. HR and LR maps are in line, except in wet zones where less HR data are edited. It shows the better capability of HR processing to retrieve clean geophysical parameters over wet zones.

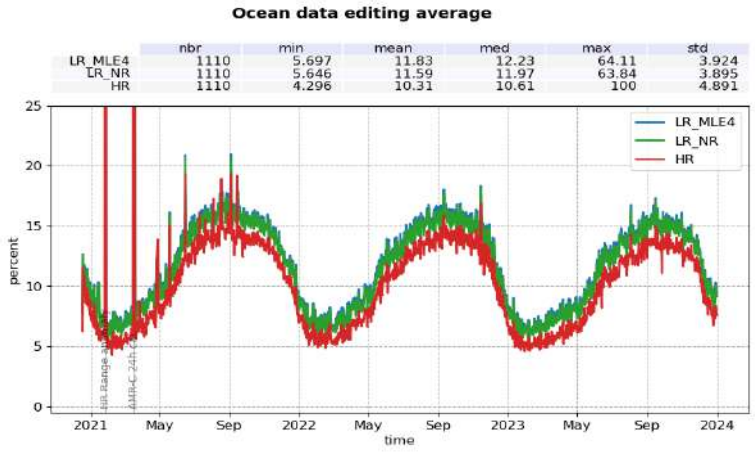

Figure 9: Percentage of edited data over ocean for LR MLE4 (blue), LR NR (green) and HR (red) per day.

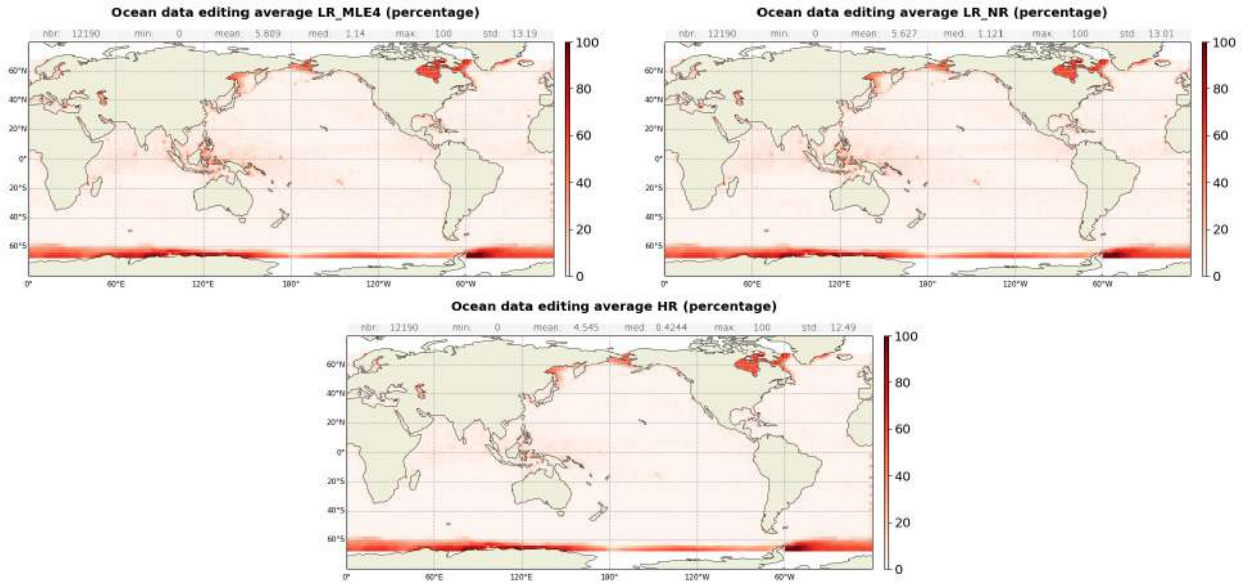

Figure 10: Maps of average percentage of edited ocean data for LR MLE4 (left), LR NR (right) and HR (bottom), computed on year 2023.

4.2.2. Flagging quality : ice

The first step of the editing process includes the removal of points where ice is detected. The ice flag (based on rad_sea_ice_flag in L2 products) is used to remove measurements affected by sea ice within the altimeter footprint.

The percentage of measurements edited on the ice flag criterium over ocean is monitored on the figure 11.

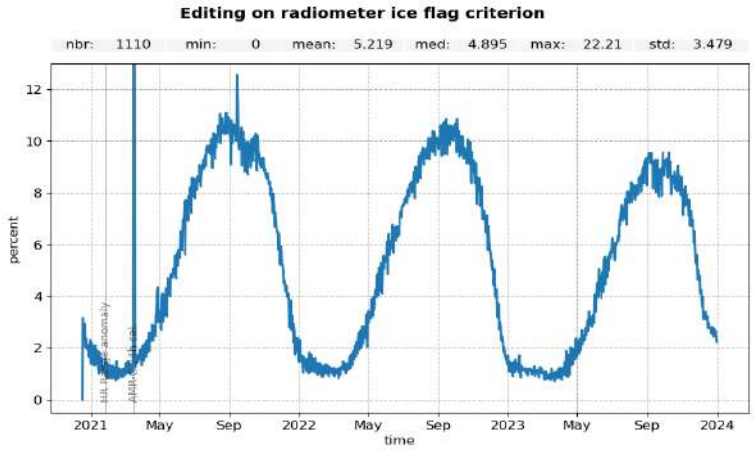

Figure 11: Percentage of data edited on ice criterion per day.

On cycle 13, from pass 20 to 45 (17/03/21 09:36 to 18/03/21 09:38), an AMR-C 24h warm target calibration caused the unavailability of the radiometer derived ice flag resulting in a spike in edited data. Over the shown period, no anomalous trend is detected but the nominal annual cycle is visible. Indeed, the maximum number of points over ice is reached during the southern winter (i.e. July - September). As Sentinel-6 MF satellite has an inclination of $66°$, it does not detect thawing of sea ice (due to global warming), which takes place especially in Northern Hemisphere over $66°$.

Note that the percentage of edited data on ice criterion is lower for Sentinel-6 MF (5.2 % in average) than on Jason-3 (9.3 % in average). Such a difference is due to the different definition of the ice flags used for this editing step. On Jason-3, the ice flag (ice_flag in L2 product) is computed using a combination of radiometer, model and altimeter parameters. On Sentinel-6 MF, the sea ice flag is only derived from radiometer outputs.

4.2.3. Thresholds

4.2.3.1. Overview

Once the measurements corrupted by sea ice surfaces are identified, the quality of the parameters retrieved by the altimeter, as well as that of the geophysical corrections are checked with respect to defined thresholds. These thresholds are detailed in table 5, with the corresponding percentage of detected outliers in LR MLE4, LR NR and HR over Sentinel-6 MF lifetime. These percentages are closely monitored cycle by cycle, day by day and pass by pass by CLS Cal/Val routines. A distinction is made between indicators at default value, and indicators out of bounds.

This allows detection of anomalies in the number of removed data, which could have instrumental, geophysical or algorithmic origins.

Parameters	Min threshold	Max threshold	Unit	% rejected		
				LR MLE4	LR NR	HR
Sea surface height anomaly	-2	2	m	3.43	3.02	3.18
Sea surface height	-130	100	m	2.47	1.95	0.01
Nb measurements of range	10	N/A		0.17	0.00	0.01
Std. deviation of range	0	See (*)	m	2.79	1.19	0.96
Backscatter coefficient	LR: 7 HR: 10	LR: 30 HR: 35	dB	2.21	0.12	0.11
Nb measurements of sigma0	10	N/A		0.16	0.00	0.01
Std. deviation of sigma0	0	1	dB	4.14	2.39	0.80
Significant wave height	0	11	m	2.62	0.27	0.11
Altimeter wind speed	0	30	m.s-1	2.40	0.96	1.36
Sea State Bias	-0.5	0	m	2.20	0.02	0.03
Ionospheric correction filtered	-0.4	0.04	m	2.98	2.81	2.97
Square off nadir angle	-0.2	0.64	deg2	0.85	1.39	N/A
Equilibrium tide	-0.5	0.5	m	0.01	0.01	0.01
Combined atmospheric correction	-2	2	m	0.00	0.00	0.00
Dry tropospheric correction	-2.5	-1.9	m	0.04	0.04	0.04
Internal tide	-5	5	m	0.00	0.00	0.00
Ocean tide	-5	5	m	0.04	0.04	0.04
Pole tide	-15	15	m	0.00	0.00	0.00
Earth tide	-1	1	m	0.00	0.00	0.00
AMR+HRMR wet tropospheric correction	-0.5	-0.001	m	0.16	0.17	0.16
Global statistics of edited measurements by thresholds				6.62	6.29	5.10

Table 5: Table of parameters used for editing and the corresponding percentages of edited measurements for each parameter for Sentinel-6 MF LR and HR.

(*) The maximum threshold for range standard deviation is set as function of significant wave height as follow:
- In LR:
  - for SWH $\leq$ 2m : 0.192
  - for SWH > 2m : 0.018 * SWH + 0.156
- In HR:
  - for SWH $\leq$ 2m : 0.087
  - for SWH > 2m : 0.033 * SWH + 0.121

The monitoring of edited data based on these thresholds criteria is shown on figure 12. On this monitoring, slightly different behaviours are observed between LR datasets. There are fewer criteria at default value in LR NR than in LR MLE4. However, the opposite is true for criteria out of bounds. This indicates that more data are retrieved in NR, but most of this additional data is of poor quality and then edited on threshold criteria.
Looking at data at default value (i.e. unavailable, right panel) and if we do not consider the events already listed above, an annual signal is visible. Part of this signal can be linked to sea ice. Indeed, as stated above, the radiometer sea ice flag performance does not allow to detect all measurements affected by sea ice. For the remaining measurements, MLE4, NR and SAMOSA retrackings failed to retrieve geophysical parameters, hence the default values detected here.
Looking at out-of-bounds data (left panel), fewer data are edited in HR (1.9 %) than in LR (3.1 % in MLE4 and 3.6 % in NR). All monitorings are stable in time, with a small annual signal of about 1%-amplitude.

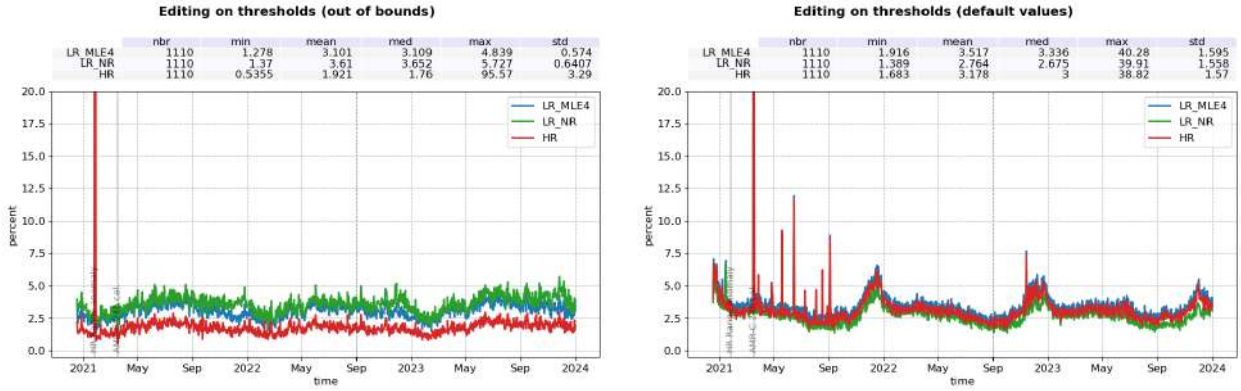

Figure 12: Percentage of data edited on threshold criteria for LR MLE4 (blue), LR NR (green) and HR (red) per day, for out of bounds (left) and default value (right) indicators.

The overall percentage of edited data with this threshold step is of 6.62 % for LR MLE4, 6.37 % for LR NR and 5.10 % for HR (table 5). These values are higher than on Jason-3 (3.45 %). In fact, the measurements that were not flagged as sea-ice by Sentinel-6 MF ice flag but by J3 ice flag are of poor quality and are therefore edited during this step (see previous section).

4.2.3.2. Individual thresholds

20 Hz range measurements number and standard deviation

1 Hz range measurements computed with less than ten 20 Hz measurements are edited. Indeed, they are considered as not consistent to compute 1Hz resolution range.

In LR, such situation usually occurs in regions with disturbed sea state or heavy rain, as shown on figure 14. Indeed, waveforms are distorted by rain cells, which makes them often meaningless for SSH calculation. As a consequence, edited measurements due to several altimetric criteria are often correlated with wet areas. Over the year 2023, the average percentage of removed measurements using this criterion is 0.14% for Sentinel-6 MF LR MLE4 whereas it is only of 0.01% for HR (figure 13) and less than 0.01% in LR NR.

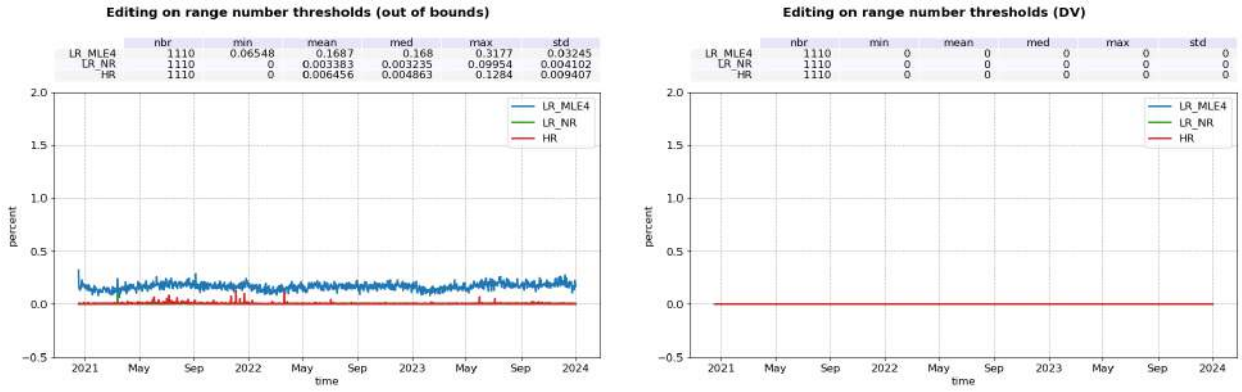

Figure 13: Percentage of data edited on range number threshold for LR MLE4 (blue), LR NR (green) and HR (red) per day, for out of bounds (left) and default value (right).

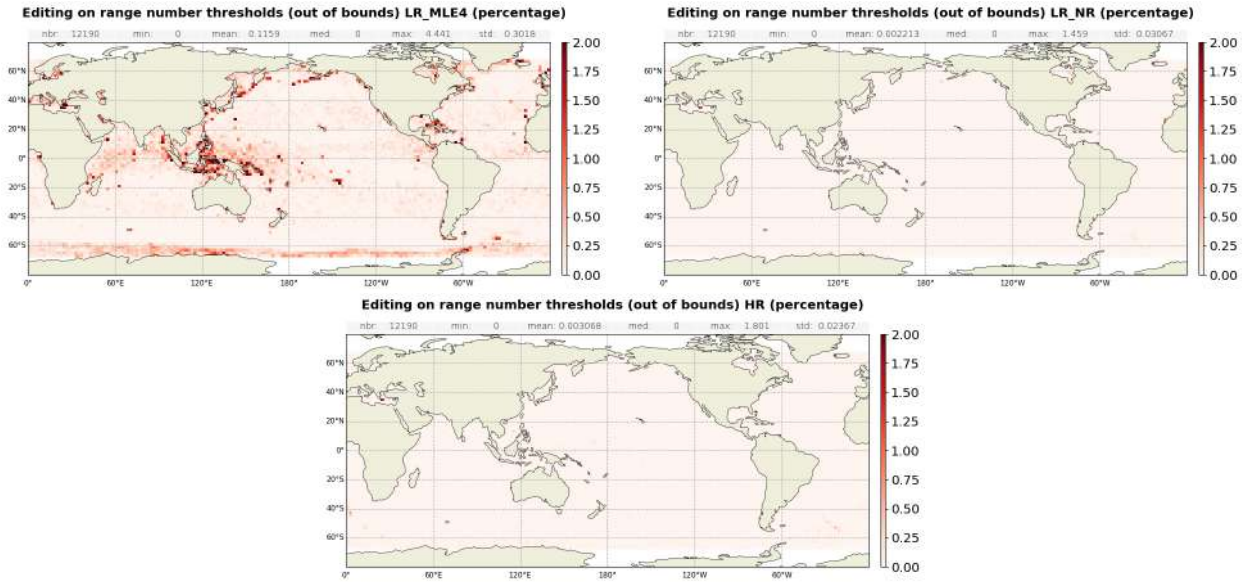

Figure 14: Maps of average percentage of data edited on range number threshold for both LR MLE4 (left), LR NR (right) and HR (bottom), for out of bounds, computed on year 2023.

Using the threshold editing on 20Hz range measurements standard deviation (figure 15), 2.75% of data are removed in average in LR MLE4, higher than in LR NR and HR (1.19 % and 0.96 % respectively). This difference is explained by a higher percentage of range standard deviation set to Default Value for LR MLE4 (figure 15, bottom panel). It highlights the LR NR and HR processings capabilities to retrieve geophysical parameters on icy regions.
Additionally, an annual signal appears here for all processings. As for 20Hz range measurements number, edited measurements are correlated with wet areas (figures 16 and 17).

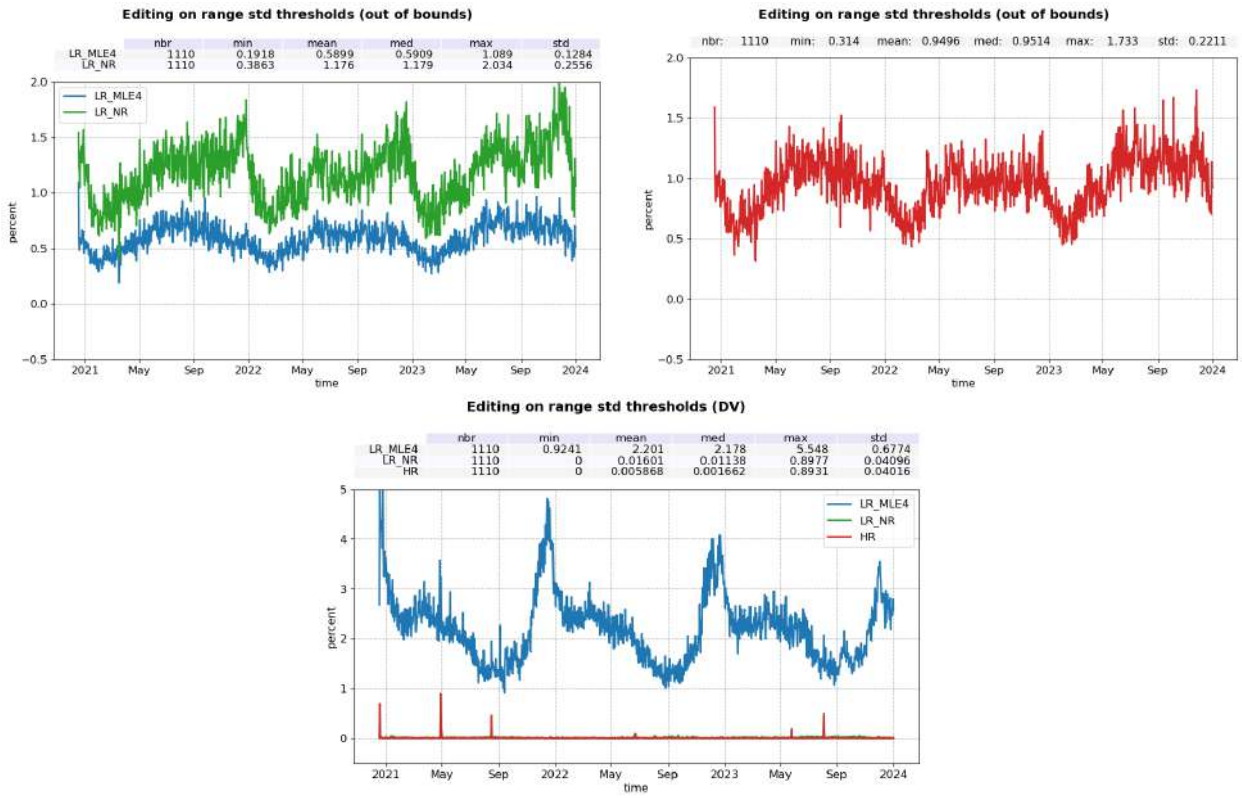

Figure 15: Percentage of data edited on range std threshold for both LR MLE4 (blue), LR NR (green) and HR (red) per cycle, for out of bounds (top) and default value (bottom).

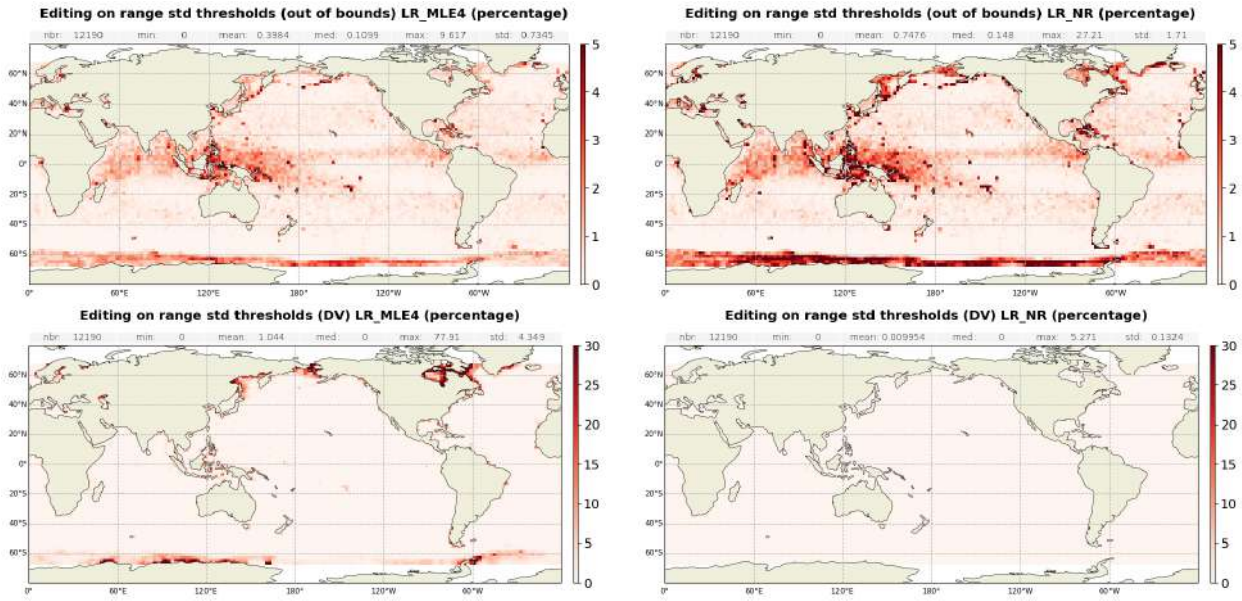

Figure 16: Maps of average percentage of data edited on range std threshold for both LR MLE4 (left) and LR NR (right), for out of bounds (top) and default value (bottom), computed on year 2023.

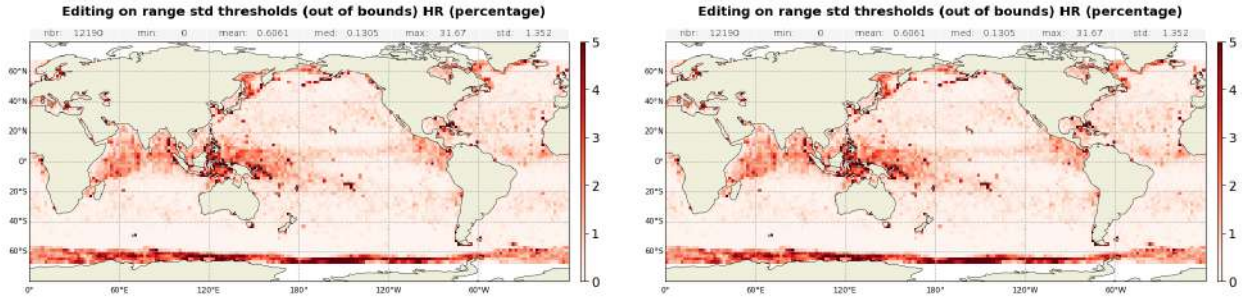

Figure 17: Maps of average percentage of data edited on range std threshold for HR, for out of bounds (left) and default value (right), computed on year 2023.

Backscatter coefficient

The percentage of edited measurements due to backscatter coefficient criterion is represented on top of figure 18. It is about 2.21% for LR MLE4, 0.12 % for LR NR and 0.11% for HR. For LR MLE4, most of these edited measurements are at DV and located in coastal areas, ice margins and wet zones (see figures 19 and 20).

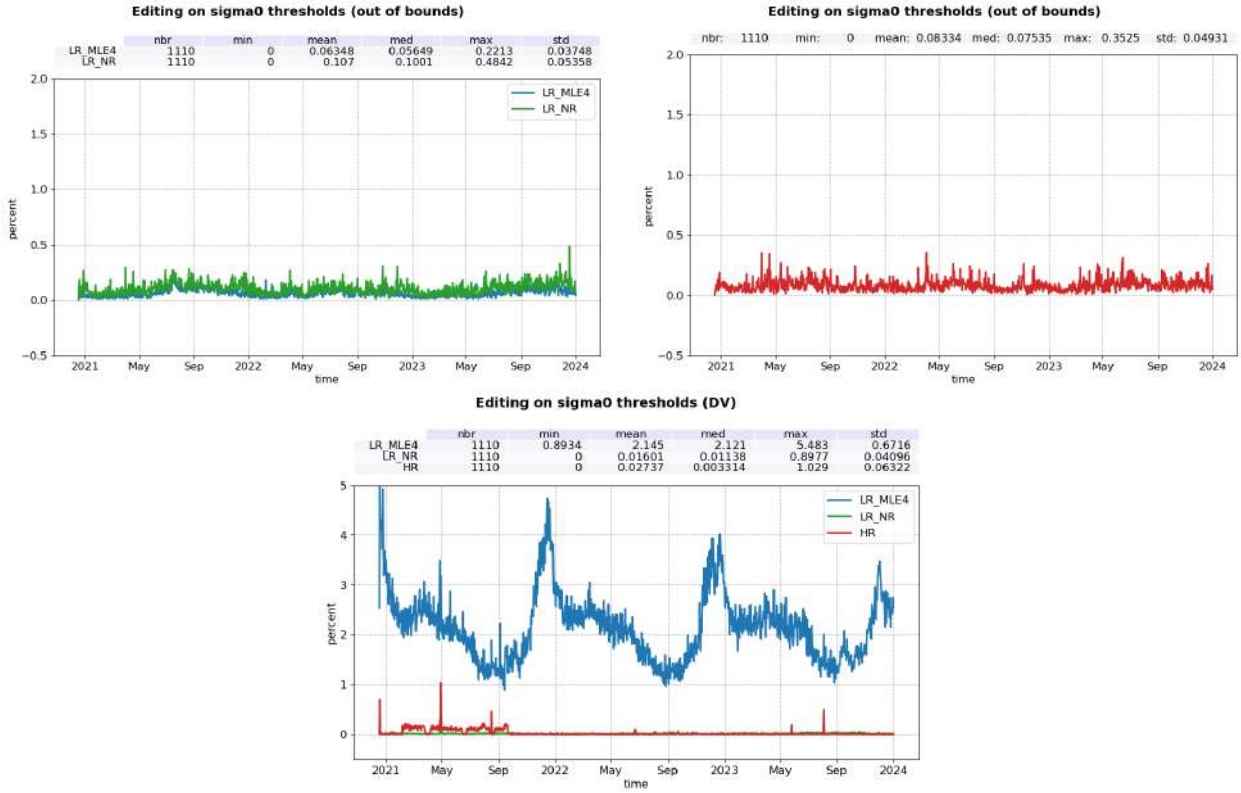

Figure 18: Percentage of data edited on sigma0 threshold for LR MLE4 (blue), LR NR (green) and HR (red) per day, for out of bounds (top) and default value (bottom).

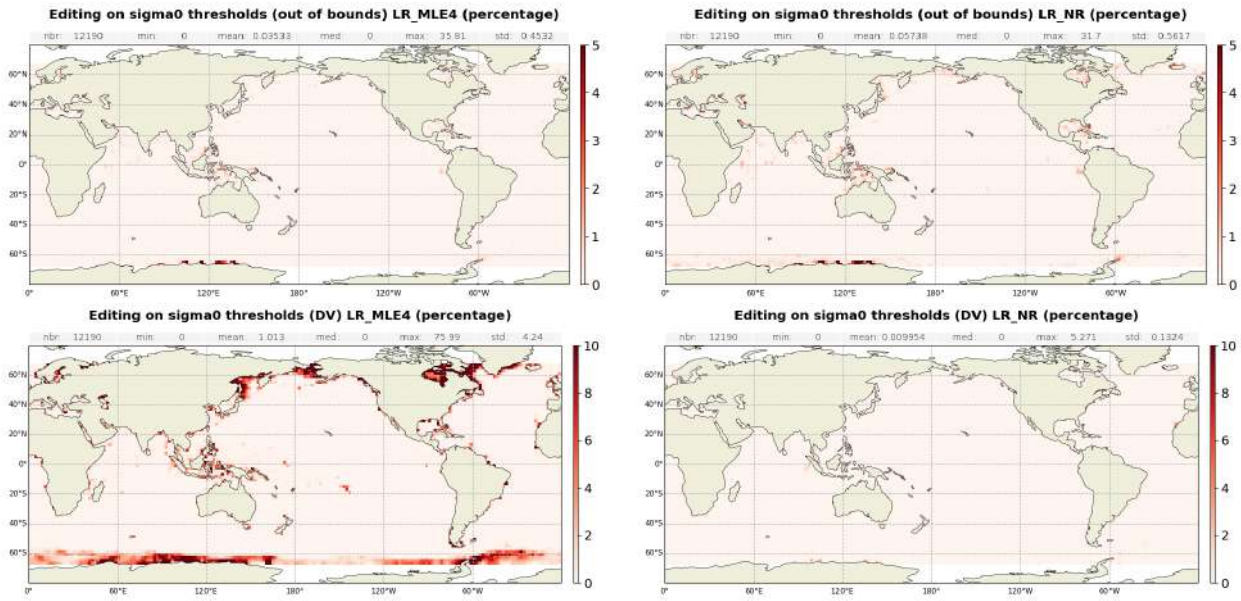

Figure 19: Maps of average percentage of data edited on sigma0 threshold for both LR MLE4 (left) and LR NR (right), for out of bounds (top) and default value (bottom), computed on year 2023.

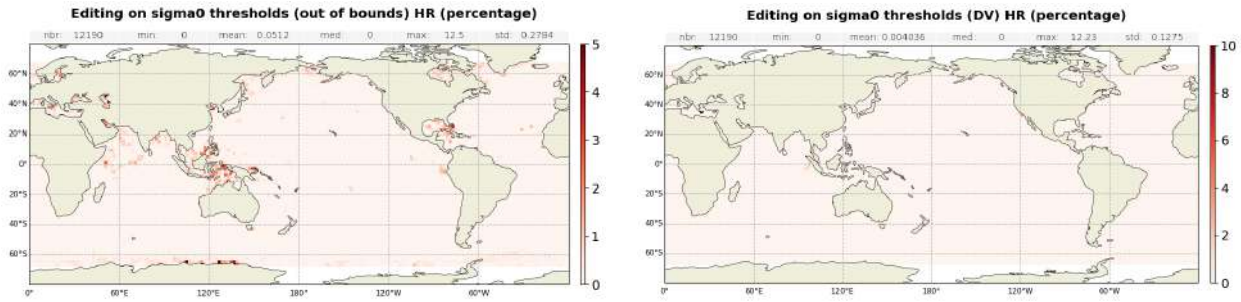

Figure 20: Maps of average percentage of data edited on sigma0 threshold for HR, for out of bounds (left) and default value (right), computed on year 2023.

Similarly to range, sigma0 computed with less than 10 full resolutions (20Hz, 20 measurements/seconds) are removed. As for the range, such situation usually occurs in regions with disturbed sea state or heavy rain (figure 22). While 0.13% of data are edited on this criterion in LR MLE4 (figure 21), LR NR and HR processings are almost unaffected with less than 0.01 % of data edited.

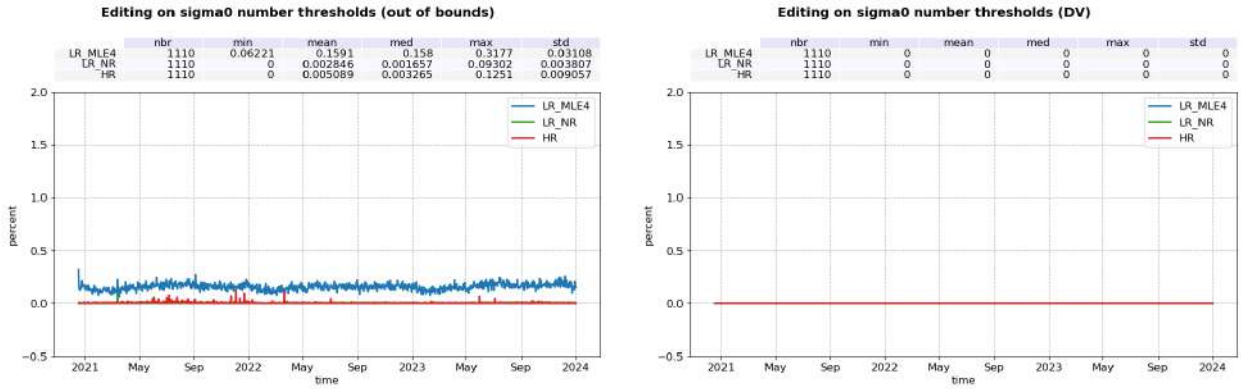

Figure 21: Percentage of data edited on sigma0 number threshold for LR MLE4 (blue), LR NR (green) and HR (red) per day, for out of bounds (left) and default value (right).

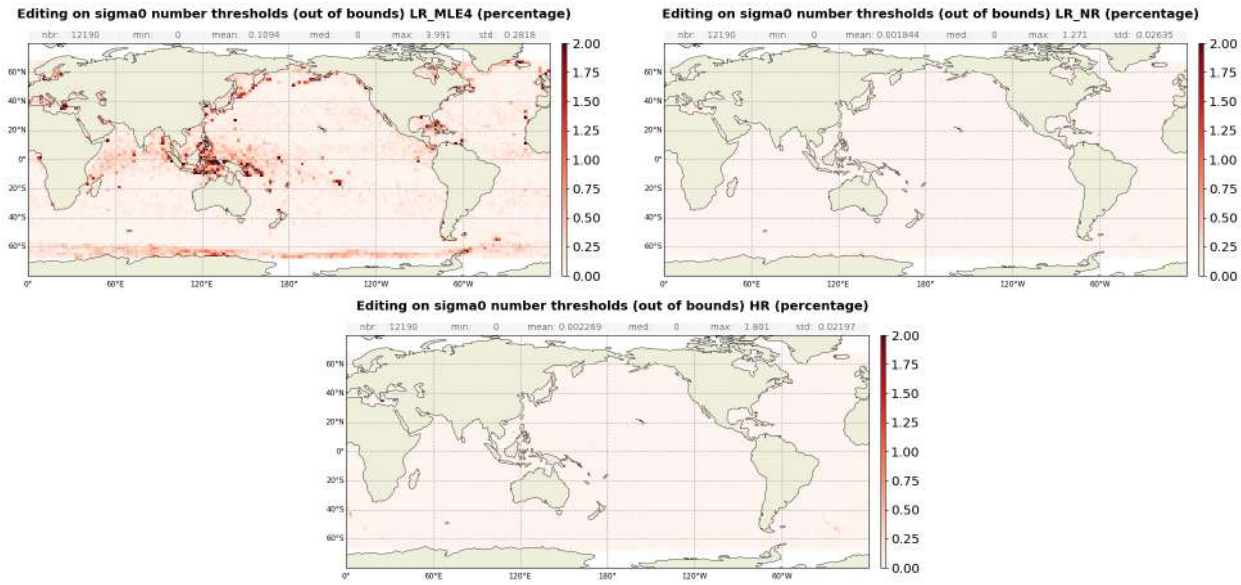

Figure 22: Maps of average percentage of data edited on sigma0 number threshold for LR MLE4 (left), LR NR (right) and HR (bottom), for out of bounds, computed on year 2023.

Figure 23 presents the percentage of data edited based on sigma0 standard deviation criterion. It is about

4.14% for LR MLE4, 2.39 % for LR NR and 0.80% for HR. Most of the out of bound sigma0 STD are located in regions with disturbed sea state or heavy rain, primarily around Indonesia (figure 24).

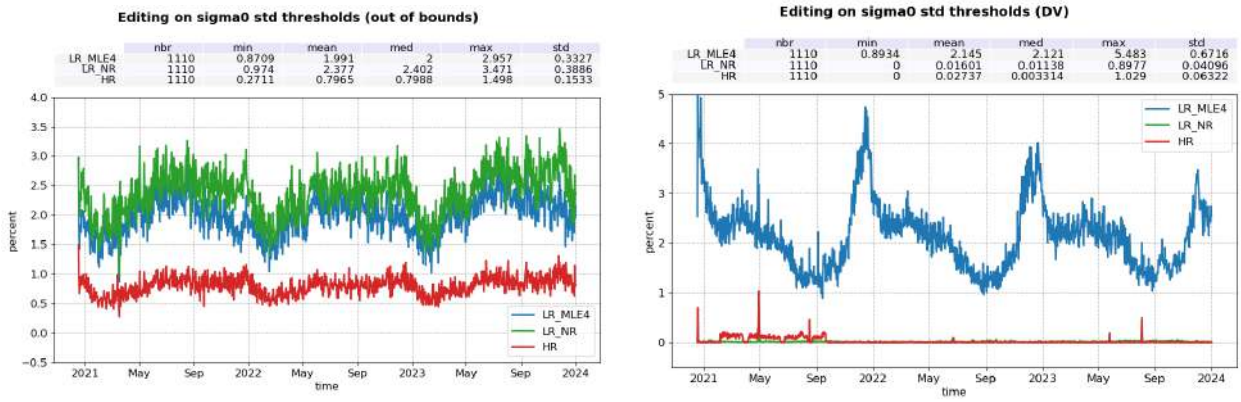

Figure 23: Percentage of data edited on sigma0 std threshold for LR MLE4 (blue), LR NR (green) and HR (red) per day, for out of bounds (left) and default value (right).

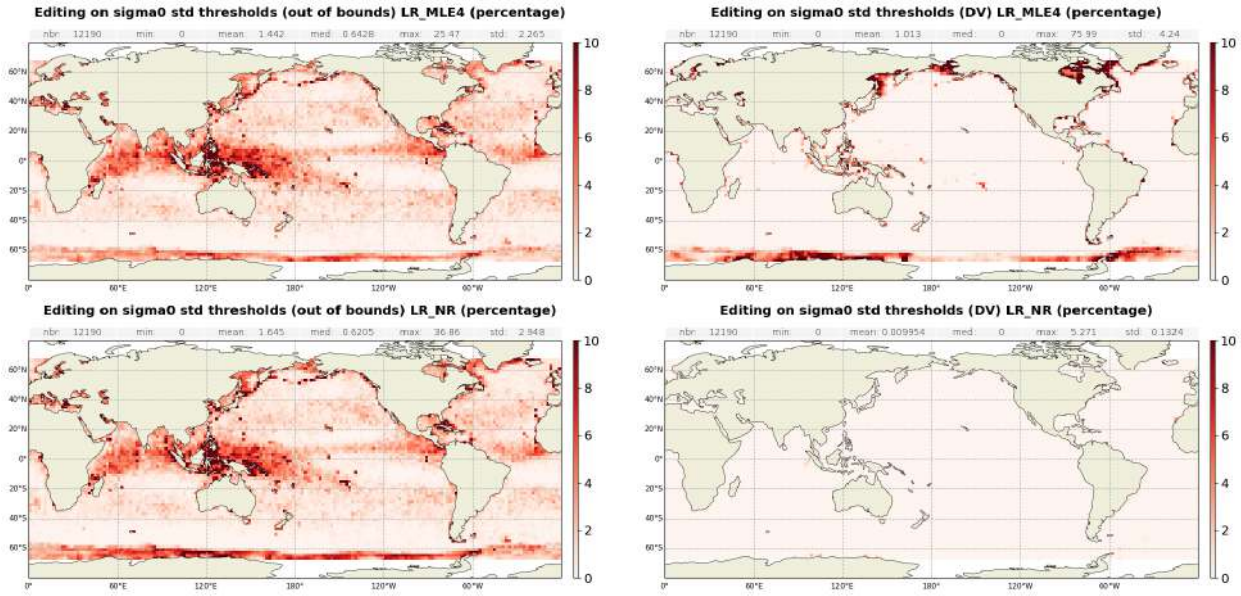

Figure 24: Maps of average percentage of data edited on sigma0 std threshold for both LR MLE4 (top) and LR NR (bottom), for out of bounds (left) and default value (right), computed on year 2023.

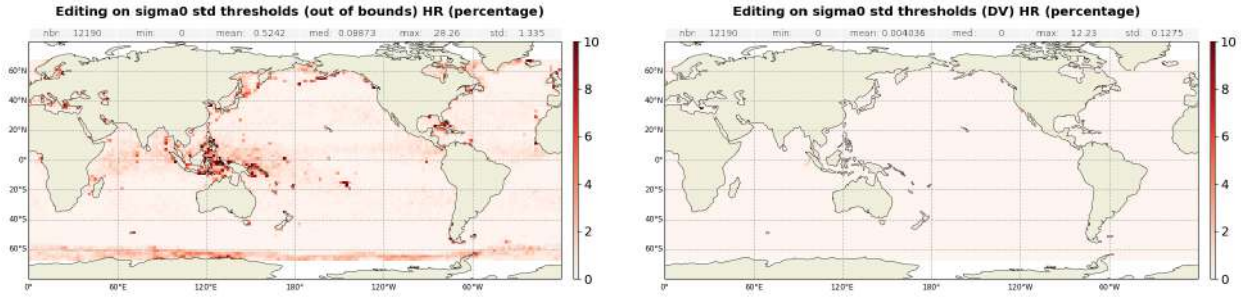

Figure 25: Maps of average percentage of data edited on sigma0 std threshold for HR, for out of bounds (left) and default value (right), computed on year 2023.

Significant wave height

The percentage of edited measurements due to significant wave heights criterion is represented on figure 26, and is about 2.62% for LR MLE4, 0.27 % for LR NR and 0.11% for HR. In LR MLE4, they are mostly due to default value data, and are located in circumpolar areas, while out of bounds values are located in coast regions, in the Mediterranean Sea and around Indonesia (figure 27).

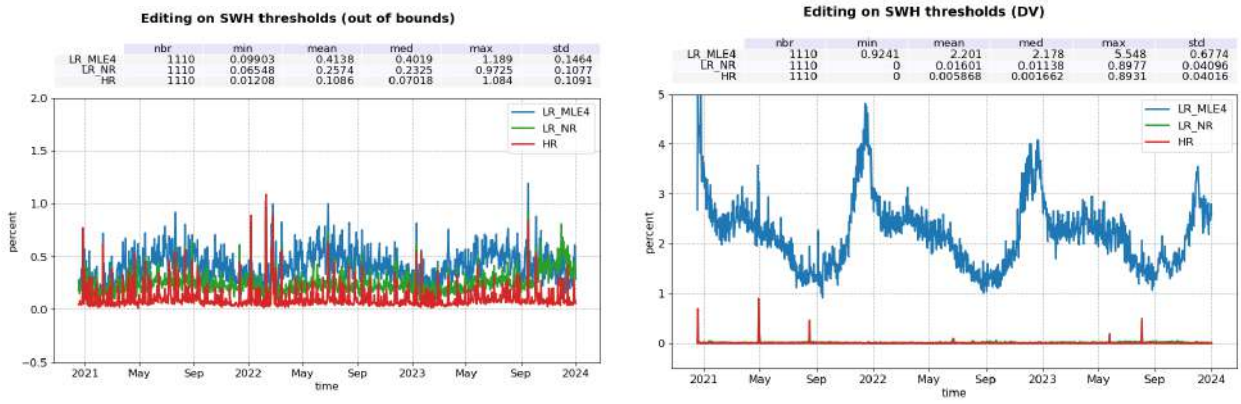

Figure 26: Percentage of data edited on SWH threshold for LR MLE4 (blue), LR NR (green) and HR (red) per day, for out of bounds (left) and default value (right).

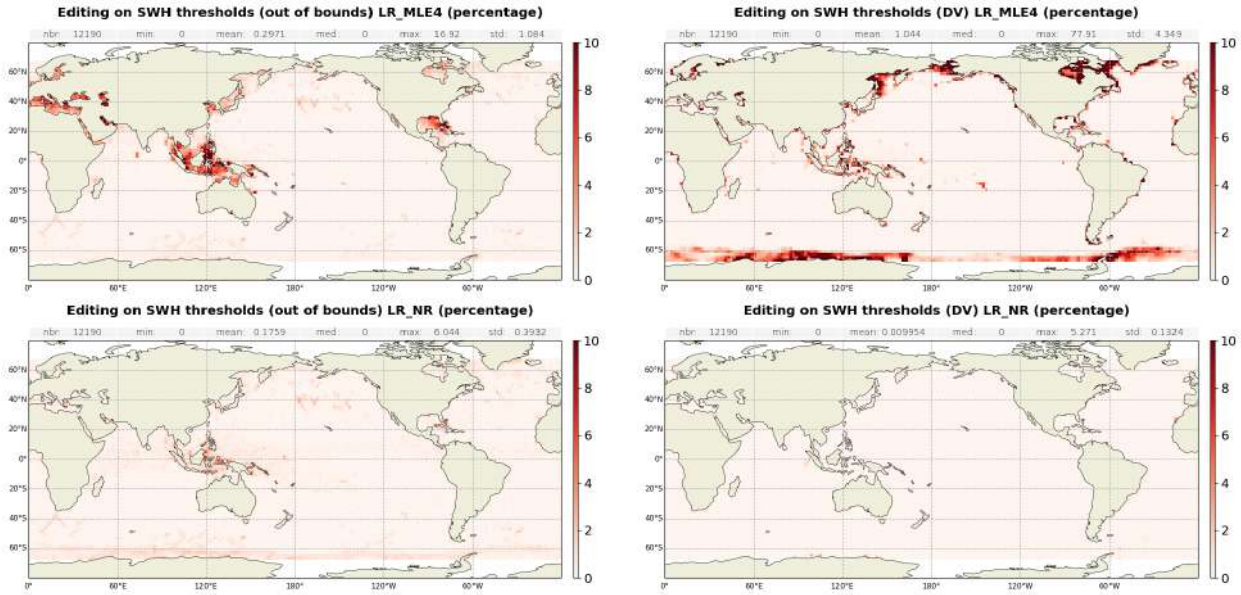

Figure 27: Maps of average percentage of data edited on SWH threshold for both LR MLE4 (top) and LR NR (bottom), for out of bounds (left) and default value (right), computed on year 2023.

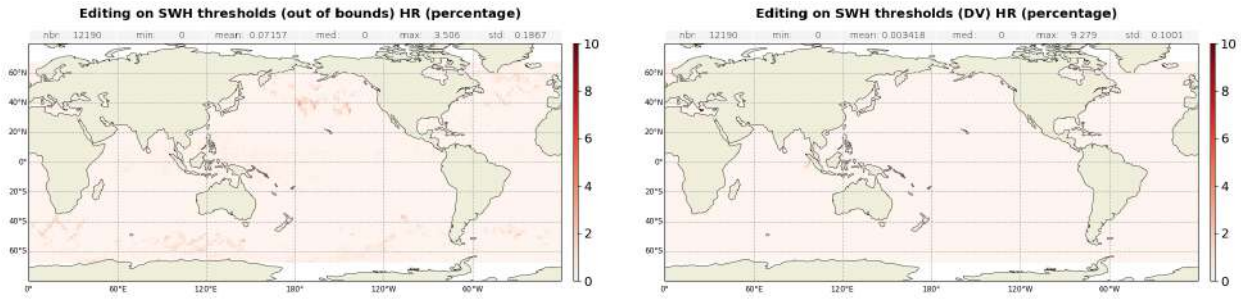

Figure 28: Maps of average percentage of data edited on SWH threshold HR, for out of bounds (left) and default value (right), computed on year 2023.

Wind speed

The percentage of edited measurements due to altimeter wind speed criterion is represented on figure 29. It is about 2.40% for LR MLE4, 0.96 % for LR NR and 1.36 % for HR. Measurements are exclusively edited because of default values.

Wind speed is also edited when it includes negative values. Nevertheless, sea state bias is available even for negative wind speed values. Therefore, the percentage of edited altimeter wind speed data is higher than the percentage of edited sea state bias data (Table 5). Maps on figure 30 showing percentage of measurements edited by altimeter wind speed criterion is correlated with maps 27, 28 (SWH) and 19 and 20 (sigma0).

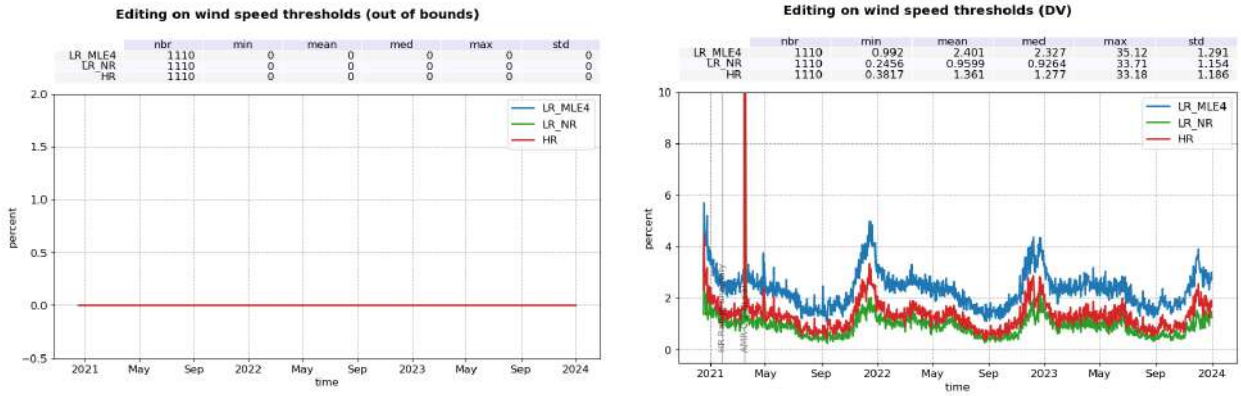

Figure 29: Percentage of data edited on wind speed threshold for LR MLE4 (blue), LR NR (green) and HR (red) per day, for out of bounds (left) and default value (right).

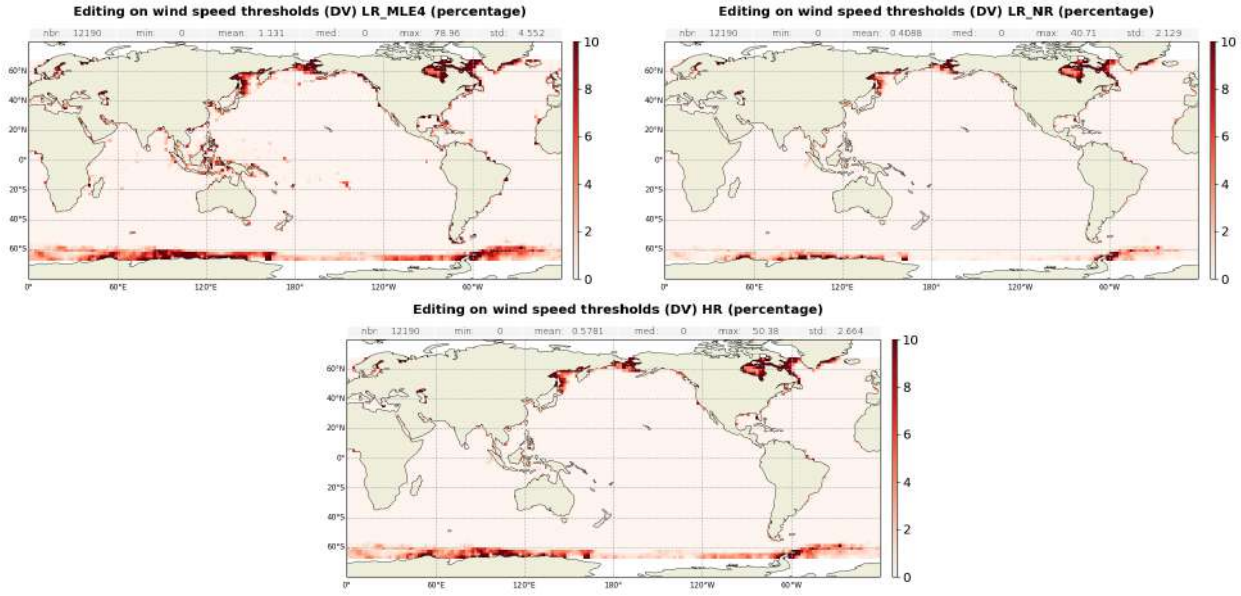

Figure 30: Maps of average percentage of data edited on wind speed threshold for LR MLE4 (left), LR NR (right) and HR (bottom), for default value, computed on year 2023.

Sea state bias

Regarding the sea state bias criterion, the percentage of edited measurements is about 2.20% in LR MLE4, 0.02 % in LR NR and 0.03 % for HR. These are exclusively due to default value data (figure 31). The difference can also be observed on wind-speed and significant wave height threshold criteria (which are both used for SSB computation).

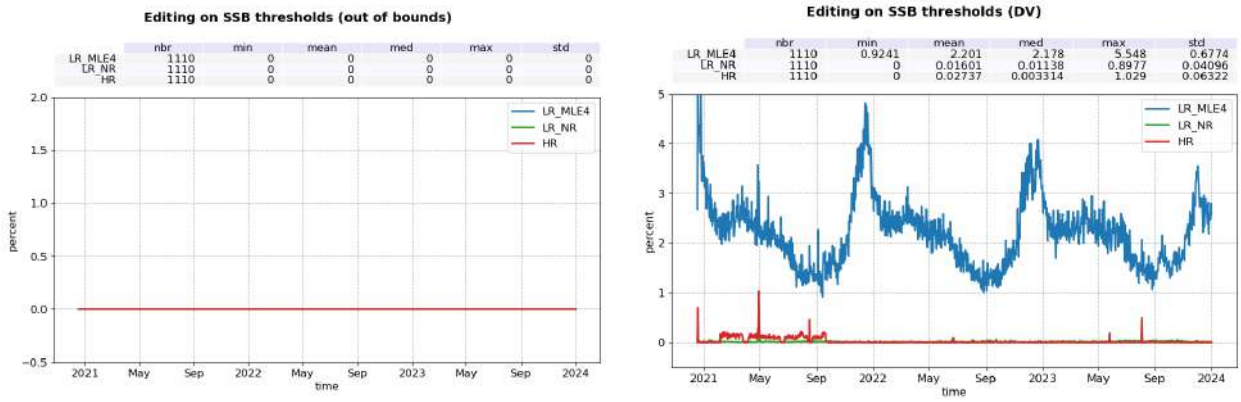

Figure 31: Percentage of data edited on SSB threshold for LR MLE4 (blue), LR NR (green) and HR (red) per day, for out of bounds (left) and default value (right).

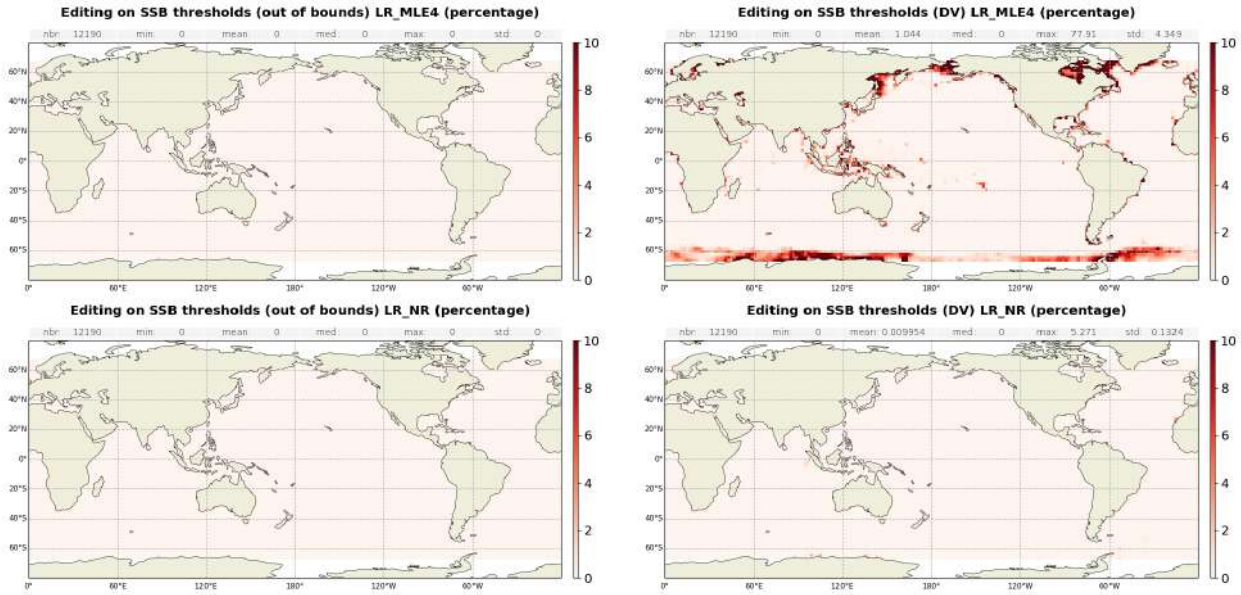

Figure 32: Maps of average percentage of data edited on SSB threshold for both LR MLE4 (top) and LR NR (bottom), for out of bounds (left) and default value (right), computed on year 2023.

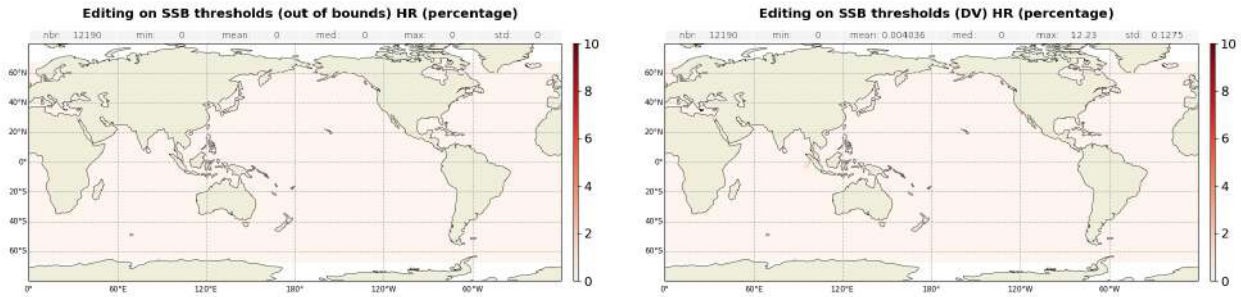

Figure 33: Maps of average percentage of data edited on SSB threshold for HR for out of bounds (left) and default value (right), computed on year 2023.

Filtered ionospheric correction

The mean percentage of edited data by threshold criterion on filtered ionospheric correction is 2.98 % for LR MLE4, 2.81 % for LR NR and 2.97 % for HR.
Note that the ionospheric correction is only computed in LR (C-band being only available in LR) and LR MLE4 ionospheric correction is used in HR products. The small differences visible between LR MLE4 and HR monitorings in figure 34 are due to the difference in data availability between the mode, especially during the Mode Mask phase.
The maps on figure 35 show that measurements edited by filtered dual frequency ionosphere correction are mostly found near coasts and at ice frontiers.

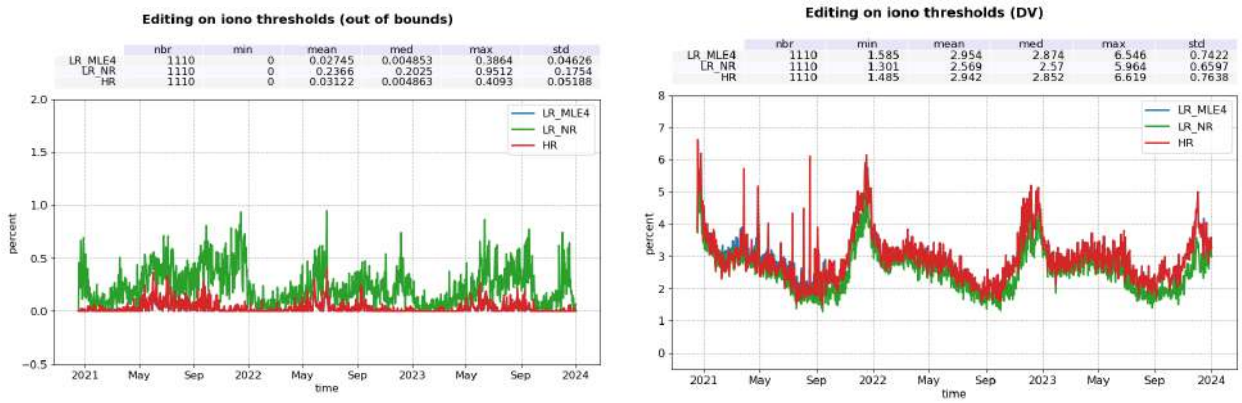

Figure 34: Percentage of data edited on filtered ionospheric correction threshold for LR MLE4 (blue), LR NR (green) and HR (red) per day, for out of bounds (left) and default value (right).

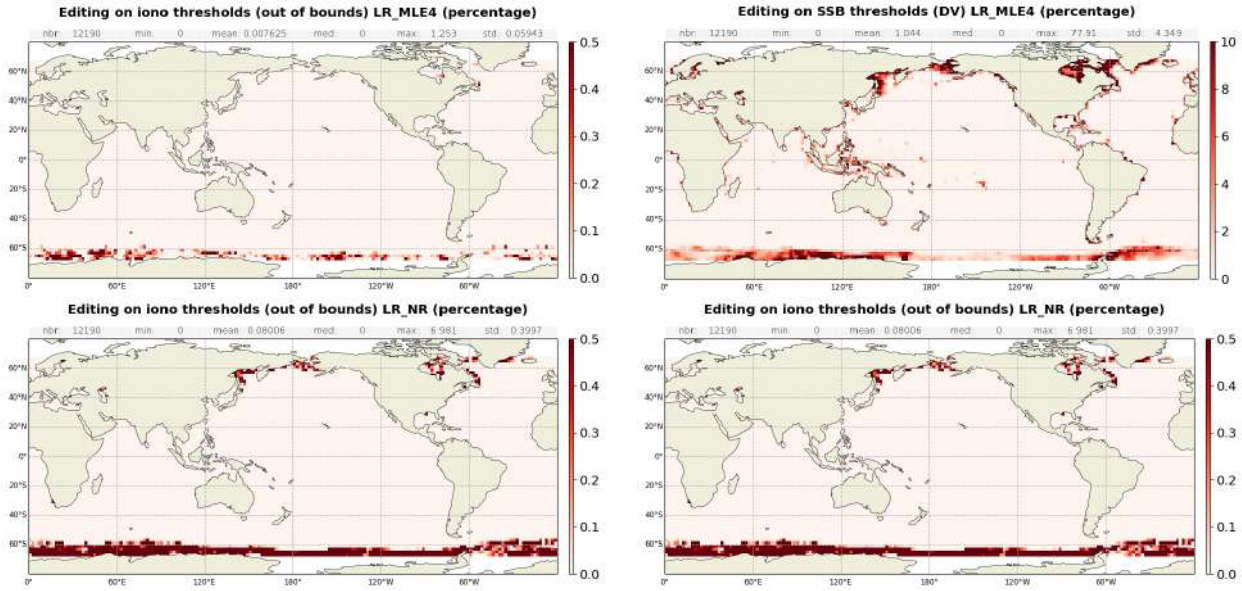

Figure 35: Maps of average percentage of data edited on LR filtered ionospheric correction threshold for both LR MLE4 (top) and LR NR (bottom), for out of bounds (left) and default value (right), computed on year 2023.

Square off nadir angle

The percentage of edited data on the square off nadir angle criterion (in LR data) is 0.85 % in MLE4 and 1.39 % in NR, as shown in figure 36. Maps on figure 37 show that edited measurements are mostly found in coastal regions and regions with disturbed waveforms.

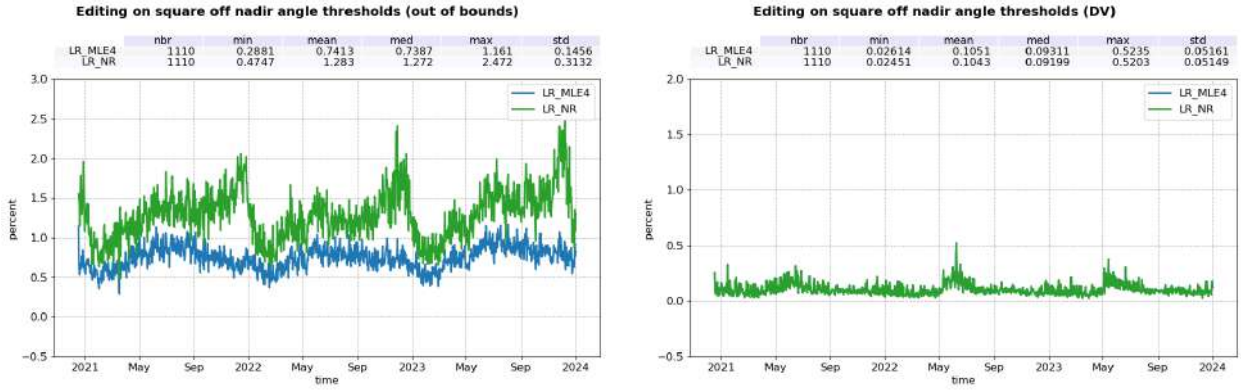

Figure 36: Percentage of data edited on square off nadir angle threshold for both LR MLE4 (blue) and LR NR (green) per day, for out of bounds (left) and default value (right).

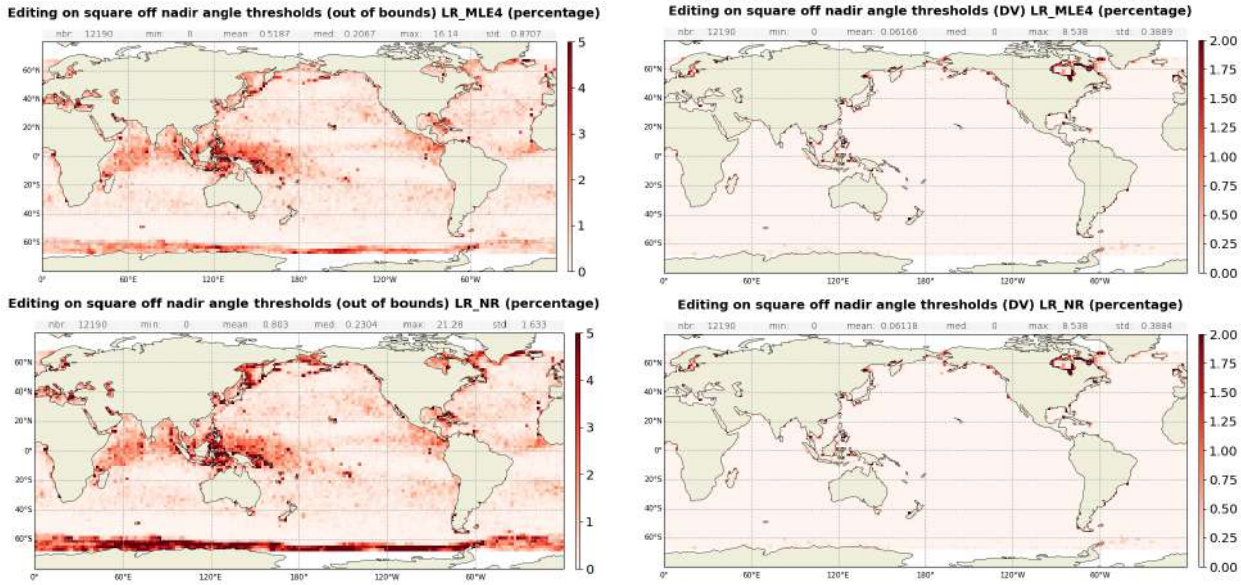

Figure 37: Maps of average percentage of data edited on square off nadir angle threshold for both LR MLE4 (top) and LR NR (bottom), for out of bounds (left) and default value (right), computed on year 2023.

Dry tropospheric correction

The editing criterion on the dry tropospheric correction has allowed to detect an anomaly in this model processing. As shown on figure 38, the dry tropospheric correction is not defined on the Greenwich meridian. Investigation has shown that it is also the case for the model wet tropospheric correction and the inverse barometer (not shown). This anomaly is related to interpolation issue of pressure files. It affects LR and HR products up to PB F09 deployed in February 2024.
All data on this line are therefore always edited.

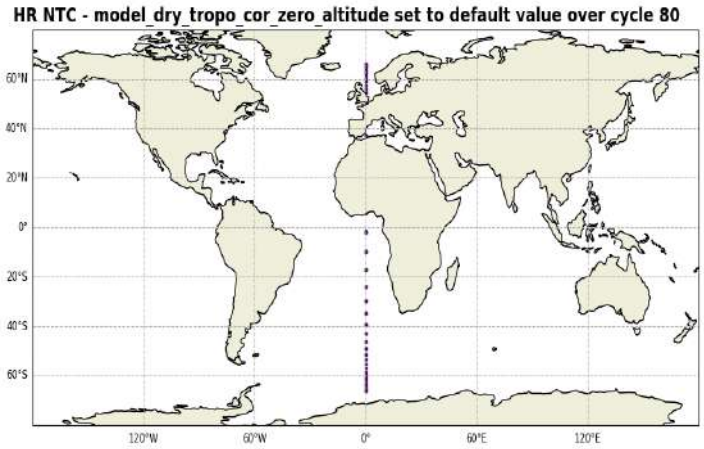

Figure 38: Map of model dry tropospheric correction set to default value. Computed for 1 cycle of HR NTC data.

Ocean tide equilibrium

A very small fraction of measurements, both in LR (MLE4 and NR) and HR, are edited based on the equilibrium ocean tide model being at default value. This impacts less than 0.01% of data in all modes (figure 39).

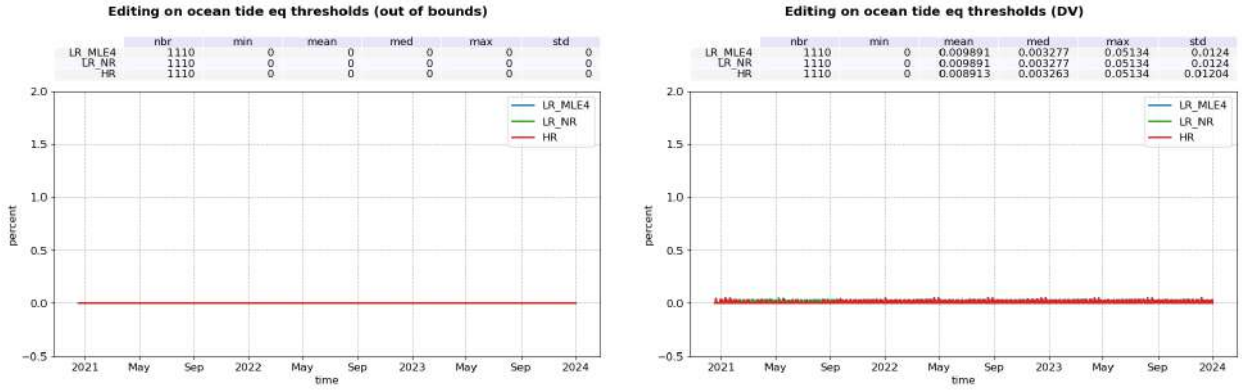

Figure 39: Percentage of data edited on equilibrium tide threshold for LR MLE4 (blue), LR NR (green) and HR (red) per day, for out of bounds (left) and default value (right).

Ocean tide

The percentage of edited measurements due to ocean tide is about 0.04% for all processings (figure 40). The ocean tide correction is a model output, there should therefore be no edited measurement. Indeed, there are no measurements edited in open ocean areas (figure 41). These measurements are exclusively at default values.

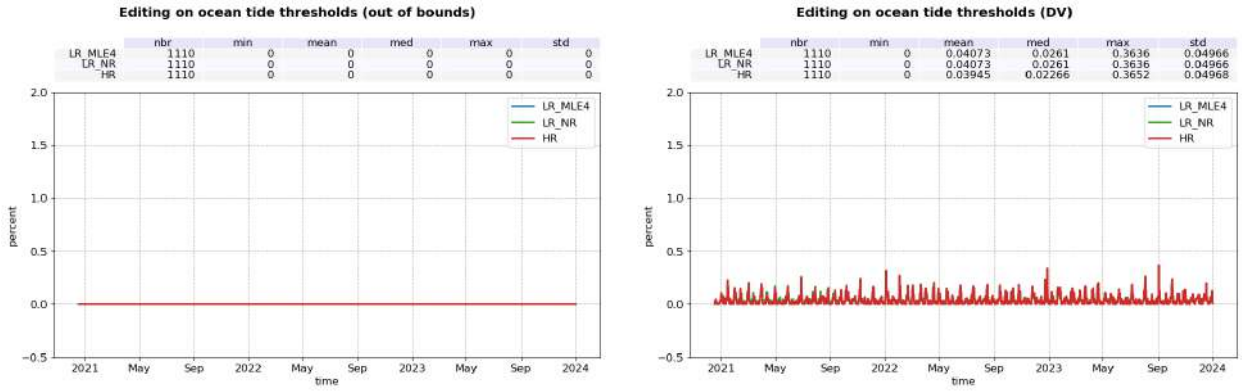

Figure 40: Percentage of data edited on ocean tide threshold for LR MLE4 (blue), LR NR (green) and HR (red) per day, for out of bounds (left) and default value (right).

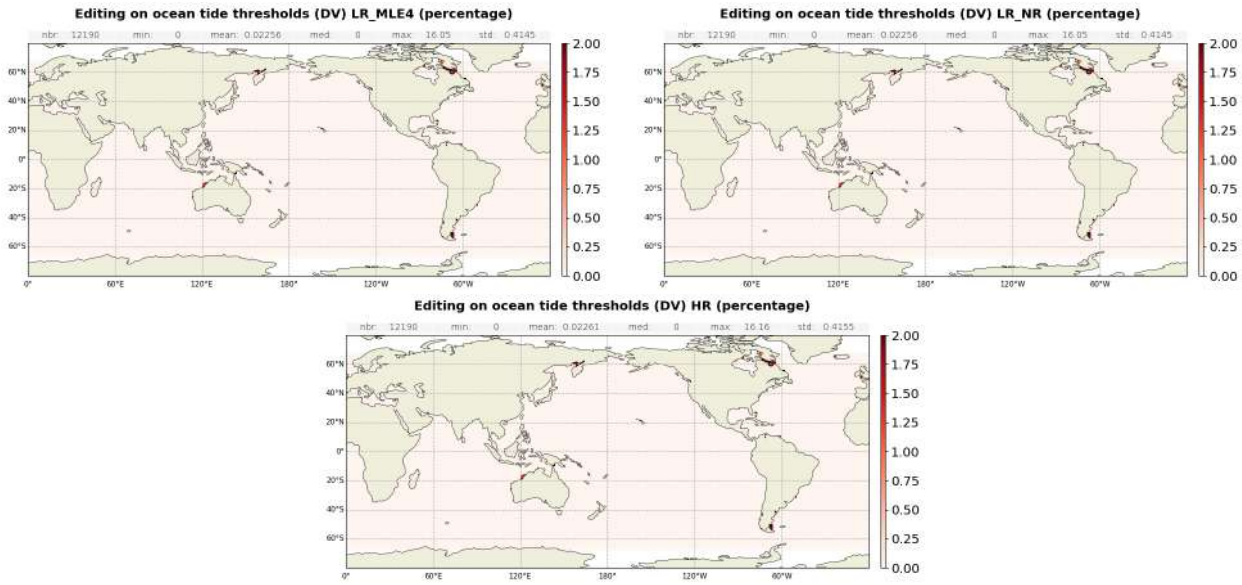

Figure 41: Maps of average percentage of data edited on ocean tide threshold for LR MLE4 (left), LR NR (right) and HR (bottom), for default value, computed on year 2023.

Wet tropospheric correction

The percentage of edited measurements due to radiometer wet troposphere correction criterion is represented in figure 42. It is 0.17 % in LR MLE4 and HR, and 0.16 % in LR NR. As expected, edited data are located in regions of high oceanic variability (see figure 43). Several spikes in the number of DV measurements for the radiometer-derived wet tropospheric correction are visible (figure 42 left panel), and are summarized in table 6.

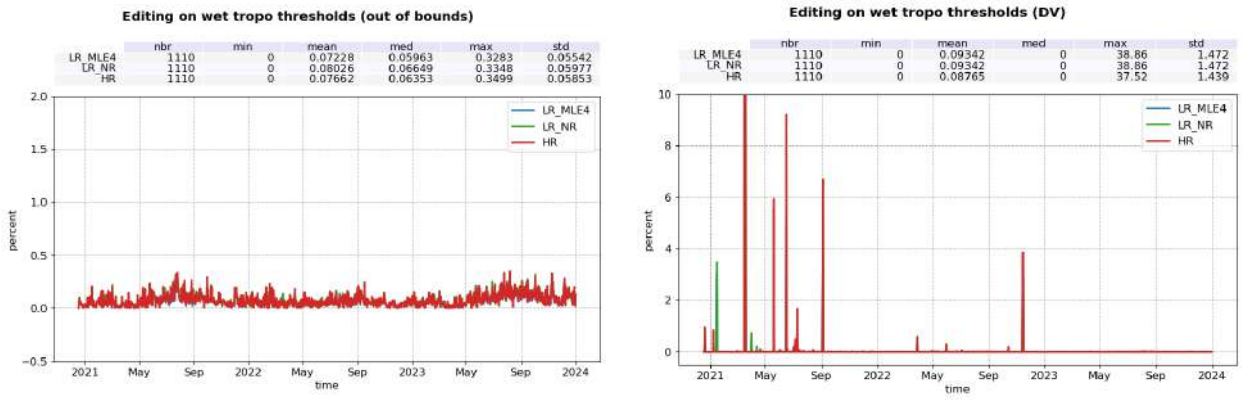

Figure 42: Percentage of data edited on wet tropospheric correction threshold for LR MLE4 (blue), LR NR (green) and HR (red) per day, for out of bounds (left) and default value (right).

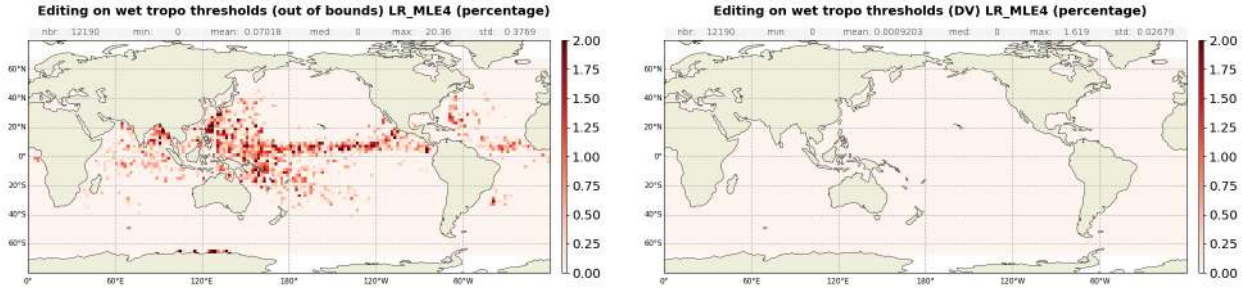

Figure 43: Maps of average percentage of data edited on radiometer wet tropospheric correction threshold, for out of bounds (left) and default value (right), computed on year 2023.

Cycle	Trace	Start date	End date	Related event
6	224 to 225	2021-01-14 23:31:38	2021-01-15 00:38:56	No related event
13	19 to 45	2021-03-17 09:39:37	2021-03-18 09:54:48	AMR-C 24h Warm target calibration
19	101 to 103	2021-05-19 02:15:31	2021-05-19 03:50:53	No related event
22	45 to 47	2021-06-15 15:35:33	2021-06-15 17:28:49	No related event
30	51 to 53	2021-09-03 05:09:07	2021-09-03 06:47:34	No related event
74	68	2022-11-14 03:10:06	2022-11-14 04:06:15	No related event

Table 6: Main events list with radiometer-derived wet tropospheric correction at DV

Sea surface height

Uncorrected sea surface height represents the difference between the orbit and the altimeter range in Ku-band. Figure 44 summarizes the editing resulting from the sea surface height threshold criterion. It removes in average 2.47% of data for LR MLE4, 1.95 % for LR NR and 0.01% of data for HR. In LR, the editing is exclusively due to range measurements at default values near coast, in wet zones, as well as regions with low significant wave heights or over sea ice (figure 45 left panel).

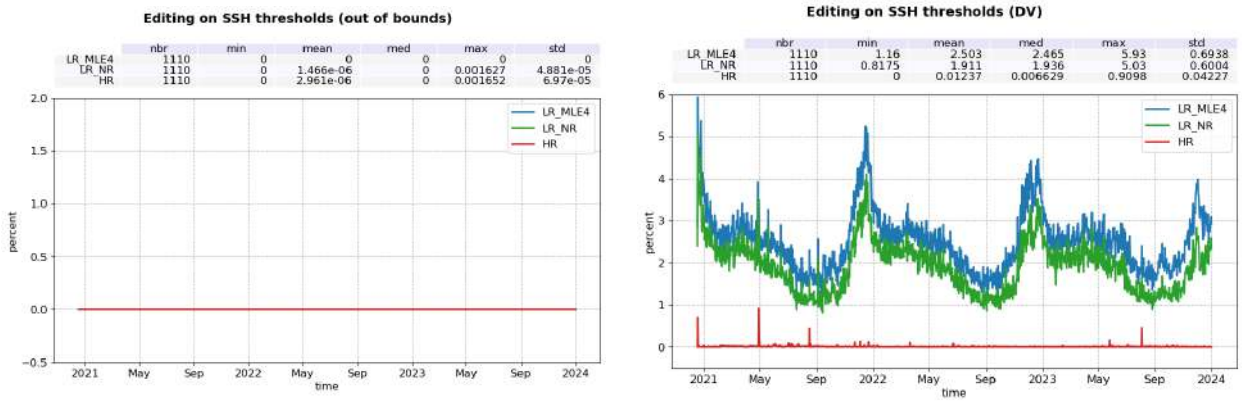

Figure 44: Percentage of data edited on SSH threshold for LR MLE4 (blue), LR NR (green) and HR (red) per day, for out of bounds (left) and default value (right).

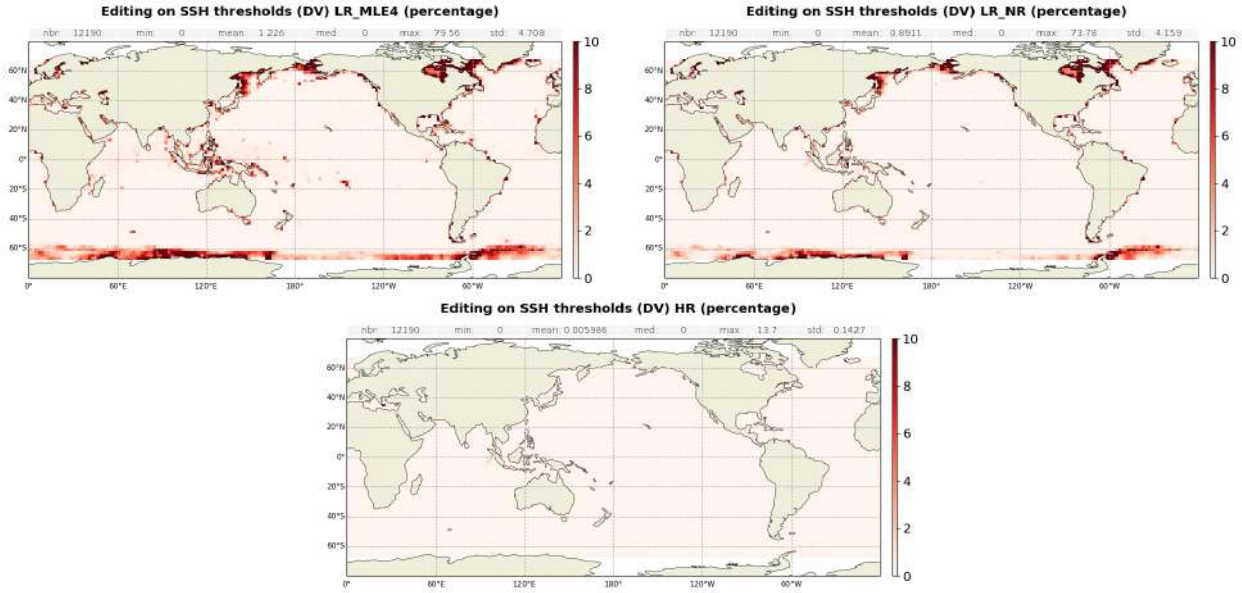

Figure 45: Maps of average percentage of data edited on SSH threshold for LR MLE4 (left), LR NR (right) and HR (bottom), for default value, computed on year 2023.

Sea level anomaly

The percentages of edited data by threshold criterion on SSHA are 6.52% in LR MLE4, 6.37 % in LR NR and 5.10 % for Sentinel-6 MF (figure 46).

The peaks already mentioned on the wet tropospheric corrections are visible here. In addition, HR monitoring present a peak end of January 2021: on cycle 8, track 12 to 60 (26-01-2021 21:19 to 28-01-2021 10:14), an anomaly in HR range (-9 m) occurred following a POS4 restart. The event was not above Sea Surface Height thresholds. SSHA thresholds are stricter and allows to edited HR data during this event.

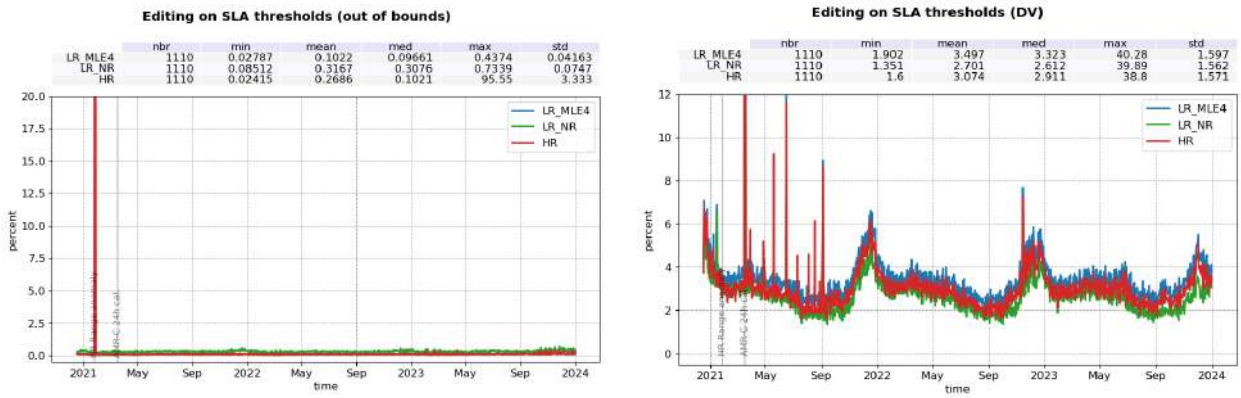

Figure 46: Percentage of data edited on SLA threshold for LR MLE4 (blue), LR NR (green) and HR (red) per day, for out of bounds (left) and default value (right).

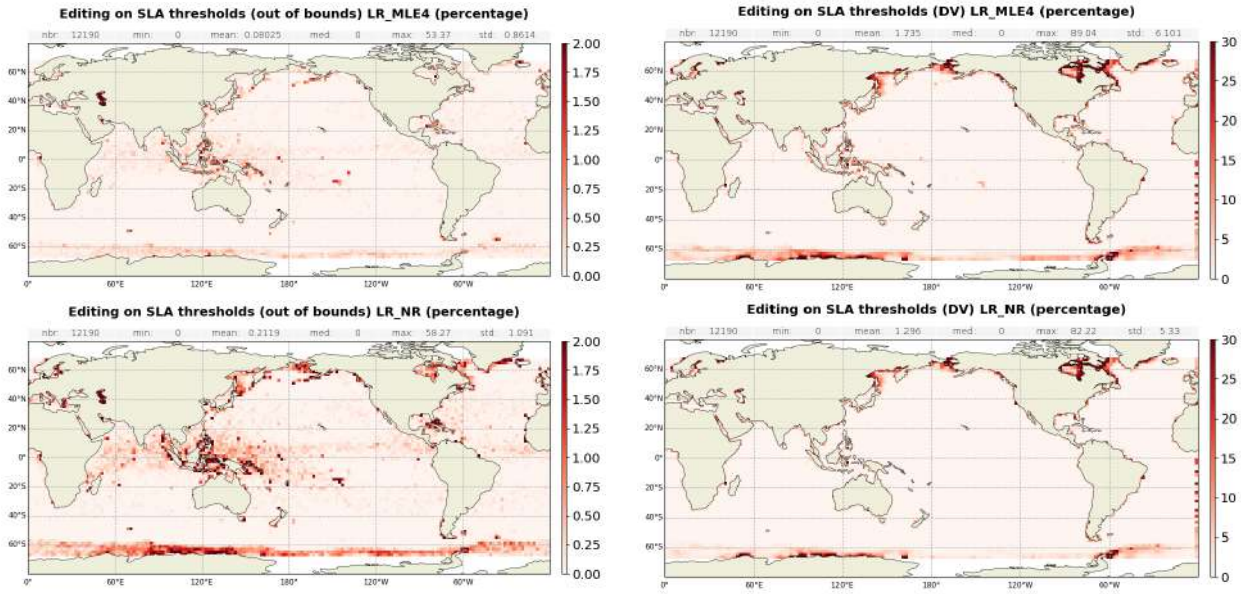

Figure 47: Maps of average percentage of data edited on SLA threshold for both LR MLE4 (top) and LR NR (bottom), for out of bounds (left) and default value (right), computed on year 2023.

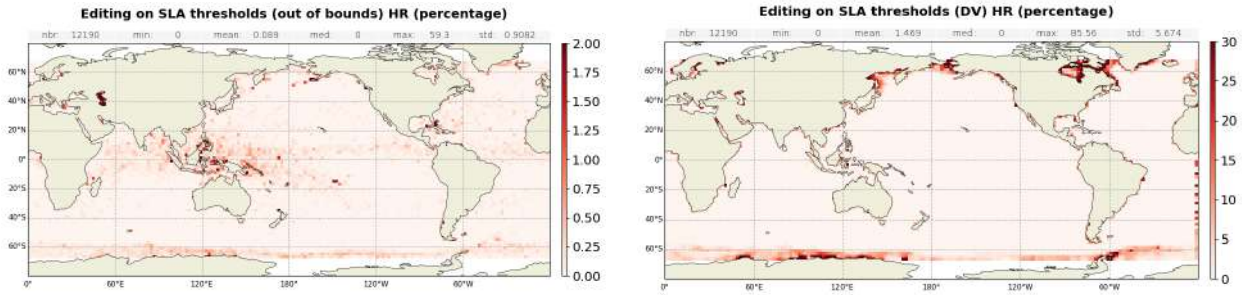

Figure 48: Maps of average percentage of data edited on SLA threshold for HR, for out of bounds (left) and default value (right), computed on year 2023.

4.2.4. Along-track SSHA consistency

Once the thresholds editing is applied, the consistency of the along-track sea surface height anomaly is checked. The statistics of the SSHA by pass are computed, with a selection over open ocean and in areas with low oceanic variability. A pair of thresholds on mean and standard deviation are set as editing criteria. The details are listed in table 7.
No pass has been edited on this criterion over the full mission lifetime.

Parameters	Set 1	Set 2
Selection		
Bathymetry	<-1000m	<-1000m
Coastal distance	>100km	>100km
Oceanic variability	<0.3m	<0.1m
Min number of measurements	3	200
Thresholds		
Mean (absolute value)	0.3m	0.15m
STD	0.4m	0.2m

Table 7: Table of parameters used for the editing on the SSHA pass statistics. These parameters are identical in HR and LR.

5 Monitoring of altimeter and radiometer parameters

Means and standard deviations of Sentinel-6 MF main parameters have both been monitored since the beginning of the mission. The goal of this chapter is to summarize these monitorings, along with Jason-3 daily monitoring for comparison.
Only the main results are included in this chapter.

Please note that from 2022-04-07 onwards, Sentinel-6 MF and Jason-3 are no longer on the same ground track (tandem phase). The analysis of the tandem phase can be found in the PB F08 Calval Assessment report [4]. The tandem phase analysis provided in the 2022 annual report [2] is no longer up to date as it was carried out on PB F06 data.

5.1. 20 Hz range measurements

The monitoring of the number and standard deviation of 20 Hz elementary range measurements used to derive 1 Hz data is presented here. These two parameters are computed during the altimeter ground processing. Before performing a regression to derive the 1 Hz range from 20 Hz data, a MQE (mean quadratic error) criterion is used to select valid 20 Hz measurements. This first step of selection consists in verifying that the 20 Hz waveforms can be approximated by a Brown echo model (Brown, 1977 [8], Thibaut et al. 2002 [9]).
Then, through an iterative regression process, elementary ranges too far from the regression line are discarded until convergence is reached. Thus, monitoring the number of 20 Hz range measurements and the standard deviation computed among them is likely to reveal changes at instrumental level.

5.1.1. 20 Hz range measurements number

Figure 49 presents the average number of 20 Hz elementary range measurements used to derive 1 Hz ranges in Ku and C-band. In Ku-band, more elementary measurements are used in average in LR mode (19.6 for both MLE4 and NR) than in HR (18.5), with LR C-band in between (19.1).
These values are stable over time and are in line with Jason-3 for LR data.

A slight latitude dependency can be seen in Ku-band for LR and HR data (figure 50, top panels and middle right panel), with lower values at high latitude. This is linked to a specific feature of Sentinel-6 MF, which has a latitude dependant PRF value. The behavior is different on Jason-3 (middle left panel), more dependent of sea state conditions. For the C band, values are lower near the coast and at high latitudes. This is expected as C band has a larger footprint than Ku band, and is more sensitive to coastline and ice presence.

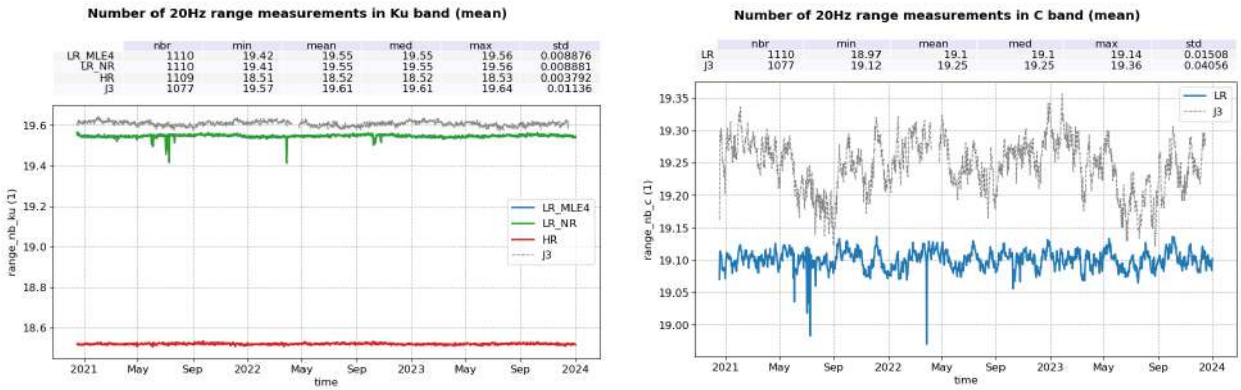

Figure 49: Mean number of 20Hz range measurements for LR MLE4 (blue), LR NR (green) and HR (red) per day, in Ku-band (left) and C-band (right, LR MLE3 only).

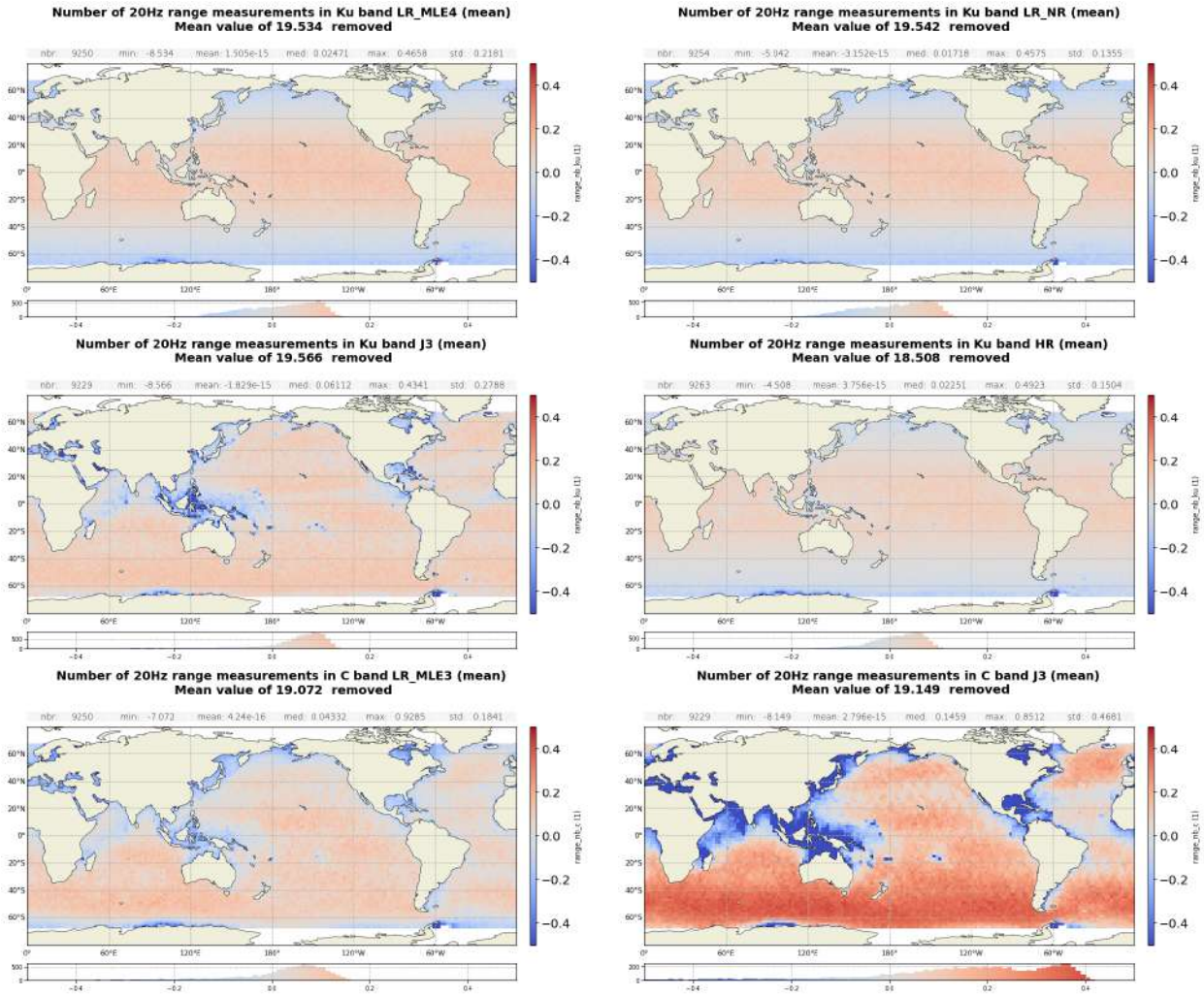

Figure 50: Centred maps of mean number of 20Hz range measurements. Top: maps for Sentinel-6 MF LR Ku-band (left : MLE4, right : NR), middle: maps for Jason-3 Ku-band (left) and Sentinel-6 MF HR (right), bottom : maps for LR C-band (left : Sentinel-6 MF, right : Jason-3). Computed on year 2023.

5.1.2. 20 Hz range measurements standard deviation

Figure 51 presents the standard deviation of the 20 Hz elementary range measurements used to derive 1Hz ranges in Ku and C-band (left and right panels respectively) per day. In Ku-band, Sentinel-6 MF LR range standard deviation is similar between MLE4 and NR, and lower than Jason-3 by 1 cm in average. It shows the improvement brought by Sentinel-6 MF in terms of noise.
Sentinel-6 MF HR range noise is even lower than LR, by 2.7 cm, thanks to the HR processing.

Due to the reduced number of pulses, C-band range standard deviation is the highest (0.26 m).

Standard deviation of measurements is correlated to significant wave height (figure 52), as shown in sections 9.1.2. and 9.1.3..

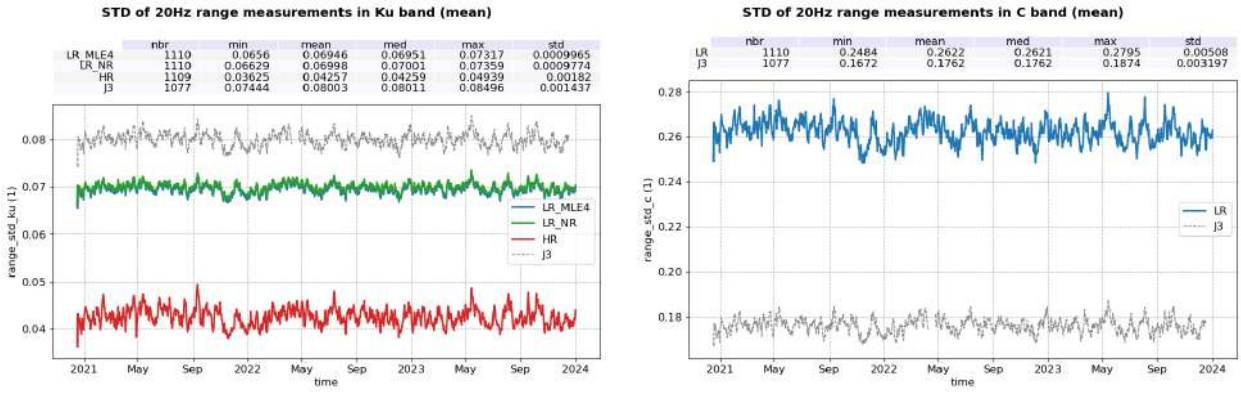

Figure 51: Mean STD of 20Hz range measurements for LR MLE4 (blue), LR NR (green) and HR (red) per day, in Ku-band (left) and C-band (right, LR MLE3 only, in blue).

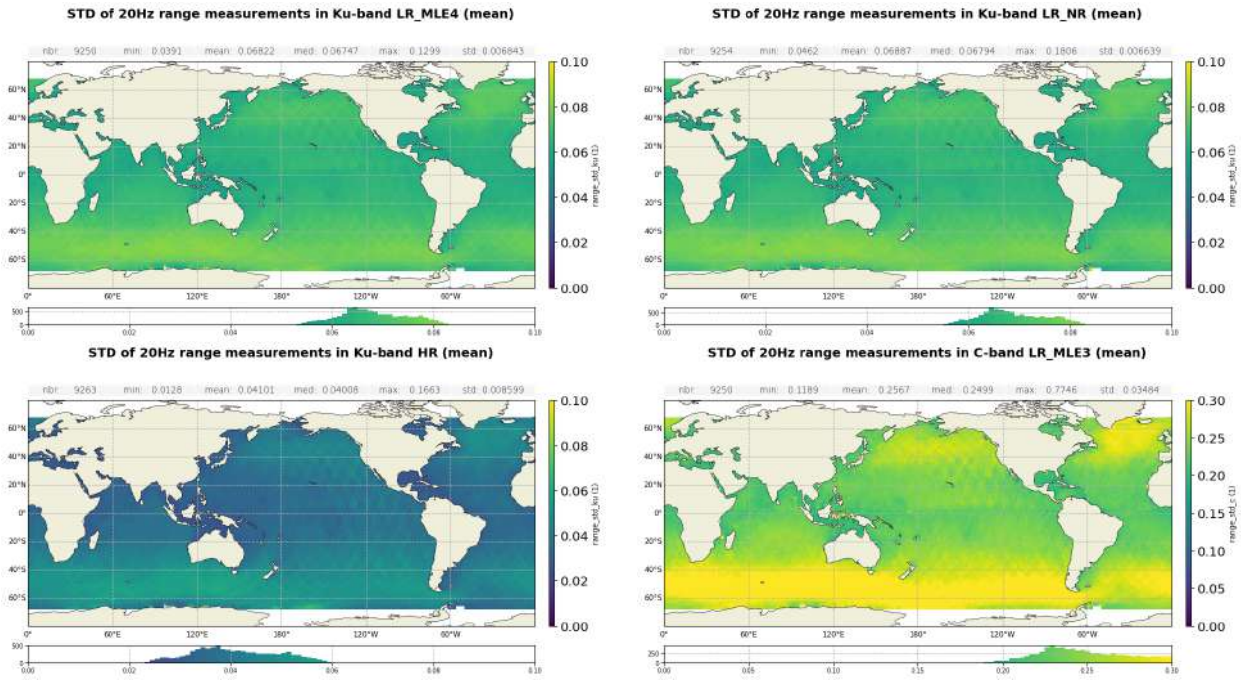

Figure 52: Maps of mean STD of 20Hz range measurements for Ku-band LR MLE4 (top left), LR NR (top right), HR (bottom left) and C-band (bottom right). Computed on year 2023.

5.2. Off nadir angle from waveform

This section analyses the square of the off-nadir angle derived from MLE4 and NR waveform retrackings from LR dataset.

The off-nadir angle is derived from the slope of the trailing edge of the waveform during the altimeter processing: it can either be caused by real platform mispointing or by backscattering properties of the surface. The square of the off-nadir angle, averaged on a daily basis (taking into account valid measurements only), has been plotted for Sentinel-6 MF and Jason-3 on figure 53. Mispointing from NR retracking is reduced from 0.008 deg^2 in MLE4 to 0.004 deg^2.

A jump is visible in both mean and standard deviation on 18/01/2021, which is related to a star-tracker update that resulted in improved pointing performance of the satellite. Spikes are visible in an otherwise stable time series, that correspond to manoeuvres during the commissioning phase.

The corresponding maps for 2023, presented on figure 54, shows higher square off nadir angle in coastal areas and around Indonesia. Figure 55 shows the dependency between the waveform mispointing and the SWH. Mispointing is higher at low SWH (above 0.04 and 0.03 deg^2 at 0 m for NR and MLE4 respectively), however there is no correlation above 2m SWH for either MLE4 and NR.
The standard deviation of the square off nadir angle (right panel) is also much higher at low SWH.
Curves for year 2023 only (solid lines) are aligned with curves for the entire time series (dotted lines).

The mispointing distributions are presented in Figure 56 for Sentinel-6 MF and Jason-3. Sentinal-6 MF distribution are centred around 0.008 and 0.004 deg^2 for MLE4 and NR respectively, while Jason-3's is centred on 0. Curves for year 2023 only (solid lines) are perfectly aligned with curves for the entire time series (dotted lines).

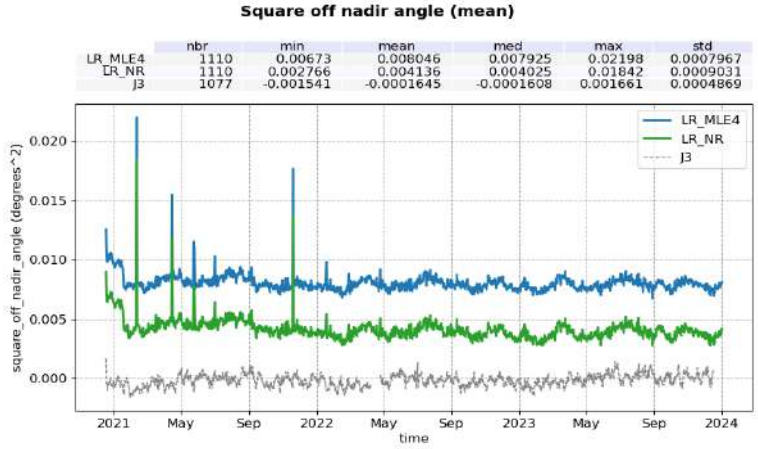

Figure 53: Mean square off nadir angle per day for LR MLE4 (blue) and LR NR (green).

During the CalVal assessment of the PB F08 reprocessing campaign, an anomaly has been detected in the stability of the Numerical Retracker in high mispointing conditions, i.e. mainly during manoeuvres. This anomaly causes differences with MLE4 retracking in mispointing up to about -0.24deg^2, in sigma0 up to 1.5dB and in range and SSHA up to 20 cm (see [4] for more information). Note that during normal operations, NR behaviour is nominal. This anomaly is corrected in PB F09.

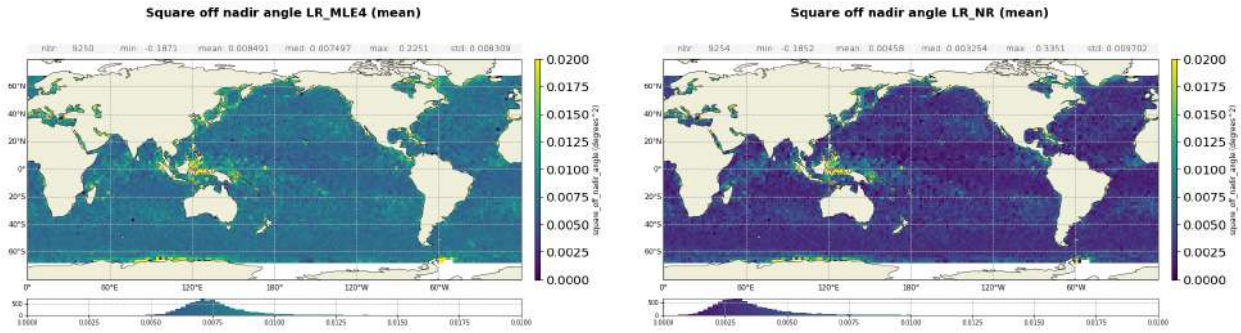

Figure 54: Map of mean square off nadir angle for LR MLE4 (left) and LR NR (right). Computed on year 2023.

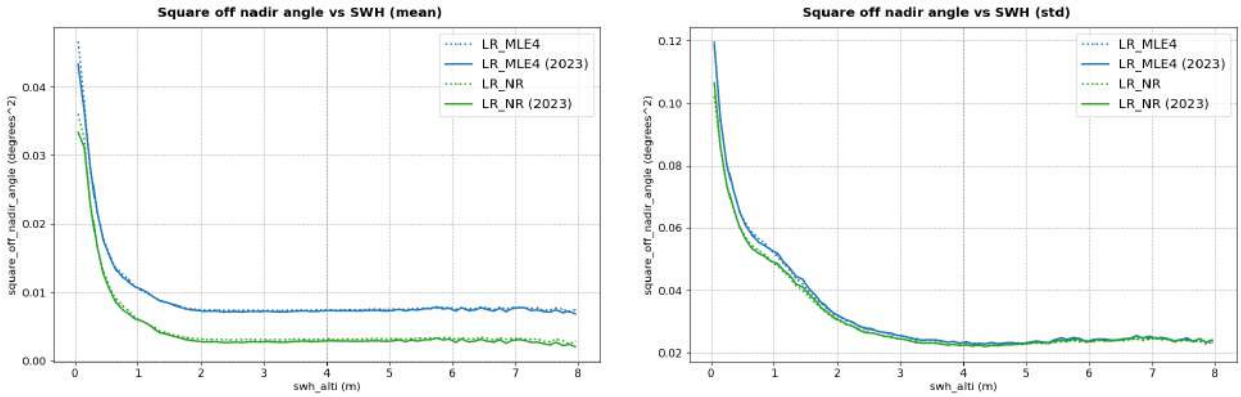

Figure 55: Square off nadir angle wrt SWH for MLE4 (blue) and NR (green). Computed on the entire time series (dotted line) and on 2023 only (solid line).

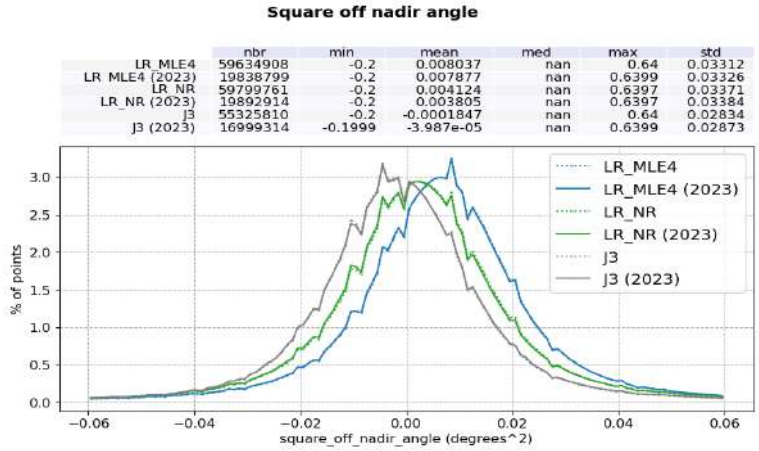

Figure 56: Histogram of square off nadir angle for Sentinel-6 MF MLE4 (blue), NR (green) and Jason-3 (black). Computed on the entire time series (dotted line) and on 2023 only (solid line).

5.3. Range

The mean difference between Sentinel-6 MF HR and LR MLE4 ranges is centred around 1.8 cm (figure 57 in black). Looking at the temporal evolution of this difference (figure 58), a slight negative drift is visible (about 2 mm in 3 years). This drift is caused by the evolution of the PTR shape in the azimuth direction, impacting HR data. The drift resulting from this degradation has been estimated at 3.1 mm/year on POS4-

B (Dinardo 2022 [10]). Please note that this analysis was performed on the 9 first months of side B, from September 2021 to June 2022, and values may be different after then because of an expected on-going stabilization.
The implementation of the range walk correction in the HR processing will correct from the range walk effects and reduce the drift. It has been deployed with the PB F09.
The use of the in flight PTR in the LR numerical retracker (in grey on figures 57 and 58), that accounts for PTR shape degradation, reduces both the bias with HR range (down to 1.2 cm from 1.8 cm) but not the drift in any significant way.

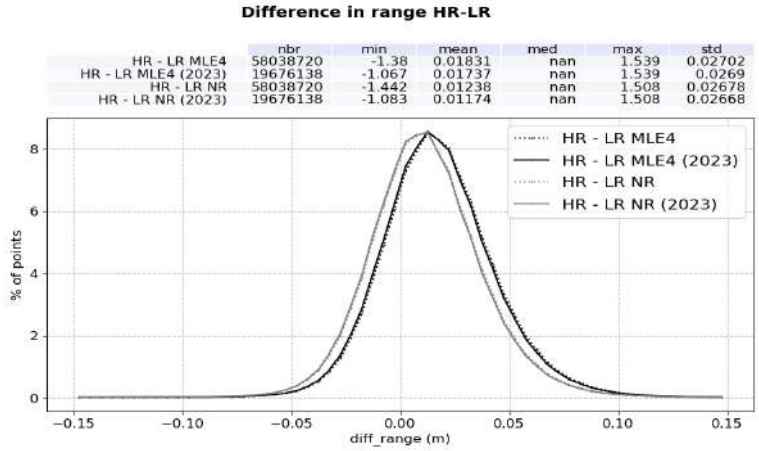

Figure 57: Histogram of HR-LR (MLE4 in black, NR in grey) difference in range. Computed on the entire time series (dotted line) and on 2023 only (solid line).

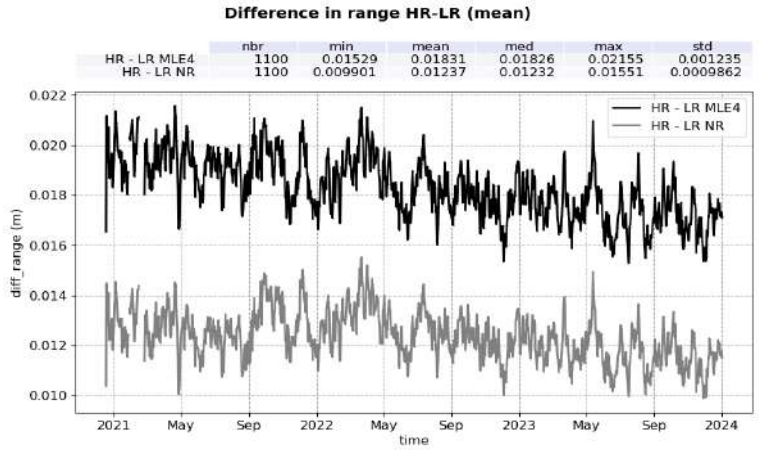

Figure 58: HR - LR (MLE4 in black, NR in grey) difference in range per day.

The biases between HR and LR ranges are strongly correlated to SWH, as shown in figure 59. With LR MLE4, the range bias increases by 3.8 cm between 2 and 7-m wave, while it is reduced to 3.3 cm with LR NR. This correlation is mostly explained by the impact of the different value of wave skewness coefficient used in the LR retrackings (skewness -0.1) and in the HR SAMOSA retracking side (skewness 0.0).

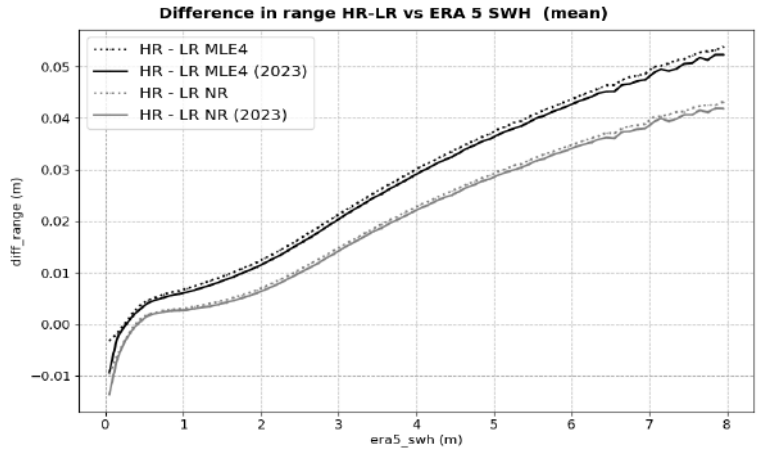

Figure 59: HR - LR (MLE4 in black, NR in grey) range difference as a function of ERA5 model SWH.

Along track wind has a known impact on HR data and more particularly on HR range [6]. To highlight this impact, two gridded maps of HR versus LR MLE4 range differences are drawn, one for ascending tracks and the other one for descending tracks. Next, the difference between these two maps is computed (ascending minus descending). Such process allows to remove all systematic error on the bias (such as waves) and to only highlight HR variations with respect to LR MLE4 that depend on track orientation. Figure 60 bottom left panel clearly shows an anti-correlation to meridional wind patterns (bottom right), ranging between -1 and 1 cm.

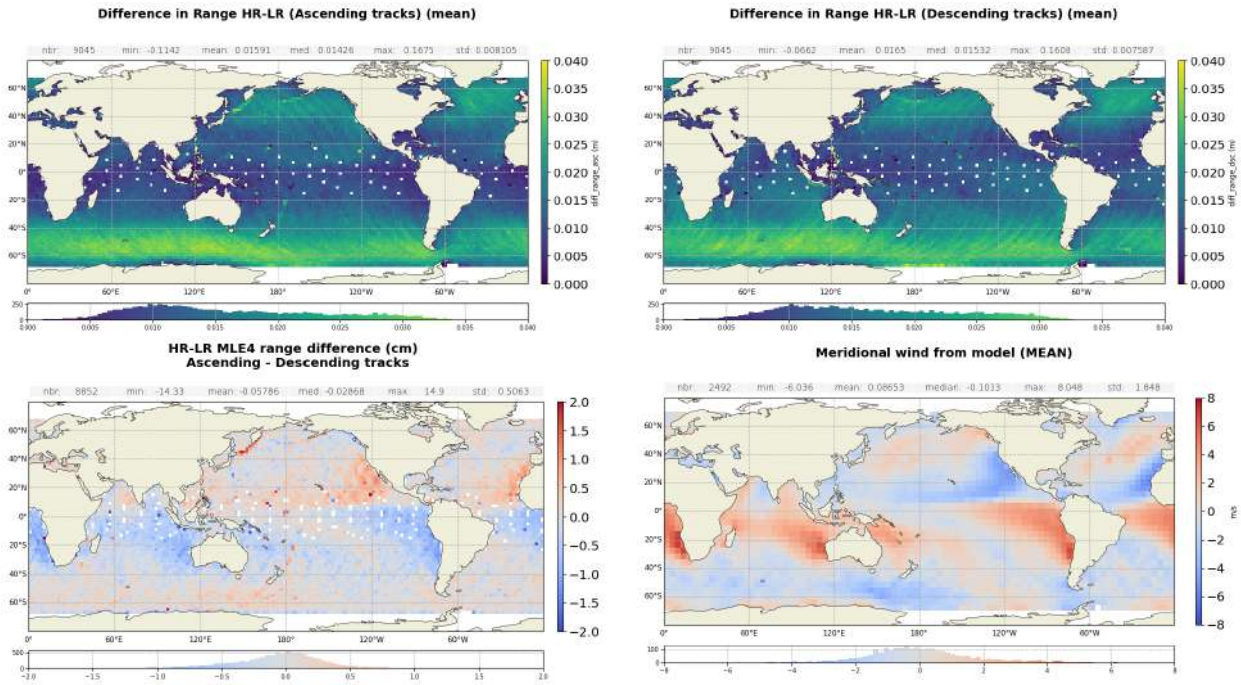

Figure 60: Maps of HR-LR MLE4 difference in range, for ascending tracks (top left) and descending tracks (top right). Bottom left: difference of the two maps above. Bottom right : along-track wind from model. Computed on year 2023.

The daily monitoring of LR reprocessed NR - MLE4 range difference is presented on figure 61. A -1 mm jump on the mean (left panel) is visible at the side B switch on 2021-09-14. Cadier et al. 2024 (under review, [5]) has shown that this jump is the result of a -1 mm jump on LR MLE4 and a -2 mm jump on LR NR. The origin to this jump is still under investigation. For MLE4, the main hypothesis is the instrumental LUT applied on MLE4 range, which is for the moment identical for both POS4-A and POS4-B. Note that the time series is still too short to quantify the impact of the NR on the long term stability with respect to MLE4. The standard deviation monitoring (right panel) presents a yearly variation with higher values from June to September and lower values from December to May, and can be linked with seasonal SWH variations (cf below).
The NR - MLE4 range distributions are presented on figure 62 for side A (left panel) and side B (right panel). Ranges are consistent between both retrackings, with only a 6.7 mm bias on side A and 5.7 mm on side B.

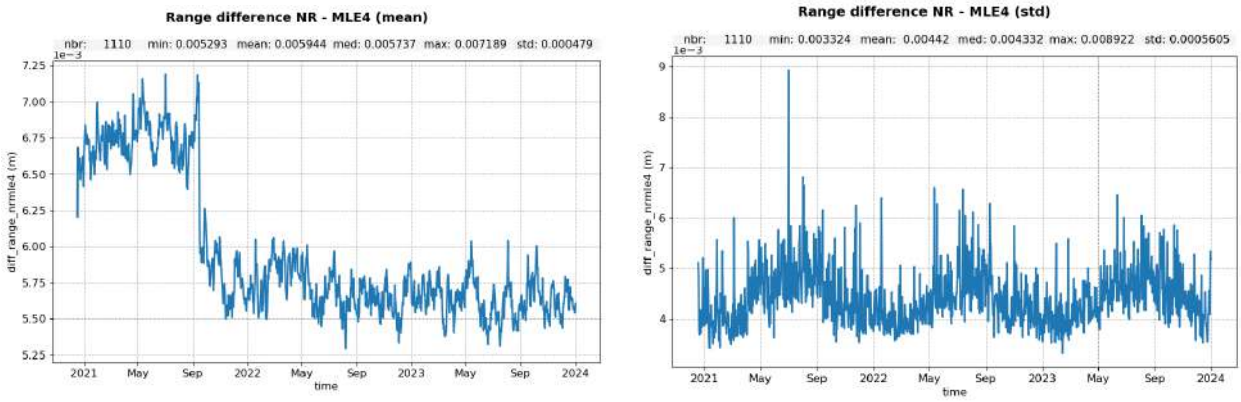

*Figure 61: Time monitoring of Sentinel-6 MF NR - MLE4 range difference per day, for the mean (**left**) and the standard deviation (**right**).*

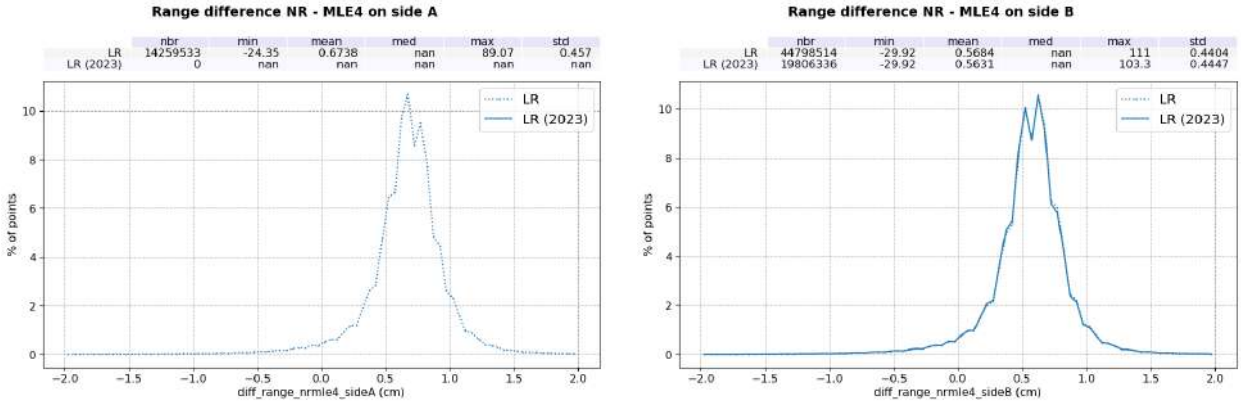

*Figure 62: Distributions of Sentinel-6 MF NR - MLE4 range difference for side A (**left**) and side B (**right**). Computed over the entire periods (dotted lines) and 2023 only (solid line on right panel).*

On figure 63 is presented the map of the F08 NR - MLE4 range difference (left panel) and its dependency to ERA 5 model SWH (right panel). The differences are correlated to SWH, with about +7.5mm increase between 0.5 and 7m SWH. This bias increase is caused by a non-optimal calibration of the MLE4 LUT.

5.4. Significant wave height

The geographical distribution of SWH over 2023 is presented on figure 64 for Ku-band LR and HR and for

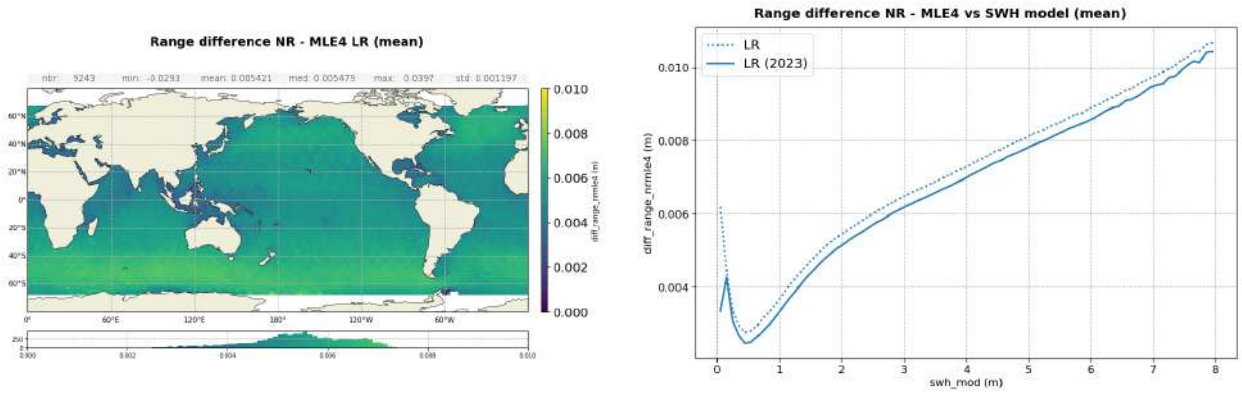

*Figure 63: Map (**left**) and ERA 5 model SWH dependency (**right**) of the LR NR - MLE4 range difference.*

C-band LR. All SWH averaged over 2023 share similar geographical patterns.

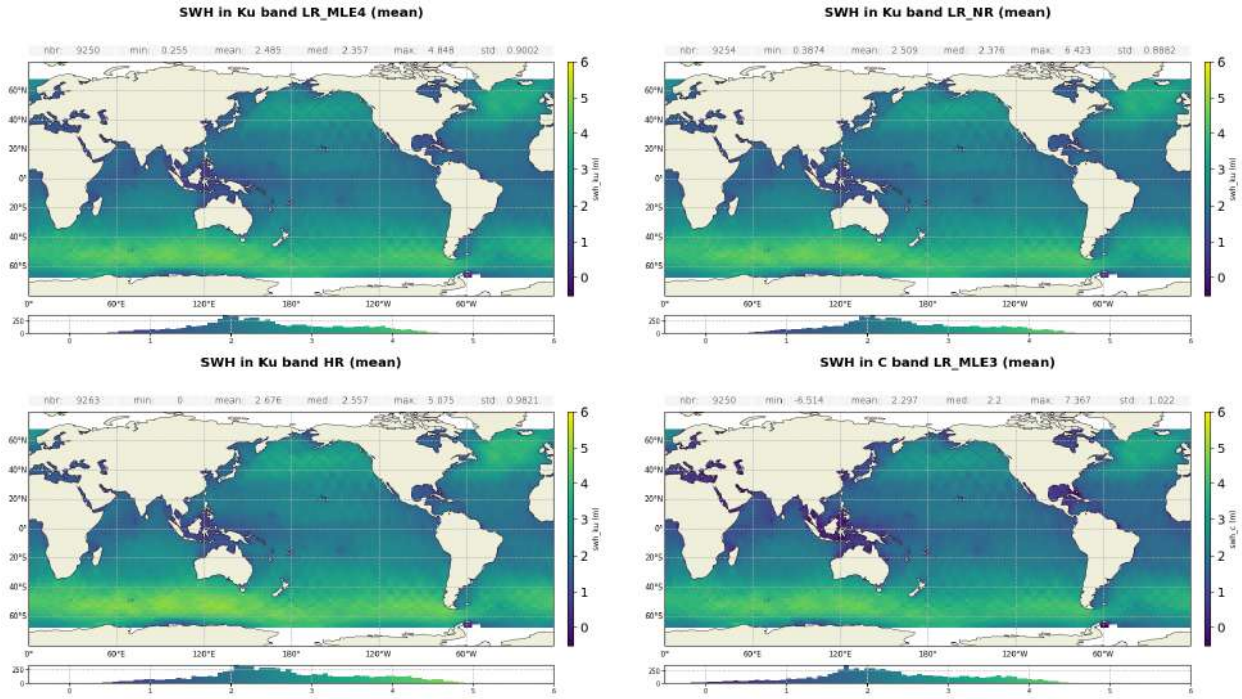

Figure 64: Maps of mean SWH for Ku band LR MLE4 (top left), LR NR (top right), HR (bottom left) and C-band (bottom). Computed on year 2023.

Ku-band SWH are centred around 2.68 m for Sentinel-6 MF LR MLE4, 2.70 m for LR NR and 2.88 m for HR. In C-band, the average SWH is of 2.51 m for Sentinel-6 MF and 2.70 m for Jason-3, due to LUT differences. These values are stable over time, as shown on figure 65.

Sentinel-6 MF LR SWH are in line with Jason-3, also centred around 2.68 m. Sentinel-6 MF and Jason-3 SWH histograms are aligned, except at very low wave heights, where Sentinel-6 MF performs better, due to its improved handling of low wave heights in the Level 2 processing.

Please note that before 2023-10-05, an anomaly (AR 2620) impacted the handling of small waves in LR NR (cf section 3.4.). It has been corrected in the patched version of PB F08 (PDAP v3.8.0).

The impact of NR SWH anomaly is also visible in figure 66, which presents the NR - MLE4 SWH difference monitoring (left panel) dependency to ERA5 model SWH (right panel) and maps before and after the patch.

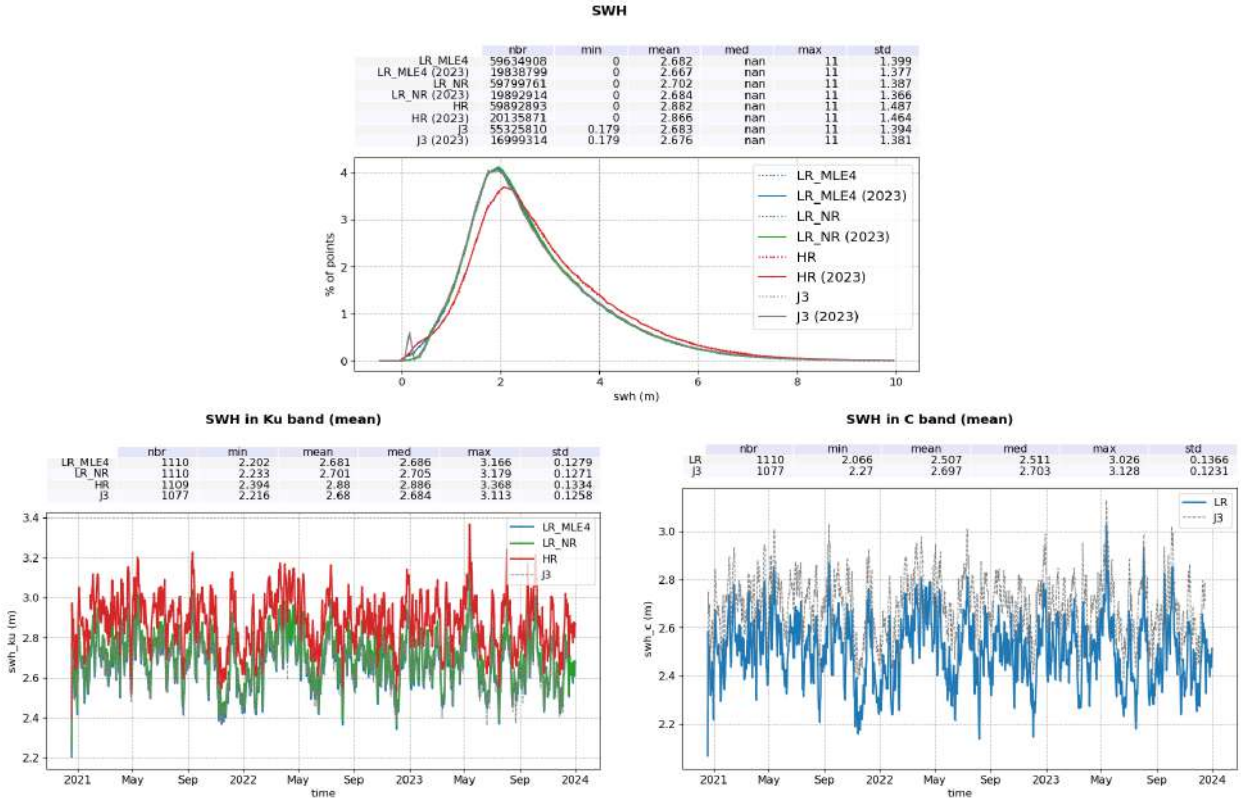

Figure 65: Top : Histogram of Ku-band SWH for Sentinel-6 MF LR MLE4 (blue), LR NR (green), HR (red) and Jason-3 (black). Computed on the entire time series (dotted line) and on 2023 only (solid line). Bottom: daily monitoring of SWH mean in Ku-band (left) and C-band (right).

On the daily monitoring, a -1 cm jump is visible at the date of the patch, the difference being reduced to about 1.3 cm after the patch. Before the patch, the bias is very significant (upwards of 25 cm) in low SWH areas, while no significant geographical distribution or SWH correlation can be seen after the patch. At higher SWH, a residual bias of about 2 cm remains, still under investigation.

Sentinel-6 MF HR SWH is not in line with Sentinel-6 MF LR and Jason-3 due to the impact of ocean vertical velocity on HR data [12]. The average HR-LR MLE4 SWH difference is centred around 22.6 cm (figure 67 left panel). This bias is stable over time but strongly depends on SWH values (figure 67 right panel). It ranges from 10 to 40 cm between 1 and 7m SWH.

Note that a correction for the ocean vertical velocity is deployed on the new HR Numerical Retracking with the PB F09.

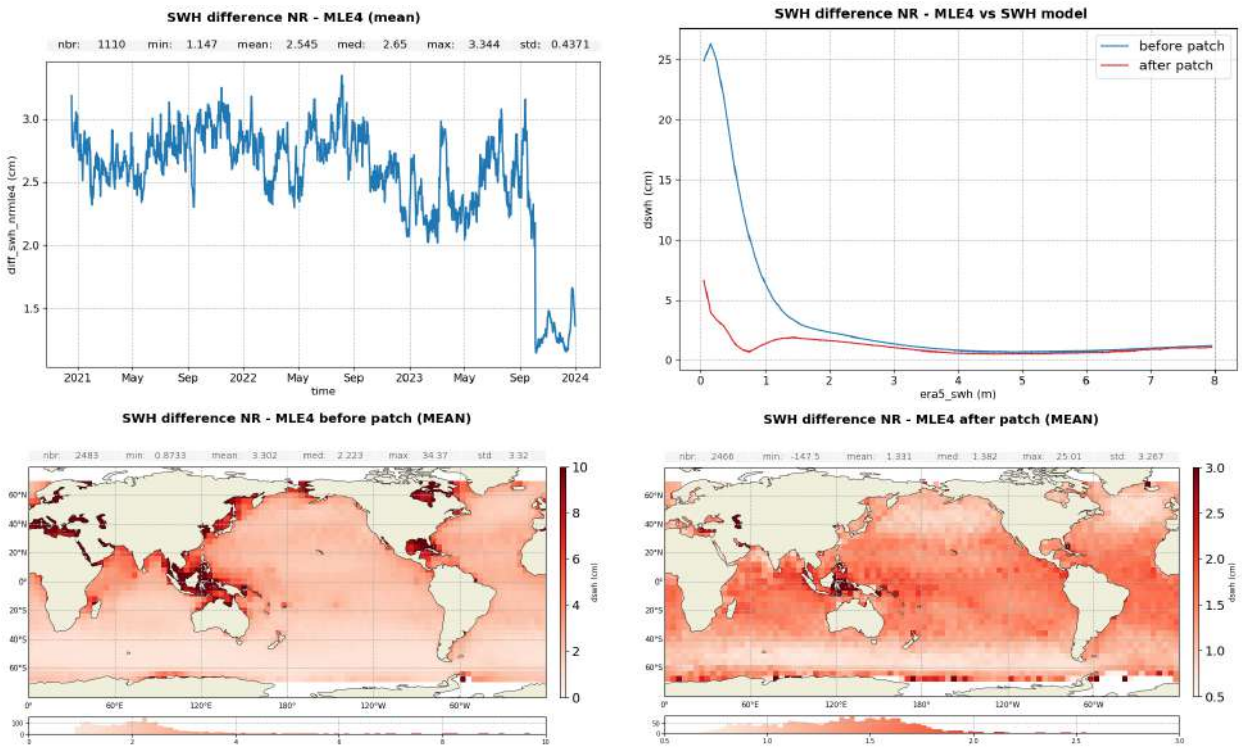

Figure 66: Top left : monitoring of the LR NR - MLE4 SWH difference in m per day. Top right : Mean differences as a function of ERA 5 model SWH computed on 2023 before (blue) and after the patch. Bottom : Maps of the difference computed on 2023 before (left) and after (right) the patch

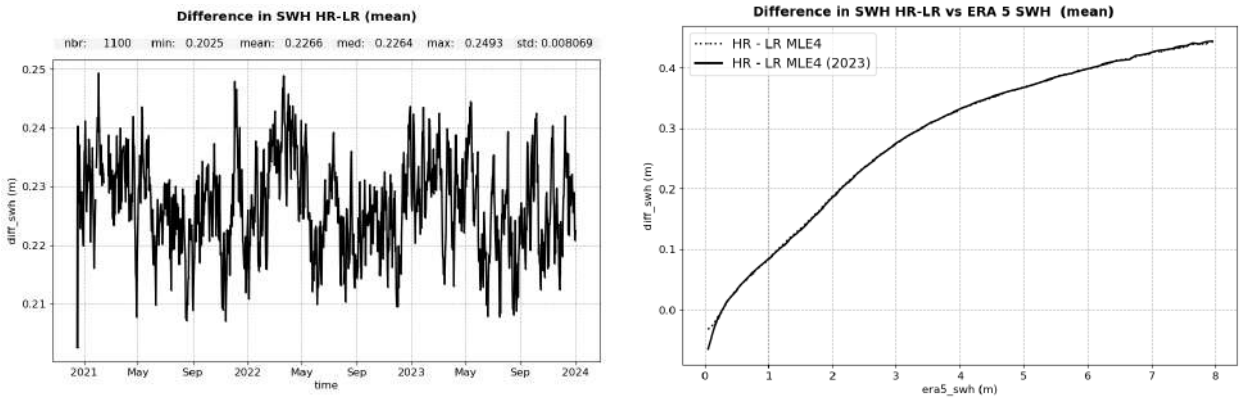

Figure 67: HR-LR MLE4 difference for Ku-band SWH. Left: mean per day. Right: difference with respect to ERA5 SWH, computed on the entire time series (dotted line) and on 2023 only (solid line).

5.5. Backscatter coefficient

The monitoring of the backscatter coefficient (sigma0) per day is presented on figure 68 along with the corresponding distribution (for Sentinel-6 MF Ku-band side B only and Jason-3 on the same time period). Ku-band Sentinel-6 MF LR sigma0 is centred around 12.3 dB and 13.2 dB for MLE4 and NR respectively, Sentinel-6 MF HR is centred around 18.1dB and Jason-3 around 13.7dB. With the PB F09 deployed in February 2024, various anomaly correction will better align sigm0 between Sentinel-6 MF and Jason-3 (+0.9 dB in LR and -6.1 dB in HR).
No jump or drift is visible in the data.

In C-band, Sentinel-6 MF sigma0 is centred around 12.3dB and Jason-3's around 13.6dB, due to processing differences. No jump or drift is visible in the data.

The geographical distributions of the Ku-band HR, Ku band LR (MLE4 and NR) and C-band sigma0 are presented on figure 69. No significant difference in geographical patterns is visible.

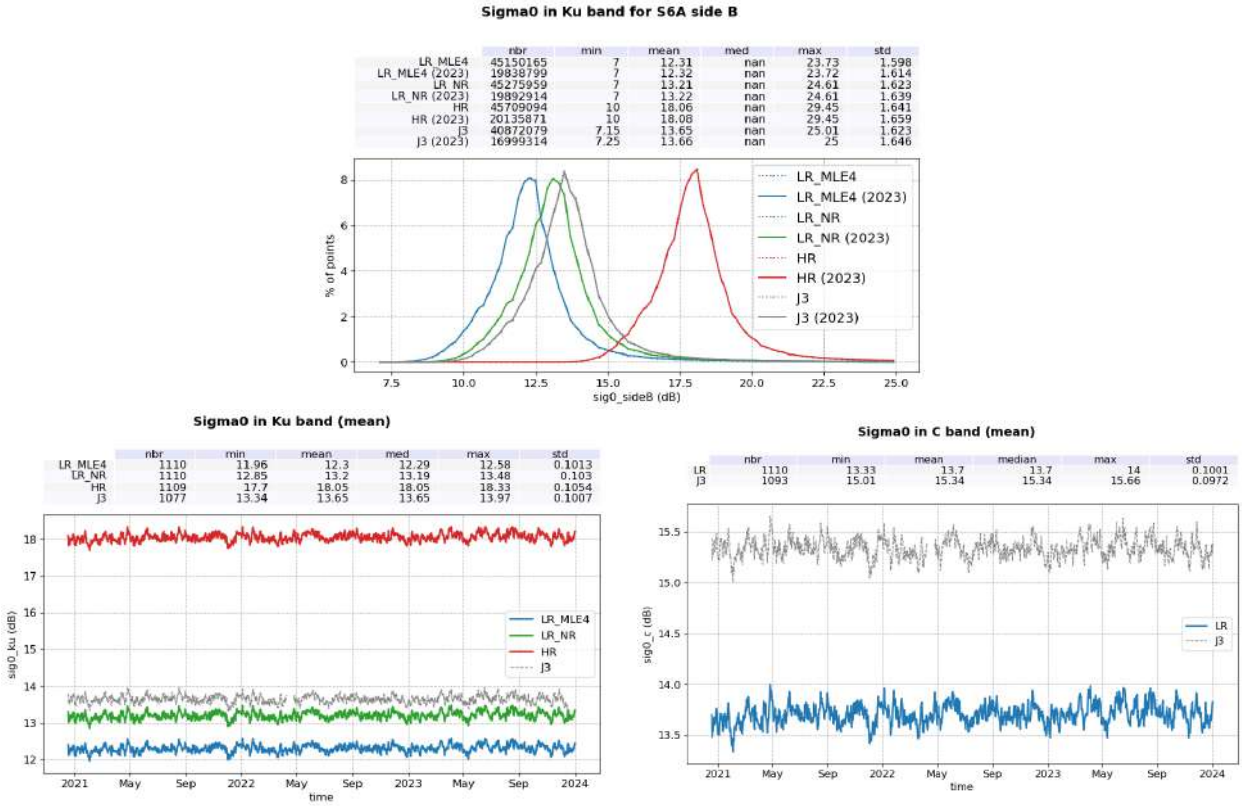

Figure 68: Top : Histogram of Ku-band Sigma0 for Sentinel-6 MF LR MLE4 (blue), LR NR (green), Sentinel-6 MF HR (red) and Jason-3 (black), computed on POS4-B entire time period (dotted line) and on 2023 only (solid line). Bottom: daily monitoring of Sigma0 mean in Ku-band (left) and C-band (right).

Figure 70 presents the sigma0 differences between reprocessed NR and MLE4. On the time series, a drift of very small amplitude can be observed from the beginning of side B to early 2023 (+0.003dB). This drift is under investigation.
In the corresponding map (right panel), the sigma0 difference is slightly correlated with high Mean Sea Surface (MSS) gradients, which corresponds to sudden changes in bathymetry. This indicates that both retrackers have different sensitivities to sea surface slopes, however the exact explanation is not yet understood. Additionally, the bias on the Caspian Sea is significantly lower than on ocean.

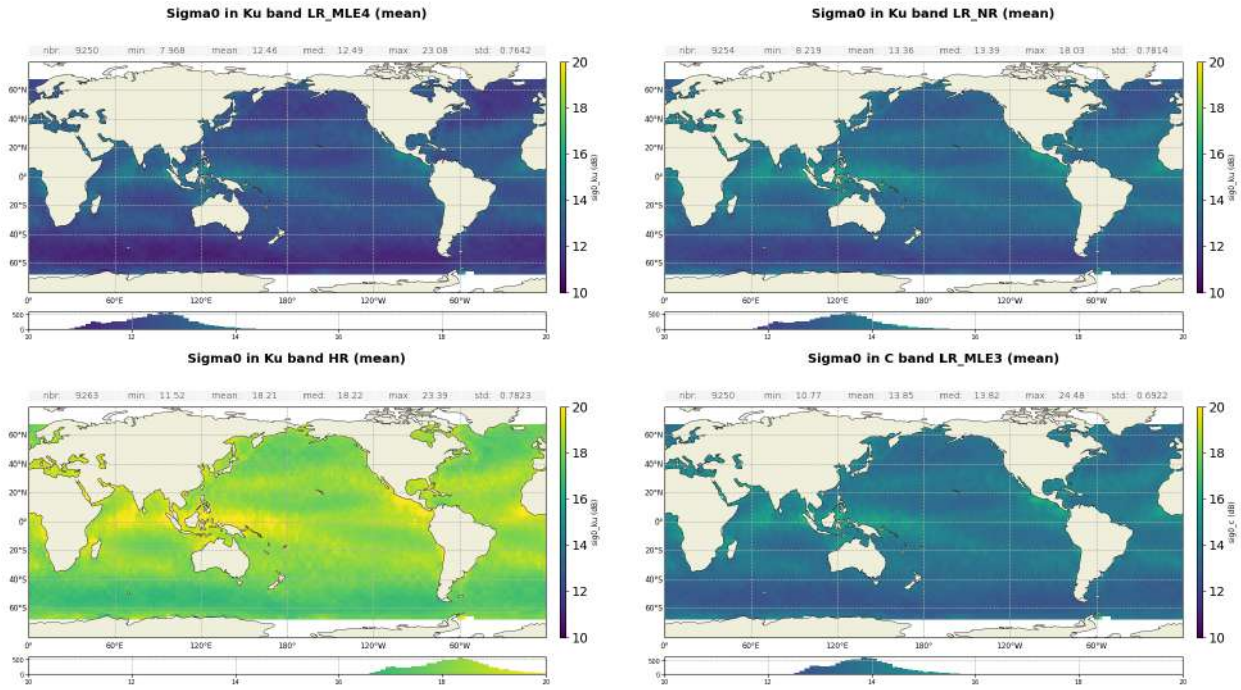

Figure 69: Maps of mean sigma0 for Ku-band LR MLE4 (top left), LR NR (top right), HR (bottom left) and C band (bottom right). Computed on year 2023.

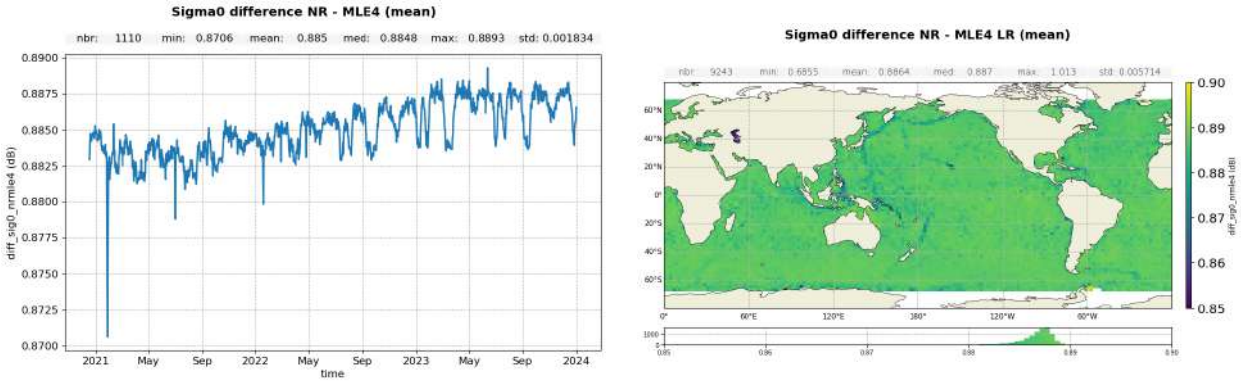

*Figure 70: Map (**right**) and monitoring (**left**) of the LR NR - MLE4 sigma0 difference per day.*

Figure 71, left panel, presents the HR-LR MLE4 sigma0 difference, which is centred around 5.69dB. At the very beginning of the time series, before a jump during cycle 7, the HR-LR MLE4 difference is about 0.02dB lower. This change can be traced back to a star-track patch on 18/01/2021 that improved the nadir satellite pointing. This impacted HR and LR sigma0 differently as in HR, SAMOSA retracking does not estimate the mispointing from the waveform, as opposed to LR with MLE4 retracking.

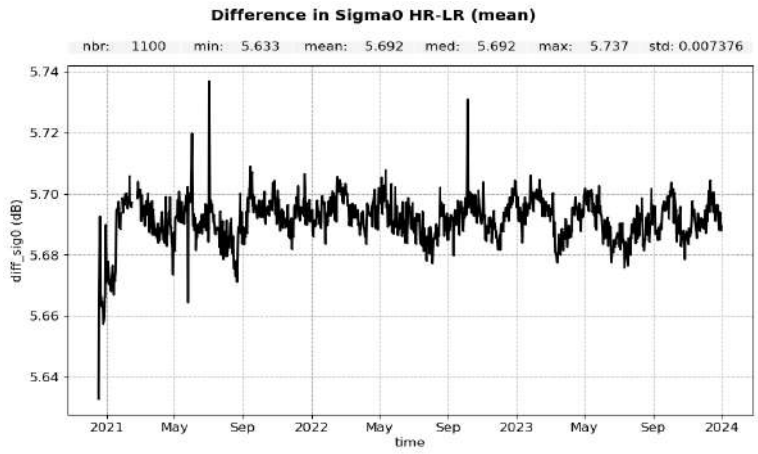

Figure 71: Daily mean of the HR-LR MLE4 sigma0 difference.

5.6. Wind speed

For Sentinel-6 MF wind speed computation, the same algorithm as for Jason-3 GDR-F is applied (Collard, 2005 [18]). The geographical distribution of altimeter wind speed over 2023 is presented on figure 64 for Sentinel-6 MF LR and HR, and Jason-3. All wind speeds averaged over 2023 share similar geographical patterns.

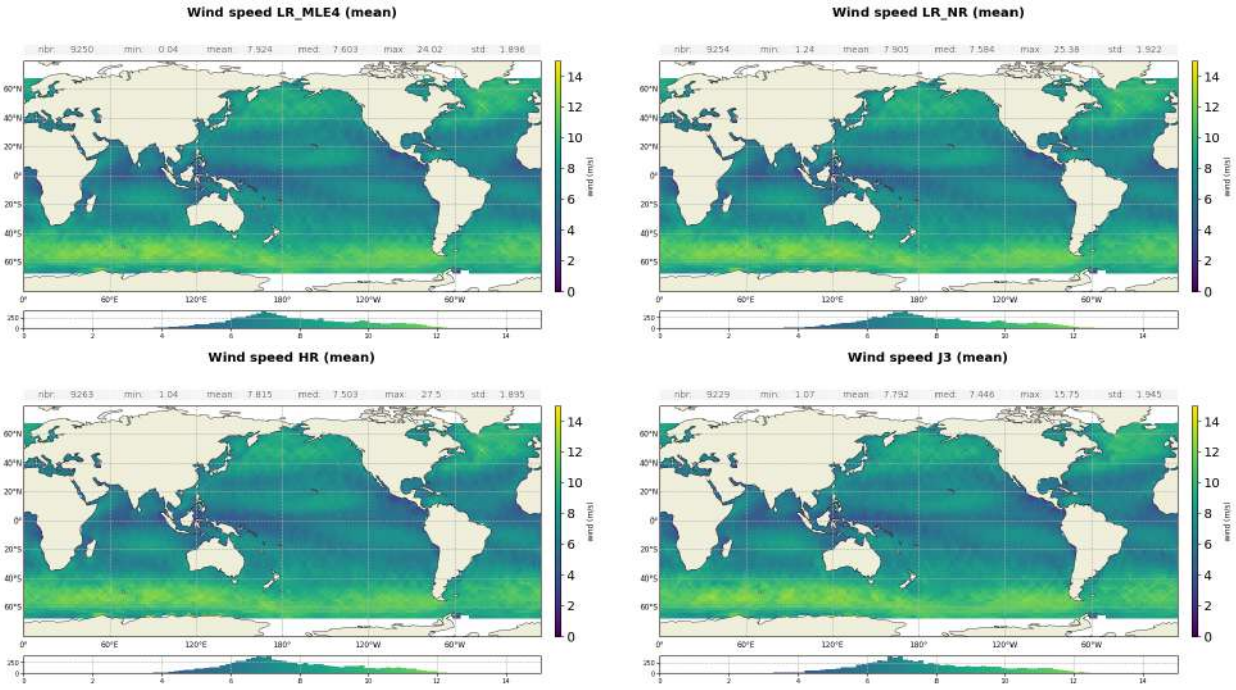

Figure 72: Maps of mean wind speed for LR MLE4 (top left), LR NR (top right), HR (bottom left) and Jason-3 (bottom right). Computed on year 2023.

The monitoring of the wind speed per day is presented on figure 73 and the corresponding distribution on figure 74. Wind speed is of the same order between LR MLE4, LR NR and HR, as well as Jason-3, and centred around 8.3 m/s, 8.3 m/s, 8.1 m/s and 8.1 m/s respectively. Variations are similar between all four datasets with no drift or jump.
In the monitoring of the standard deviation, a yearly cycle is visible, due to seasonal evolution of the wind speed : higher standard deviation during northern hemisphere summer (about 3.8m/s) than during the northern hemisphere winter (about 3.6m/s).

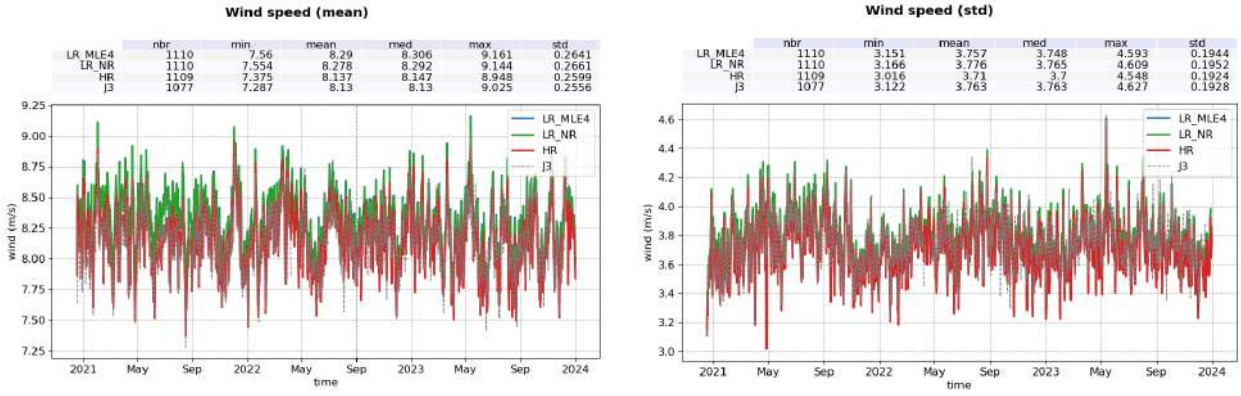

Figure 73: Mean (left) and standard deviation (right) wind speed per day for LR MLE4 (blue), LR NR (green), HR (red) and Jason-3 (black).

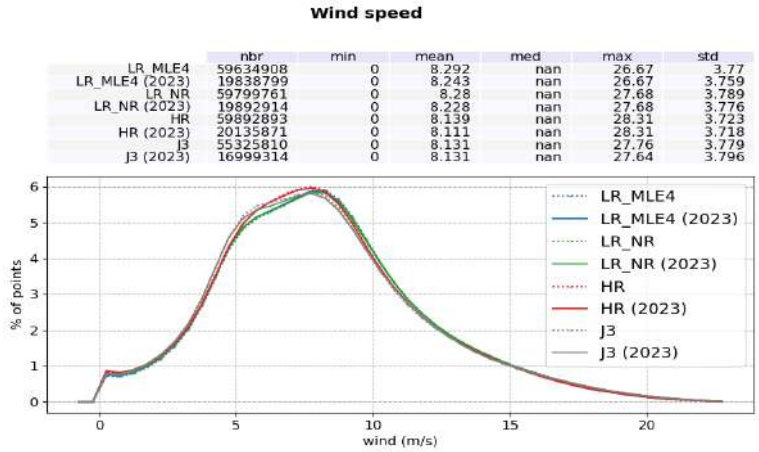

Figure 74: Histogram of wind speed for Sentinel-6 MF LR MLE4 (blue), LR NR (green), HR (red) and Jason-3 (black). Computed on the entire time series (dotted line) and on 2023 only (solid line).

Figure 75 presents the wind speed differences between reprocessed NR and MLE4. On the time series, as for the sigma0, a drift of very small amplitude can be observed from the beginning of the side B to the beginning of 2023 (-1 cm/s). This drift is under investigation.
Unsurprisingly, the corresponding map (right panel) presents similar features to the NR - MLE4 sigma0 differences map presented on figure 70, with a correlation with high Mean Sea Surface (MSS) gradients and a different bias on the Caspian Sea.
The differences are correlated to the SWH (bottom panel), with a +1.5 cm/s increase between 1 and 8 m-SWH in 2023.

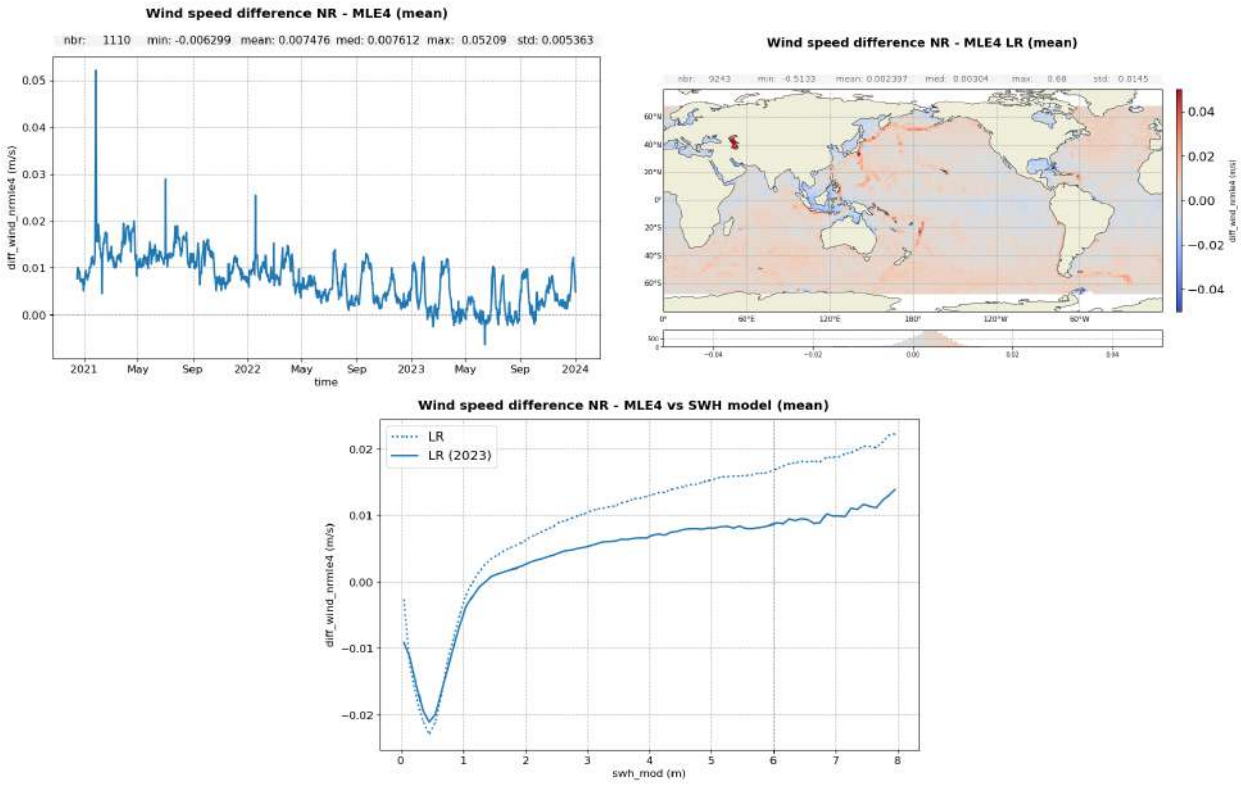

*Figure 75: Map (**right**) and monitoring (**left**) of the LR NR - MLE4 wind speed difference in m/s per day. **Bottom** : Mean differences as a function of ERA 5 model SWH.*

The monitoring of the HR-LR MLE4 wind speed difference is presented on figure 76. A first jump is visible in the beginning of the time series on 18/01/2021 that corresponds to a star-tracker update that improved the satellite pointing. This impacted HR and LR MLE4 wind speed differently through the sigma0 (cf section 5.5.) as in HR, SAMOSA retracking does not estimate the mispointing from the waveform, as opposed to LR with MLE4 retracking. The second jump (about +10 cm/s) happens at the side B switch on 2021-09-14. Indeed, if calibration biases on the sigma0 are different between sides A and B since the PB F08, they are not properly adjusted. Refined calibration biases have been proposed in the PB F08 reprocessing calval assessment report ([4]). On side B, difference is centred around -0.05 m/s and stable in time, with a seasonal variability (the variability is higher in summer and lower in winter).

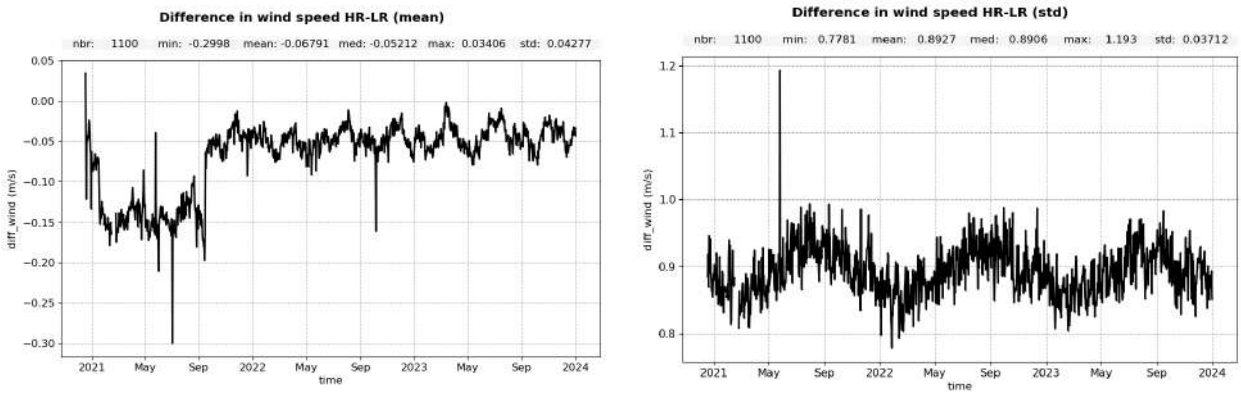

Figure 76: Mean (left) and standard deviation (right) HR-LR MLE4 wind speed difference per day.

The monitoring of the difference between the altimeter-derived wind speed and the model is plotted on figure 77. The mean difference per day is higher for Sentinel-6 MF (33.0 cm/s, 34.3 cm/s and 26.1 cm/s for LR MLE4, LR NR and HR respectively) than for Jason-3 (20.9 cm/s). From the beginning of Sentinel-6 MF to the side B switch (mid September 2021), LR MLE4 and LR NR differences with respect to the model are significantly higher than for Jason-3, indicating that the calibration biases applied on LR sigma0 for POS4-A are not perfectly calibrated. All curves are much more in line on side B.
The monitoring of the standard deviation yields close values in average (1.46 m/s for Sentinel-6 MF LR MLE4, 1.47 for LR NR, 1.39 m/s for Sentinel-6 MF HR and 1.41 m/s for Jason-3), but yearly oscillations in the Sentinel-6 MF data have a significantly higher amplitude (about 30 cm/s) than Jason-3 (about 15 cm/s). These differences in behavior between Sentinel-6 MF and Jason-3 are under investigation.

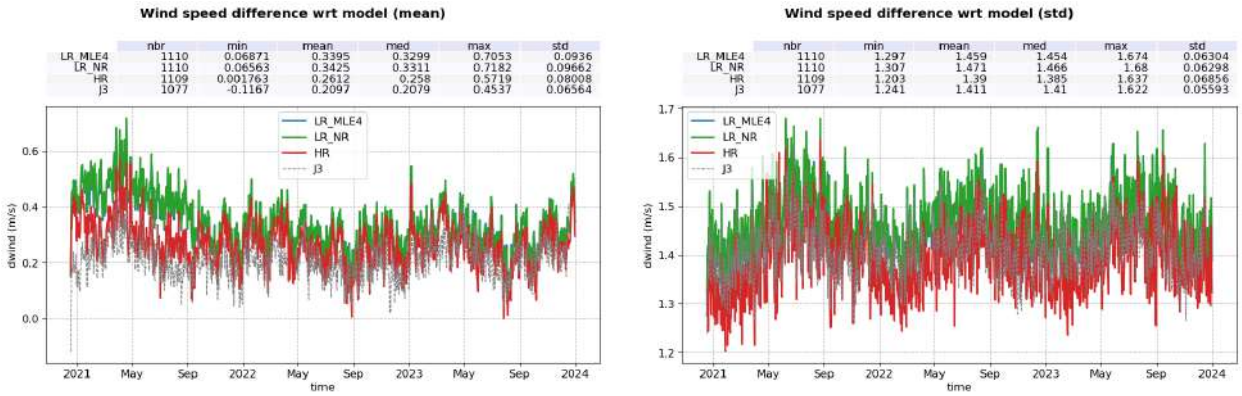

Figure 77: Mean (left) and standard deviation (right) wind speed difference wrt model per day for LR MLE4 (blue), LR NR (green), HR (red) and Jason-3 (grey).

5.7. Sea state bias

Sentinel-6 MF sea state biases (SSB) are computed using Jason-3 GDR-F SSB parameterizations.

Maps of Ku-band SSB averaged over the year 2023 show the same geographical patterns between Jason-3 and Sentinel-6 MF LR MLE4, LR NR and HR (figure 78).

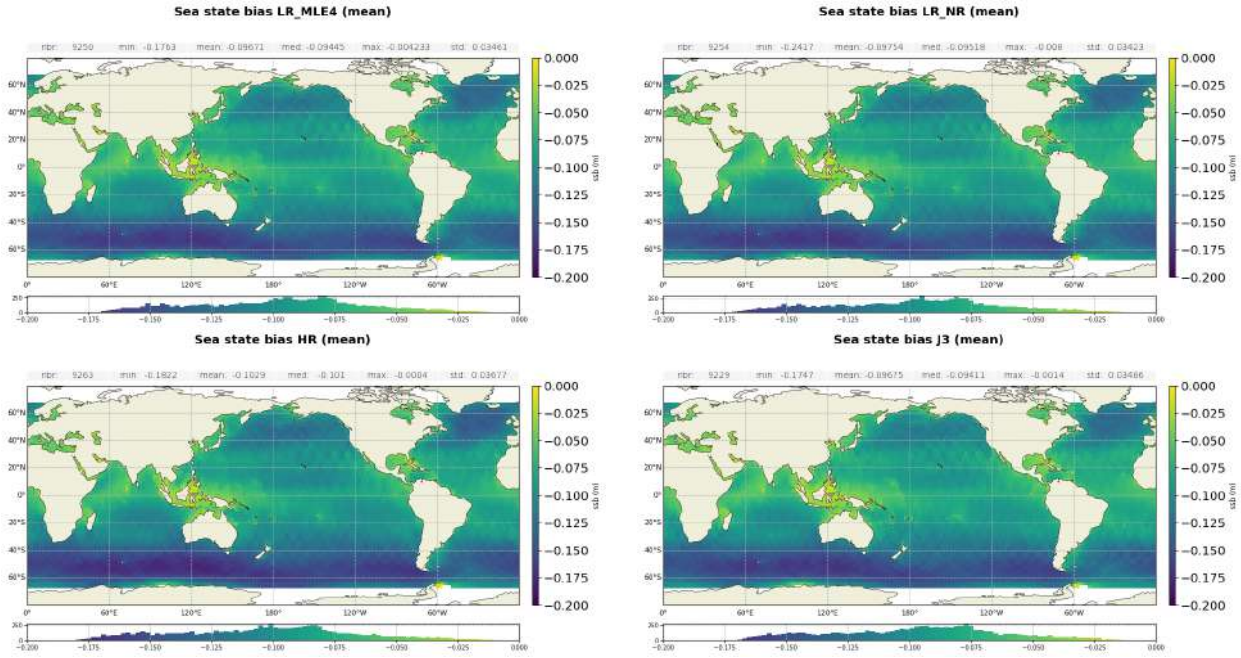

Figure 78: Maps of mean SSB for LR MLE4 (top left), LR NR (top right), HR (bottom left) and Jason-3 (bottom right). Computed on year 2023.

Ku-band SSB are centred around -10.4 cm for Sentinel-6 MF LR MLE4, -10.5 cm for LR NR and -11.1 cm for Sentinel-6 MF HR. Sentinel-6 MF LR SSB is very good agreement with Jason-3, also centred around -10.4 cm.
In C-band, the average SSB is of -9.5 cm for Sentinel-6 MF and Jason-3. These values are stable over time, as shown on figure 79.

Figure 80 presents the SSB differences between NR and MLE4. A jump of about +0.4 mm is visible on the date of the PDAP v3.8.0 patch (2023/10/05, see section 3.4.) that impacted NR data. A significant SWH correlation is visible on the corresponding map (right panel) and in the mean difference as a function of ERA 5 model SWH (bottom panel), with an about +4 mm increase between 0.5 an 8 m-SWH in 2023.

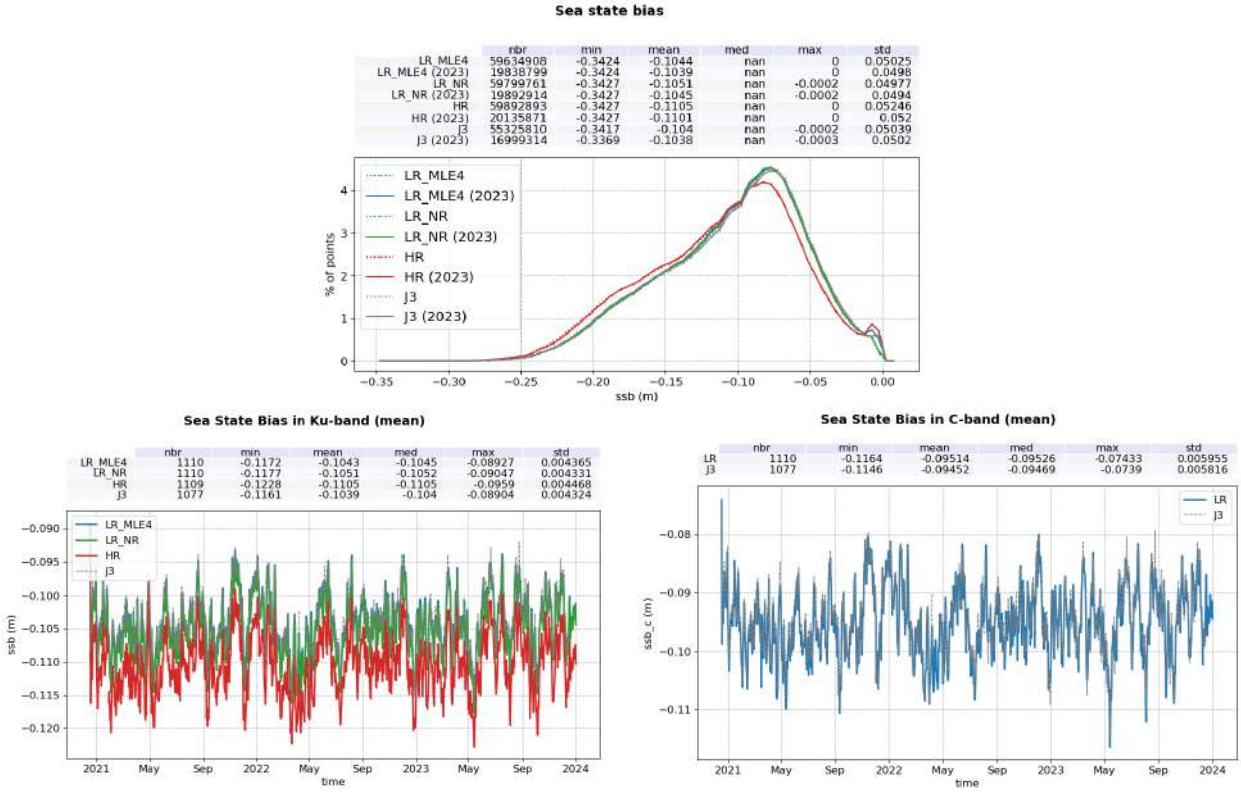

Figure 79: Top : Histogram of Ku-band SSB for Sentinel-6 MF LR MLE4 (blue), LR NR (green), HR (red) and Jason-3 (black), Computed on the entire time series (dotted line) and on 2023 only (solid line). Bottom: daily monitoring of SSB mean in Ku-band (left) and C-band (right).

The monitoring of the HR-LR MLE4 SSB difference is presented on figure 81. The difference is centred around -0.72 cm in average and 0.58 cm in standard deviation with yearly oscillations in both cases, as observed on the wind speed (figure 76, right panel). This seasonal variability is induced by the SWH.

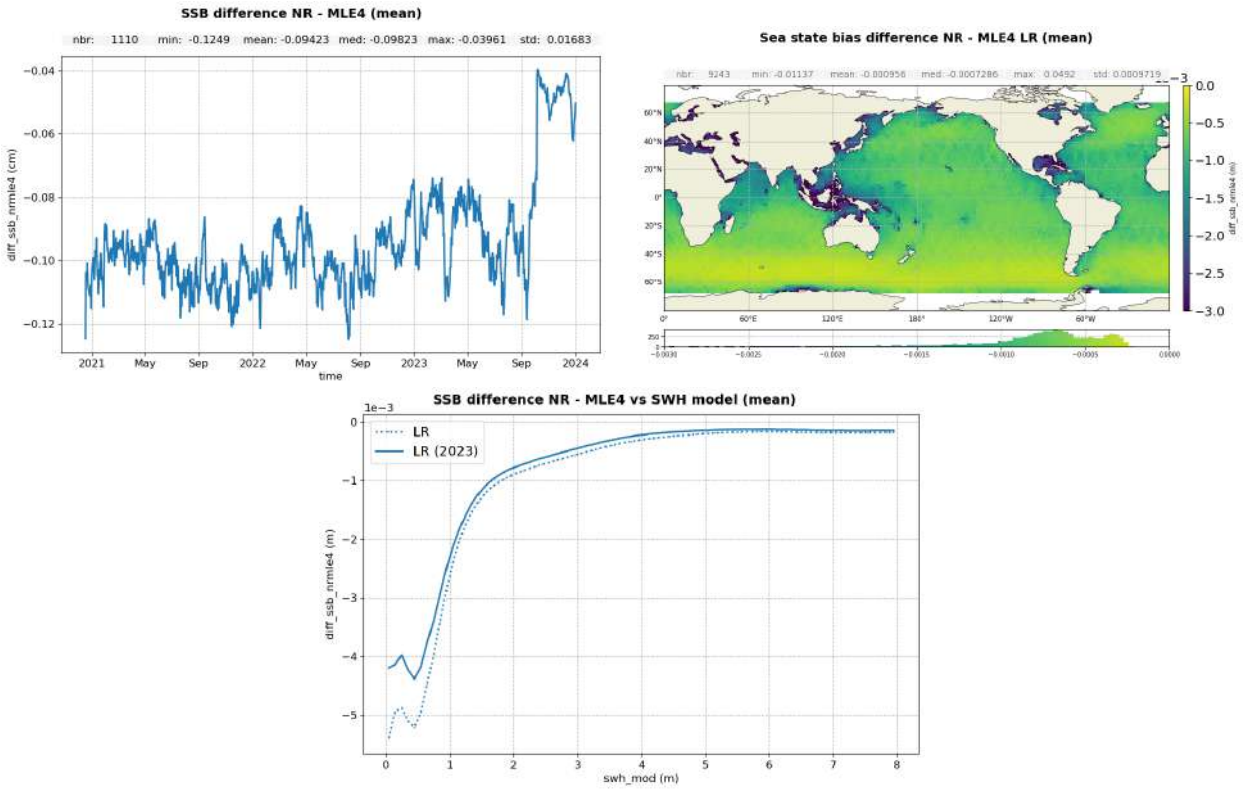

*Figure 80: Map (**right**) and monitoring (**left**) of the LR reprocessed NR - MLE4 SSB difference per day in cm. **Bottom** : Mean differences in meters as a function of ERA 5 model SWH.*

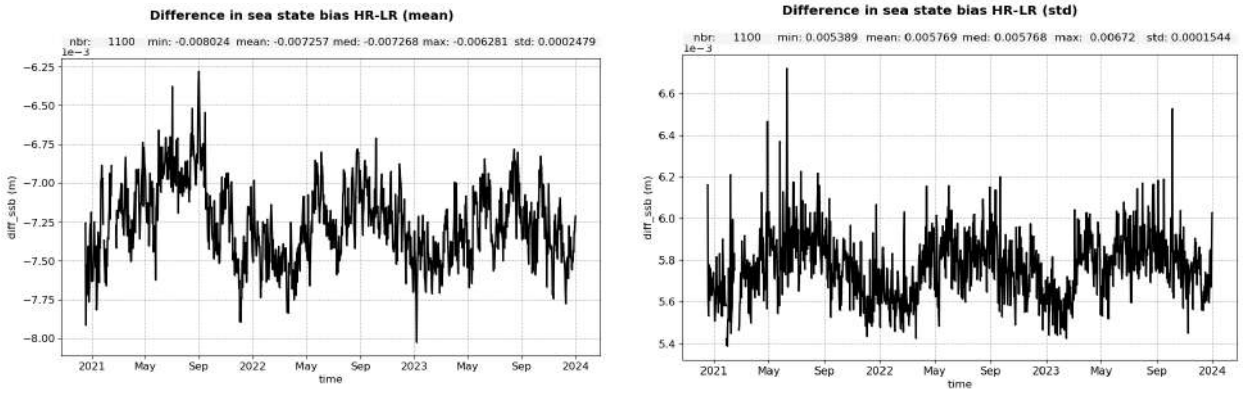

Figure 81: Mean (left) and standard deviation (right) HR-LR MLE4 SSB difference per day.

5.8. Ionospheric correction

Sentinel-6 MF altimeter ionosphere correction is derived from LR data, in Ku and C-band. The ionosphere correction in HR products is copied from LR MLE4 products and thus identical.

The filtering process of dual-frequencies ionospheric correction is described in [14].

The monitoring of the filtered dual-band ionospheric correction is presented on figure 82, along with the corresponding distributions. There is a very good agreement between Sentinel-6 MF LR MLE4, LR NR and Jason-3 ionospheric corrections, that follow the same variations with a downward trend due to the intensification of the current solar cycle. Averages over the whole period are -4.0 and -3.9 cm for Sentinel-6

MF LR MLE4 and LR NR respectively and -3.5 cm for Jason-3, the bias being stable over time.
The geographical distribution of Sentinel-6 MF filtered ionospheric correction is presented on figure 83.

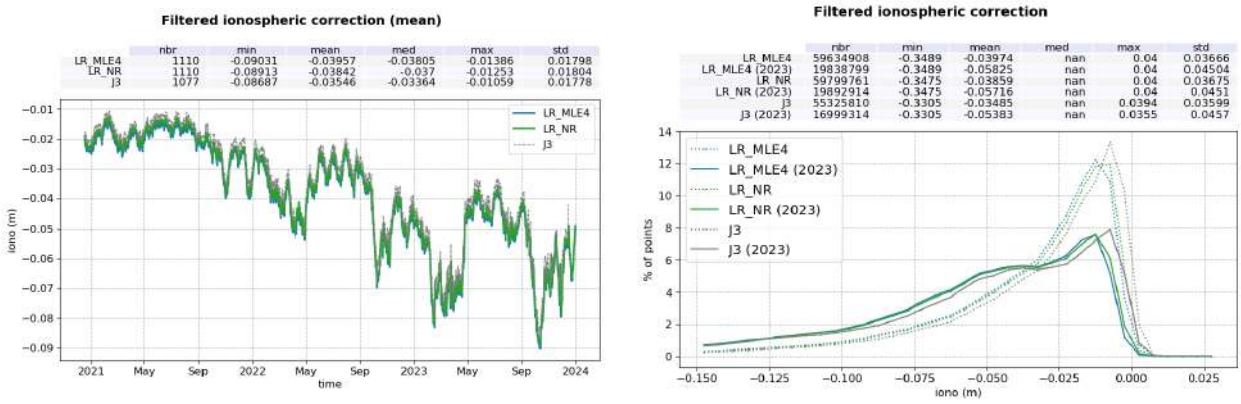

Figure 82: Monitoring of filtered ionospheric correction for Sentinel-6 MF LR MLE4 (blue), LR NR (green) and Jason-3 (black). Left: Mean per day. Right : Histogram computed on the entire time series (dotted line) and on 2023 only (solid line).

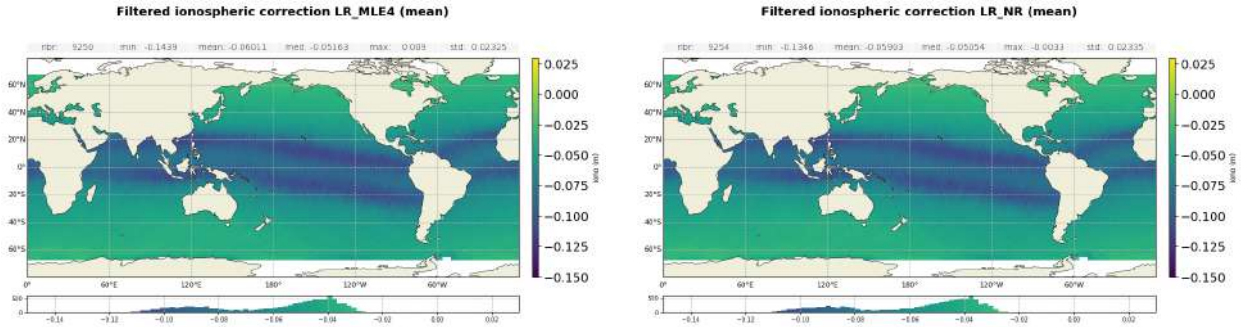

Figure 83: Maps of mean filtered ionospheric correction for Sentinel-6 MF LR MLE4 (left) and LR NR (right). Computed on year 2023.

Figure 84 presents the daily monitoring of the NR - MLE4 filtered ionospheric correction difference. An about -0.25 mm jump is visible at the side B switch due to range (cf section 5.3.).

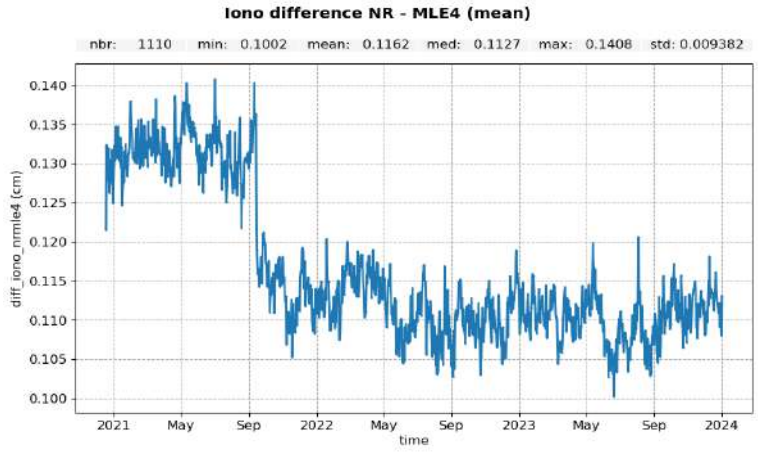

Figure 84: Time monitoring of the NR - MLE4 filtered ionospheric correction difference per day in cm.

The monitoring of the filtered minus GIM model ionospheric corrections differences are presented on figure 85. As expected, both Sentinel-6 MF MLE4 and NR curves, as well as Jason-3, follow identical variations. Sentinel-6 MF altimeter ionosphere corrections show in average a better consistency to GIM model than

Jason-3. The biases with respect to GIM are centred around 1.0 cm and 1.1 cm for Sentinel-6 MF LR MLE4 and LR NR respectively, while it is of 1.4 cm for Jason-3. However, looking at the corresponding maps of altimeter versus GIM difference (figure 86), the amplitudes of the differences are stronger for Sentinel-6 MF than Jason-3. This behavior could be linked to the fact that the C-band SSB in the ionospheric correction computation for Sentinel-6 MF is computed using Jason-3 C-band SSB parameterization and might not be adapted to the differences in wavelength (5.41 GHz and 5.31 GHz for Sentinel-6 MF and Jason-3 respectively), cf Cadier et al. 2024, under review [5]. This is also visible in the higher standard deviations for Sentinel-6 MF LR MLE4 and LR NR compared to Jason-3 (0.9 cm, 0.9 cm and 0.8 cm respectively, see figure 85, right panel).

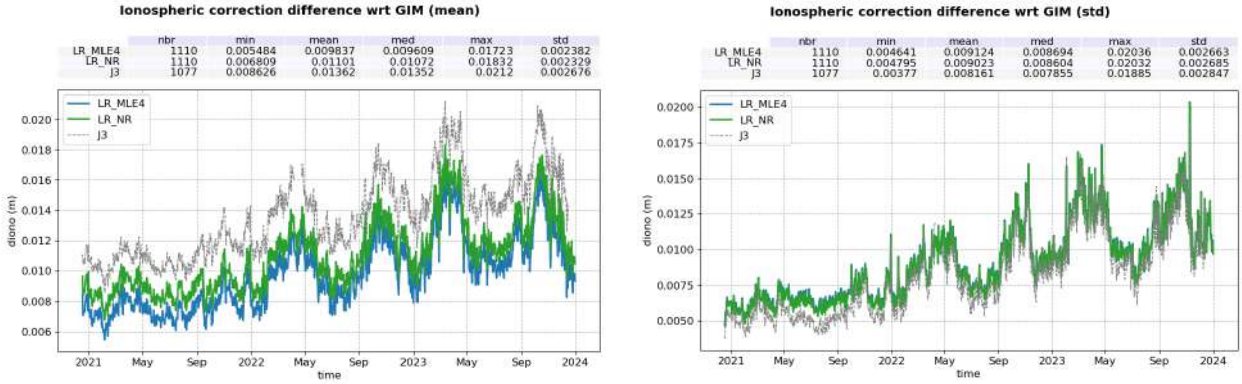

Figure 85: Mean (left) and standard deviation (right) filtered iono - GIM iono per day for Sentinel-6 MF LR MLE4 (blue), LR NR (green) and Jason-3 (black).

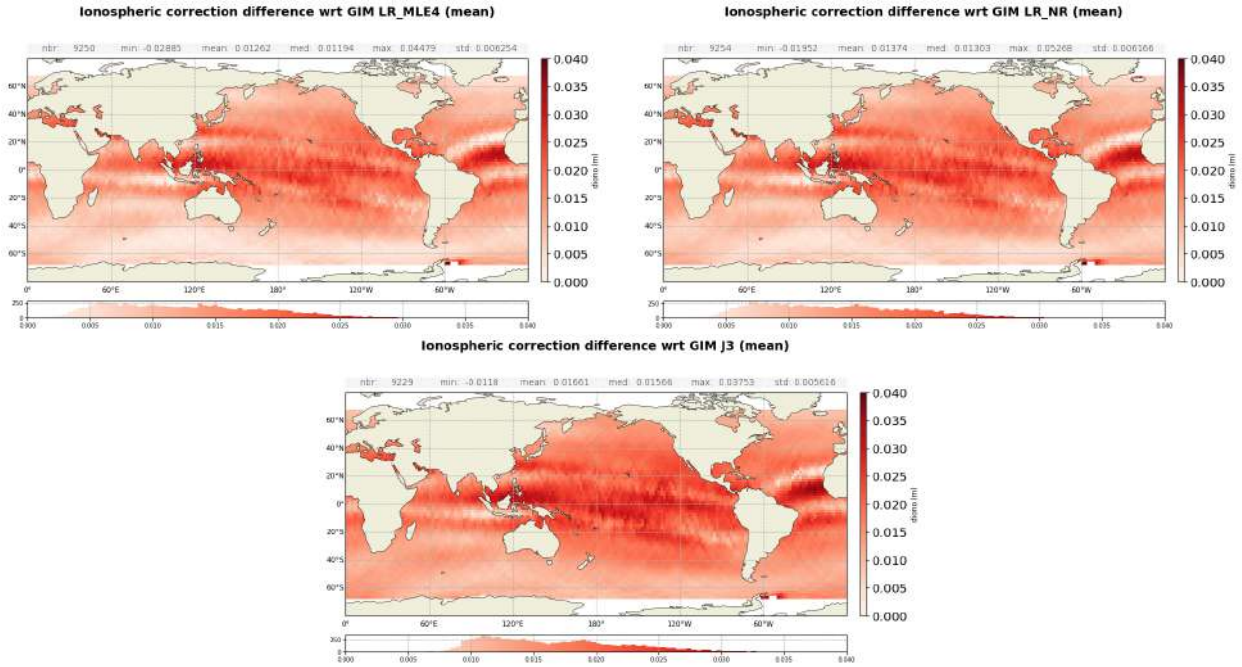

Figure 86: Maps of mean filtered ionospheric correction - GIM iono for Sentinel-6 MF LR MLE4 (left), LR NR (right) and Jason-3 (bottom). Computed on year 2023.

5.9. AMR wet troposphere correction

5.9.1. Overview

In order to evaluate radiometer wet troposphere correction, liquid water content, water vapour content and atmospheric attenuation, Sentinel-6 uses a three-frequencies AMR radiometer (18.7, 23.8 and 34.0 GHz), similar to the one used on Jason-3, in combination to HRMR data for more reliable measurements in coastal areas.

Note that the 23.8 GHz channel is the primary water vapour sensing channel, meaning a higher water vapour concentration leads to larger 23.8 GHz brightness temperature values. As a consequence, top right and bottom right parts of figure 87 are anti-correlated. Moreover, the 34 GHz channel and the 18.7 GHz channel, which have less sensitivity to water vapour, facilitate the removal of the contributions from cloud liquid water and excess surface emissivity of the ocean surface due to wind, which also act to increase the 23.8 GHz brightness temperature.

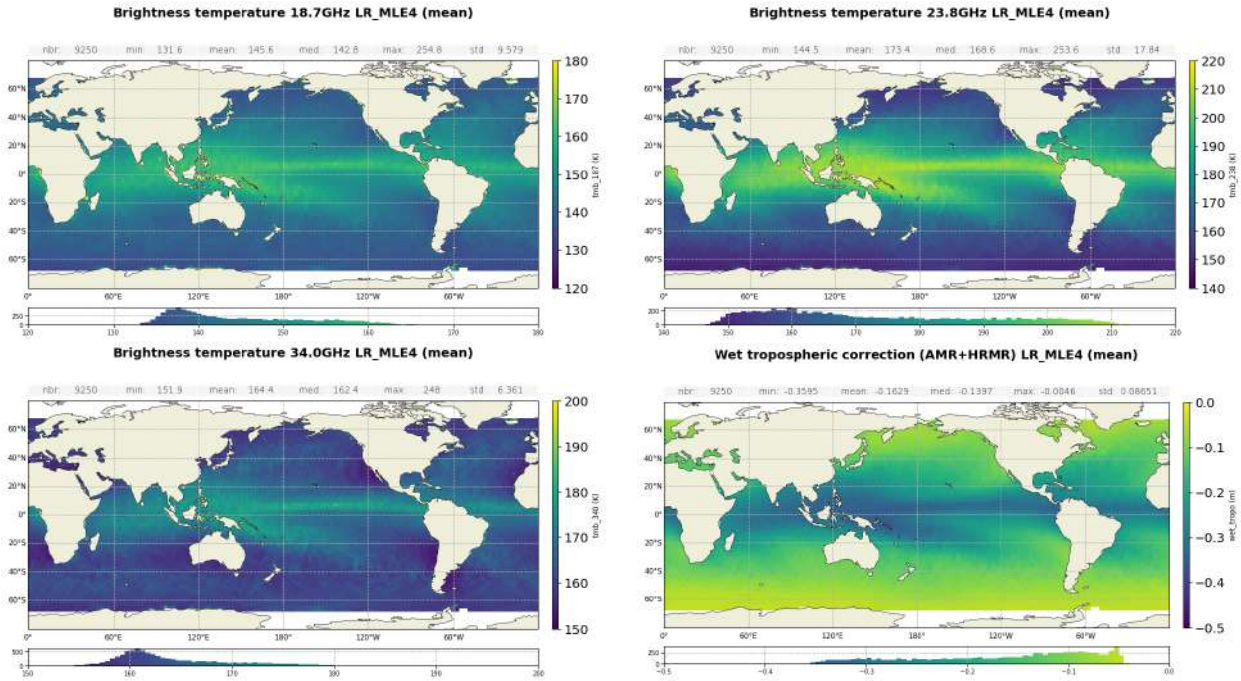

Figure 87: Maps of mean brightness temperature for channels 18.7 GHz (top left), 23.8GHz (top right), 34.0GHz(bottom left) in K and mean wet tropospheric correction (bottom right) in m. Computed on year 2023.

The distributions of the wet tropospheric corrections for Sentinel-6 MF and Jason-3 are presented on figure 88. Both distributions are similar, with Sentinel-6 MF centred around -15.2 cm and Jason-3 around -15.1 cm.
Curves for year 2023 only (solid lines) are aligned with curves for the entire time series (dotted lines).

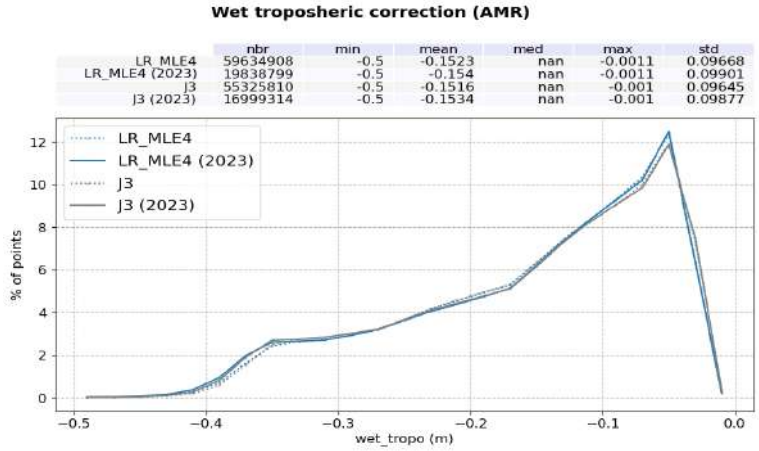

Figure 88: Histogram of wet tropospheric correction in m for Sentinel-6 MF (blue) and Jason-3 (black). Computed on the entire timeseries (dotted line) and on 2023 only (solid line).

5.9.2. Comparison with model

The wet troposphere correction computed from ECMWF model data has been used to check the Sentinel-6 MF and Jason-3 radiometer corrections. The cross-comparison between all radiometers and models available is necessary to analyse the stability of each wet troposphere correction. An overview of the wet troposphere correction importance for mean sea level is given in Obligis et al. [15]. The difference between measured and model data is computed on a daily basis and is plotted on figure 89 for Sentinel-6 MF and Jason-3 for comparisons. Looking more closely to Sentinel-6 MF data, the monitoring per day of the bias between radiometer and model highlights two events (figure 89 left panel):

- on 27-28 April 2021, a jump of -4 mm is observed in the bias preceded by a progressive increase of the bias (from beginning of March 2021) by the same amplitude. The jump visible on 27-28 April 2021 is concomitant with a satellite restart and follows an AMR deep sky calibration occurring on the 25/04/2021. It is not observed in Jason-3 time series (figure 89 left panel). This jump is most likely linked either to the AMR calibration or to the satellite restart that occurred on the 22/04/2021, during which significant thermal variations could have permanently impacted the radiometer antenna.
- on 13 October 2021, a jump of +2 mm is observed on both Sentinel-6 MF and Jason-3 monitoring. It is linked to an update in the ECMWF model (see [11] for more details).

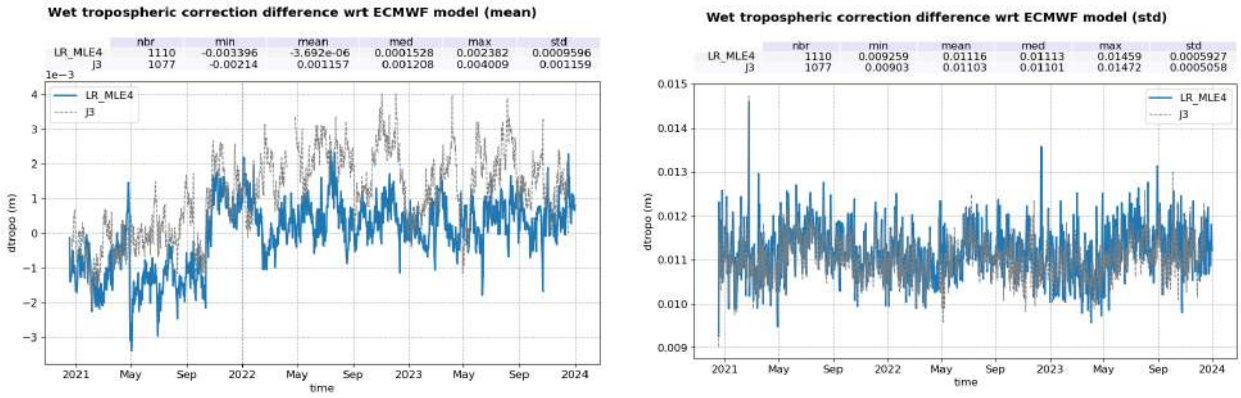

Figure 89: Mean (left) and standard deviation (right) HRMR+AMR wet troposhperic correction - ECMWF model per day for Sentinel-6 MF (blue) and Jason-3 (black).

6 SSH crossover analysis

6.1. Overview

Sea Surface Height crossover differences are the SSH differences between ascending and descending passes where they cross each other. Sea Surface Heights are computed as follow :

$$SSH = Orbit - AltimeterRange - \sum(GeophysicalCorrections)$$

Crossover differences are systematically analysed to estimate data quality and the Sea Surface Height (SSH) performance. SSH crossover differences are computed from the valid data set on a one cycle basis, with a maximum time lag of 10 days, in order to limit the effects of ocean variability which are a source of error in the performance estimation. The mean SSH crossover differences should ideally be close to zero and standard deviation should ideally be small.

Nevertheless, SLA varies also within 10 days, especially in high variability areas. Furthermore, due to lower data availability (due to seasonal sea ice coverage), models of several geophysical corrections are less precise in high latitude. Therefore, an additional geographical selection - removing shallow waters, areas of high oceanic variability and high latitudes ($> |50|$ deg) - is applied for cyclic monitoring.

6.2. Mono-mission SSH crossovers

The cycle by cycle mean of SSH crossover differences is plotted in figure 90. All curves follow similar variations and average close to zero, Sentinel-6 MF HR having a slightly higher mean at 0.9 mm compared to Sentinel-6 MF LR MLE4, LR NR and Jason-3 (-0.1 mm, -0.1 mm and -0.2 mm respectively). These results are summarized in table 8. Similarly to Jason-3, a 120-day signal is observed for Sentinel-6 MF monitorings. This signal disappear with the use of JPL orbits instead of CNES POE-F (cf Cadier et al. 2024, under review [5]). Further investigations are required to fully understand this behavior.

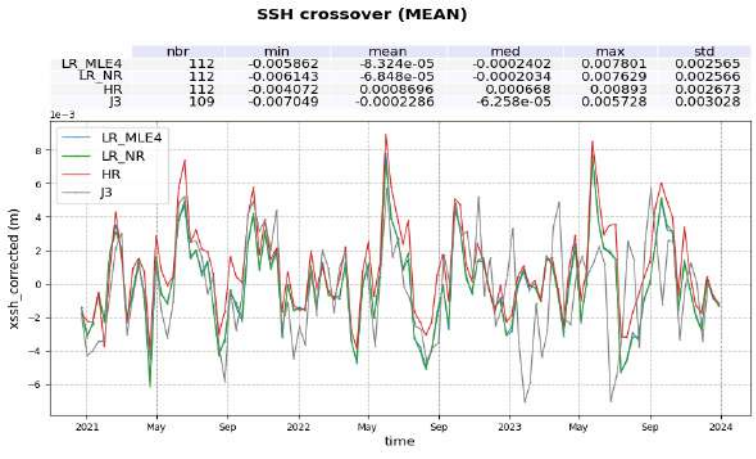

Figure 90: Mean SSH differences at crossovers by cycle for Sentinel-6 MF LR MLE4 (blue), LR NR (green), HR (red) and Jason-3 (black).

Figure 91 presents the monitoring of the error of crossover SSH differences, for Sentinel-6 MF LR, HR, and Jason-3. All datasets show very good performance, very similar and stable in time. No anomaly is detected. Sentinel-6 MF LR MLE4, LR NR and Jason-3 have similar errors, at 3.3 cm in average, while Sentinel-6 MF HR error is slightly lower at 3.2 cm. These results are summarized in table 8.

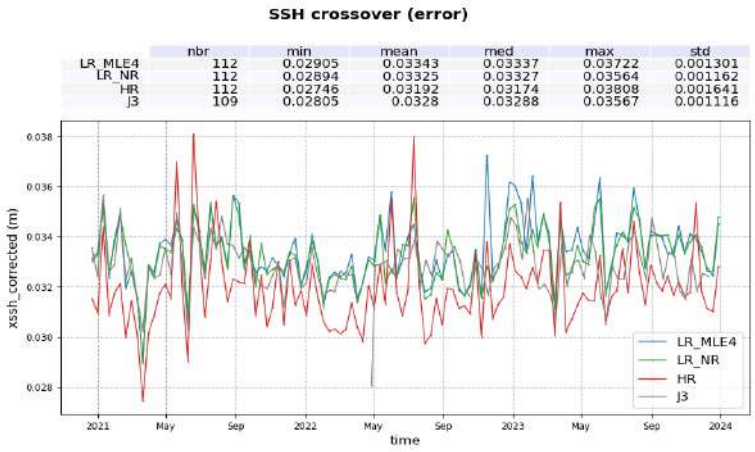

Figure 91: Error of SSH differences at crossovers by cycle for Sentinel-6 MF LR MLE4 (blue), LR NR (green), HR (red) and Jason-3 (black).

The cyclic monitoring of the crossover differences of the SSH using model wet tropospheric correction is plotted on figure 92. The means of the Sentinel-6 MF LR MLE4, LR NR and Jason-3 datasets with model WTC (-0.3 mm in all three cases) are slightly higher in absolute value than with AMR+HRMR WTC. The mean of the HR dataset is slightly closer to zero than with the radiometer WTC (0.7 mm vs 0.9 mm).
The differences in errors are more significant. For all datasets, the use of model wet tropospheric correction degrades the error of the SSH crossover differences, by about 2 mm for LR MLE4 and LR NR and 1 mm for HR and Jason-3. These results are summarized in table 8.

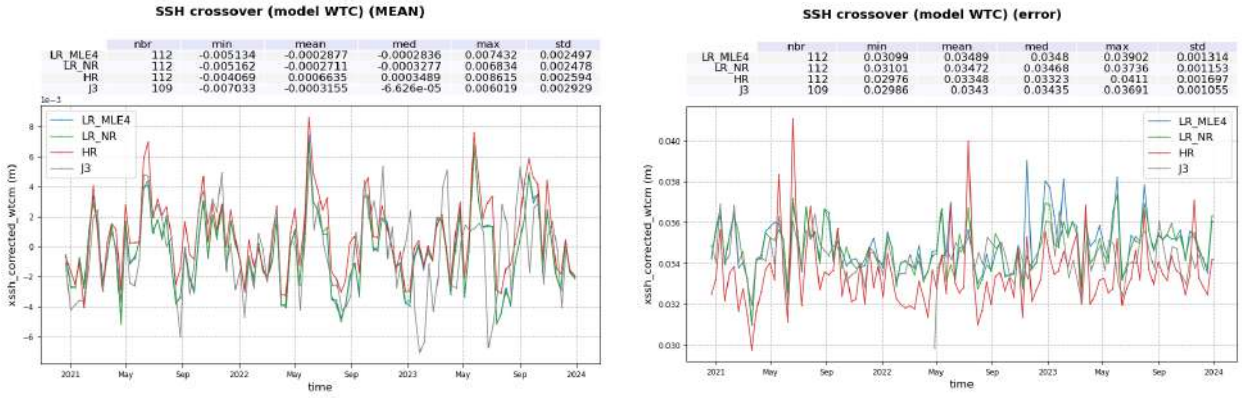

Figure 92: Mean (left) and error (right) SSH differences at crossovers by cycle for Sentinel-6 MF LR MLE4 (blue), LR NR (green), HR (red) and Jason-3 (black), using model wet tropospheric correction.

The maps of LR SSH differences at crossovers are smooth and do not highlight any strong discrepancies between ascending and descending tracks in terms of SSH (figure 93 top panels). The map of HR SSH difference at crossover highlight patterns correlated to along-track wind (bottom panel). It is linked to the impact of along-track wind on HR data and more particularly on HR range (see section 5.3.).

Mission	Mean (mm)		Error (cm)	
	AMR WTC	Model WTC	AMR WTC	Model WTC
Sentinel-6 MF LR MLE4	-0.1	-0.3	3.3	3.5
Sentinel-6 MF LR NR	-0.1	-0.3	3.3	3.5
Sentinel-6 MF HR	0.9	0.7	3.2	3.2
Jason-3	-0.2	-0.3	3.3	3.4

Table 8: Mean and standard deviation of monomission SSH crossover differences for Sentinel-6 MF LR and HR and Jason-3

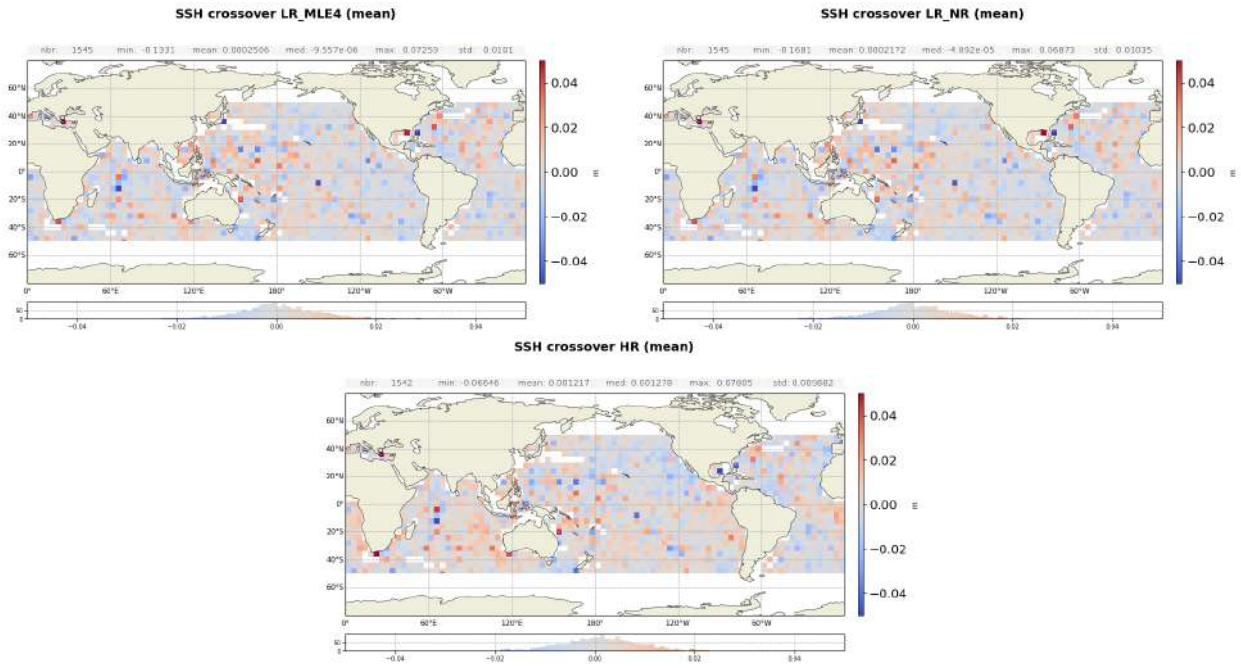

Figure 93: Maps of mean SSH differences at mono-mission crossovers in m for LR MLE4 (top left), LR NR (top right) and HR (bottom), computed on year 2023.

6.3. Multi-mission SSH crossovers

The monitoring of multi-mission SSH differences at crossovers is plotted on figure 94. All three cases, LR MLE4/Jason-3, LR NR/Jason-3 and HR/Jason-3, follow the same variations, with means of -1.7 cm, -1.1 cm and 0.1 cm respectively.
On all curves, a jump of about -3 mm is visible at the end of April 2021, concomitant with a Sentinel-6 MF restart on April 27-28th, 2021. Then, on both S6-MF LR NR/J3 and S6-MF HR/J3 datasets, a downward drift is visible until approximately the end of the tandem phase in April 2022. These drifts might be caused by the evolution of the Jason-3 PTR shape in the first case, that would not be compensated by a similar effect in Sentinel-6 MF LR NR due to the use of the in-flight PTR, and by the range walk effect impacting HR data in the second case.

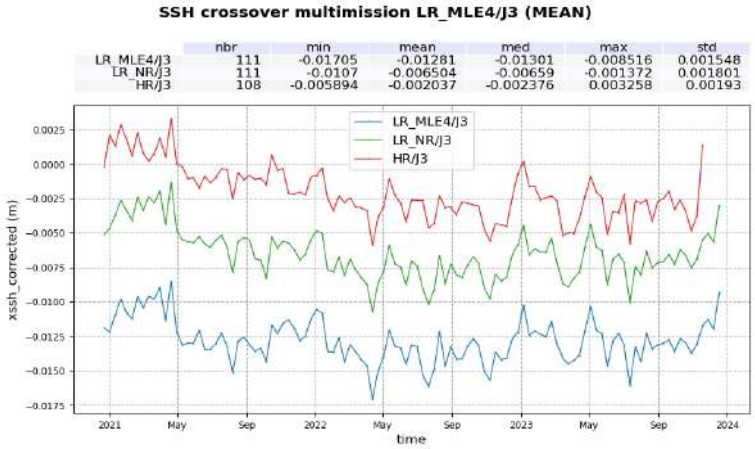

Figure 94: Mean multimission SSH differences at crossovers by cycle for Sentinel-6 MF LR MLE4/Jason-3 (blue), LR NR/Jason-3 (green) and HR/Jason-3 (red).

Figure 95 presents the monitoring of the standard deviation of multimission crossover SSH differences, for LR MLE4/Jason-3, LR NR/Jason-3 and HR/Jason-3. All datasets show very good performance at 4.7 cm.

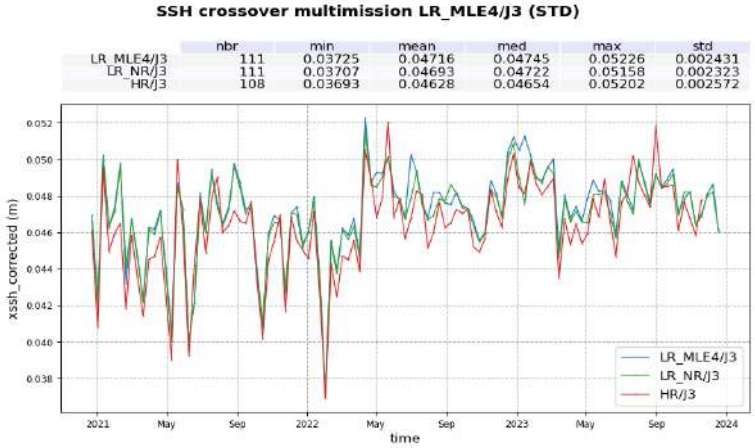

Figure 95: STD multimission SSH differences at crossovers by cycle for Sentinel-6 MF LR MLE4/Jason-3 (blue), LR NR/Jason-3 (green) and HR/Jason-3 (red).

The cyclic monitoring of the multimission crossover differences of the SSH using model wet tropospheric correction is plotted on figure 96. The average SSH crossover difference per cycle follows the same variation as the crossover SSH with radiometer-derived WTC, with only minor value differences. As for monomission crossover differences, however, using a wet troposphere model derived from model degrades the standard deviation of the multimission SSH crossover differences by about 2 mm in all three datasets.

The corresponding geographical distributions and their differences are presented in figure 97. While no significant regional pattern can be seen in the Sentinel-6 MF LR/Jason-3 SSH crossovers differences, Sentinel-6 MF HR/Jason-3 SSH crossovers differences are higher at high latitudes. This difference in geographical pattern in clearly visible in the bottom panel, with differences up to about 1 cm at high latitudes, while it is about -2 cm in the equatorial regions. This is expected as no skewness is used in HR processing, unlike for LR and Jason-3 processings, leading to a strong correlation of the range to sea state conditions (see section 5.3.).

6.4. Pseudo time tag bias

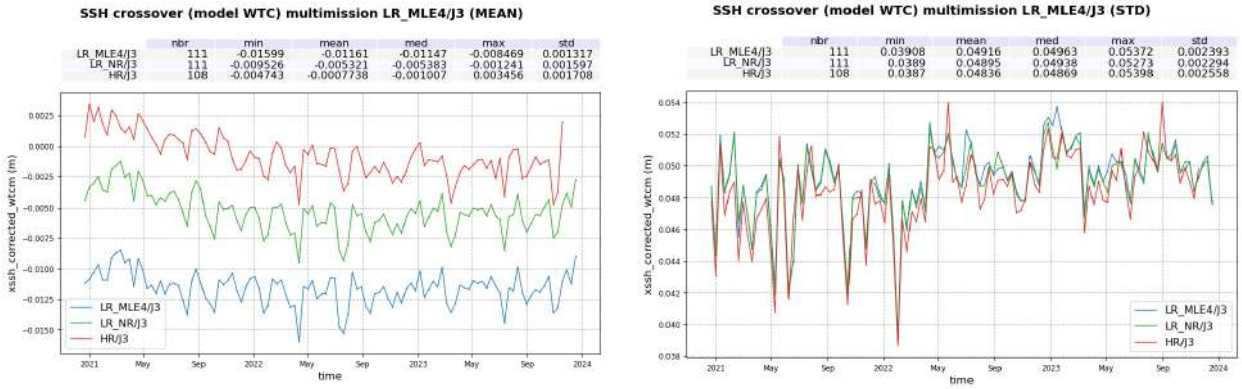

Figure 96: Mean (left) and standard deviation (right) of multimission SSH differences at crossovers by cycle for Sentinel-6 MF LR MLE4 / Jason-3 (blue), LR NR / Jason-3 (green) and HR / Jason-3 (red). SSH is computed using model WTC.

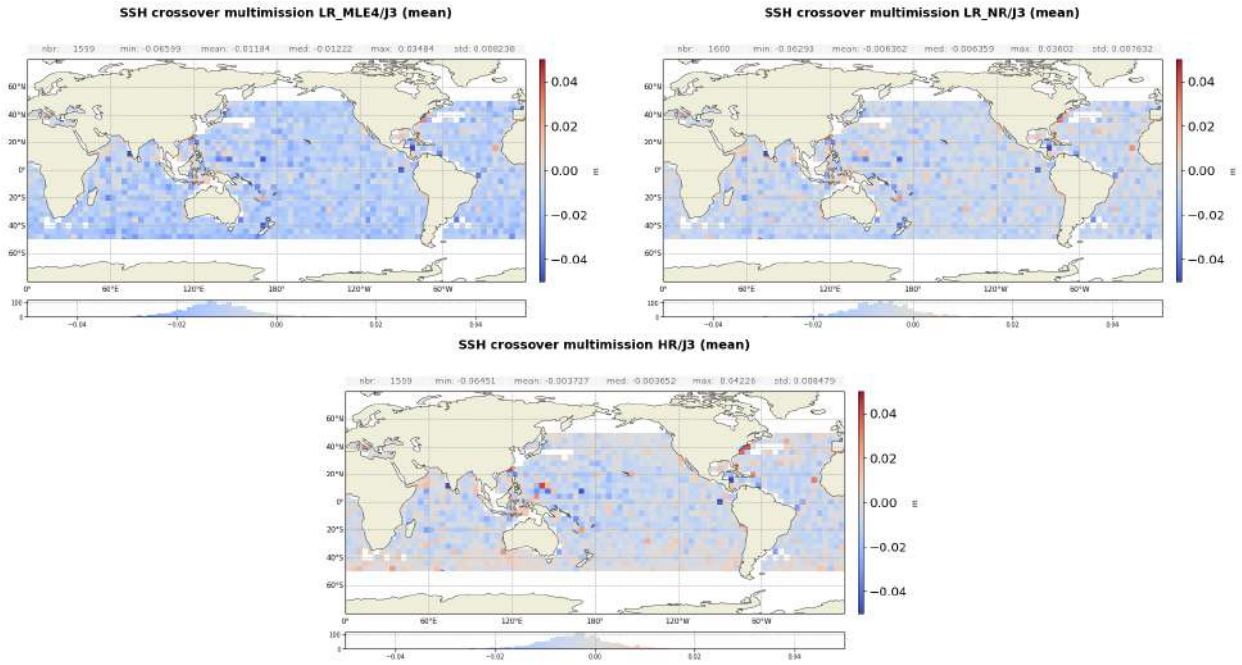

Figure 97: Maps of multimission mean SSH differences at crossovers for LR MLE4/Jason-3 (top left), LR NR/Jason-3 (top right) and HR/Jason-3 (bottom). Computed on year 2023.

The pseudo time tag bias (α) is found by computing at mono-mission SSH crossovers a regression between SSH and orbital altitude rate ($\dot{H}$), also called satellite radial speed: SSH = $\alpha\dot{H}$. This empirical method allows us to estimate the potential real time tag bias but it can also absorb other errors correlated with $\dot{H}$. Therefore it is called “pseudo” time tag bias. The monitoring of this coefficient estimated at each cycle is performed for Sentinel-6 LR and HR in figure 98.

Its mean is -24 μs for LR MLE4, -23 μs for LR NR and -4 μs for HR mode, and never exceeds a few hundreds microseconds.

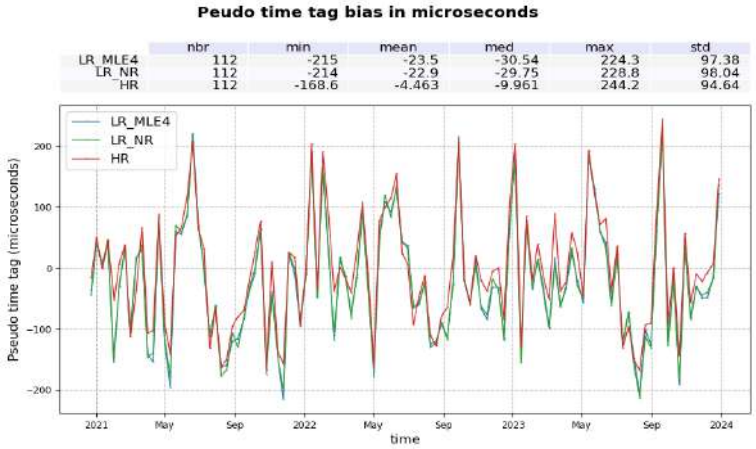

Figure 98: Pseudo time tag bias by cycle for LR (blue) and HR (red).

6.5. Transponder analysis

An absolute calibration of the Poseidon-4 altimeter is performed over the CDN1 transponder in West Crete mountains for each descending Sentinel-6 MF pass number 18.

The range bias (see figure 99) is calculated for each waveform seeing the CalVal site by taking the difference between the transponder-altimeter distance (accurately determined using a precise positioning of the satellite and the transponder site) and the altimeter range derived from the retracking (based on a sinc-function fit) of the transponder-generated waveform. Note that the altimeter bias is further corrected for transponder and altimeter related errors, the Doppler range shift, and delays through the atmosphere.

The datation bias is also computed and presented on figure 100.

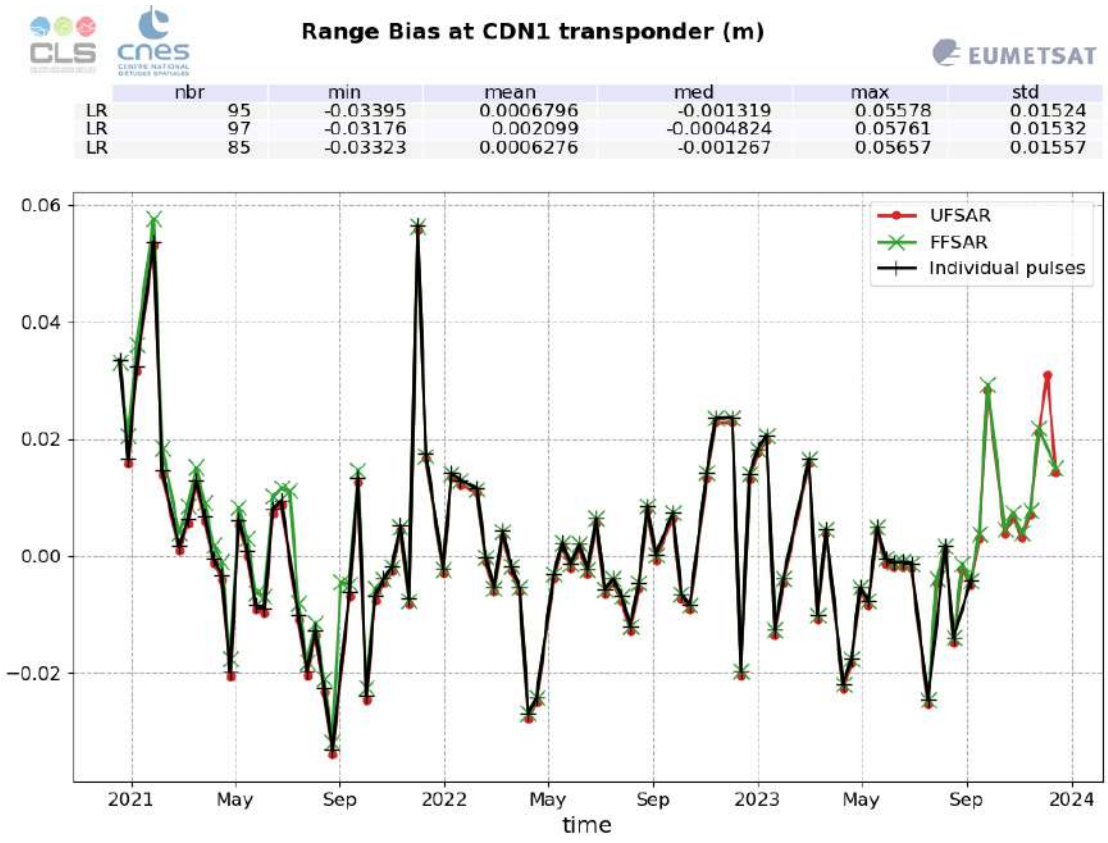

Figure 99: Monitoring of the range bias at CDN1 transponder, from cycle 34 to 115.

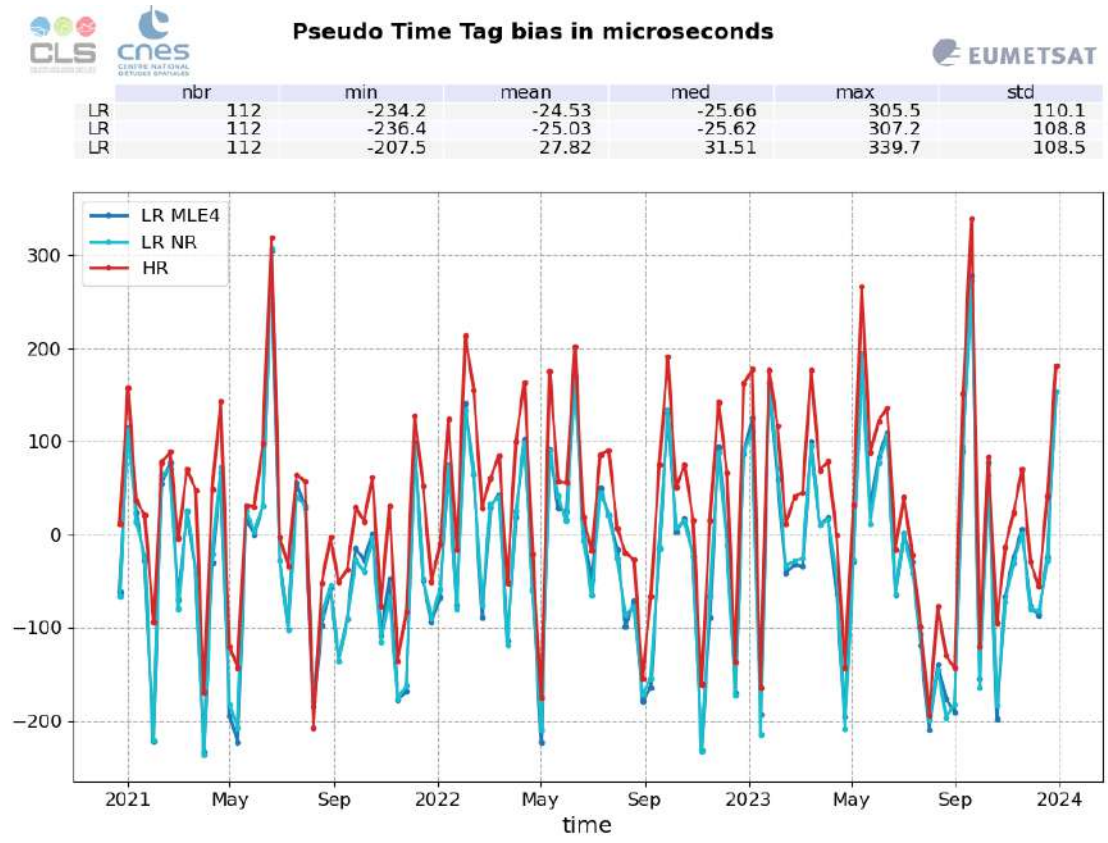

Figure 100: Monitoring of the datation bias at CDN1 transponder, from cycle 34 to 115.

7 SSHA along-track analysis

7.1. Overview

The Sea Surface Height Anomaly (SSHA) is the most well-known parameter estimated from altimetry. It corresponds to the elevation of sea surface, with respect to a reference called Mean Sea Surface (MSS), generated by oceanic variability and climatic phenomena (such as Gulf stream current, El Nino, ...). It is computed as follow:

$$SSHA = Orbit - AltimeterRange - \sum(GeophysicalCorrections) - MeanSeaSurface$$

The details of the geophysical corrections can be found in Sentinel-6 ALT Level 2 Product Generation Specification [16].

SSHA analysis is a complementary indicator to estimate the altimetry system performance. It enables the study of the evolution of the SSHA mean (detection of jump, abnormal trend or geographical correlated biases), and also the evolution of the SSHA variance highlighting the long-term stability of the altimetry system performance.

The SSHA distributions are plotted on figure 101 for Sentinel-6 MF LR MLE4, LR NR and HR as well as Jason-3. Mean values are of 4.9 cm for Sentinel-6 MF LR MLE4, 4.2 cm for Sentinel-6 MF LR NR and 3.8 cm for Sentinel-6 MF HR. The latter is very close to Jason-3 mean value (3.6 cm). Curves for year 2023 only (right panel) are aligned with curves for the entire time series (left panel).

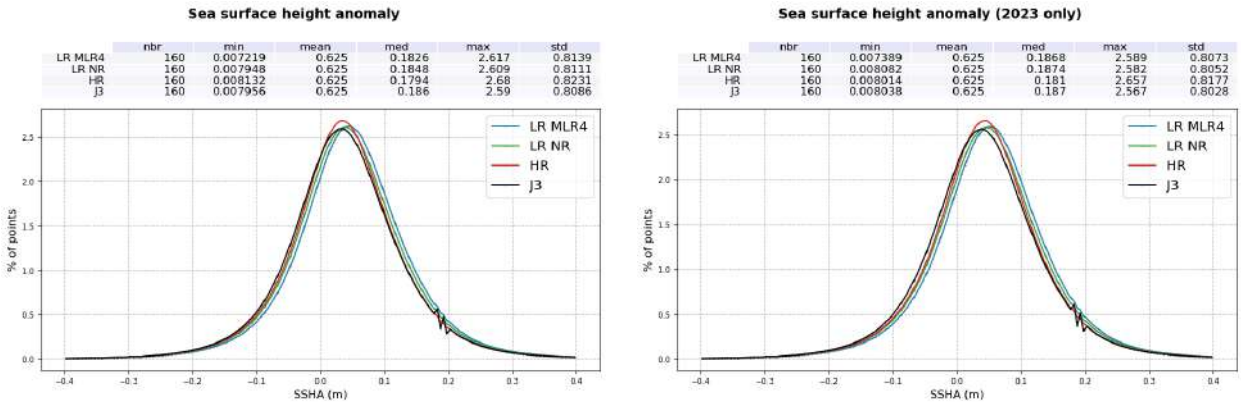

Figure 101: Histograms of SSHA in m for Sentinel-6 MF LR MLE4 (blue), LR NR (green), HR (red) and Jason-3 (black). Computed on the entire time series (left) and on 2023 only (right).

The mean SSHA daily monitoring is presented on figure 102, left panel. Sentinel-6 MF HR and Jason-3 SSHA are very close. As observed on the histogram, Sentinel-6 MF LR SSHA curves are slightly higher. All curves follow similar seasonal cycles and variations. The seasonal cycle on year 2023 has a higher amplitude due to the current El Nino phenomenon. The spike in HR on April 28th, 2021, visible on both mean and standard deviation, is caused by a higher number of missing passes on that day (cf tables 3 and 4) compared to LR, proportionally increasing the weight of the Caspian Sea in the daily monitoring.

On figure 102, right panel, is plotted the daily monitoring of the SSHA standard deviation. The Caspian

Sea has been excluded from this monitoring for it creates spikes in the standard deviation on days that this region is observed, reducing the readability of the figure and preventing from comparisons with Jason-3, that does not have SSHA available on the Caspian Sea. All curves present similar variations, averaging at 11.4, 11.5, 11.5 and 11.4 cm for Sentinel-6 MF LR MLE4, LR NR, HR and Jason-3 respectively.

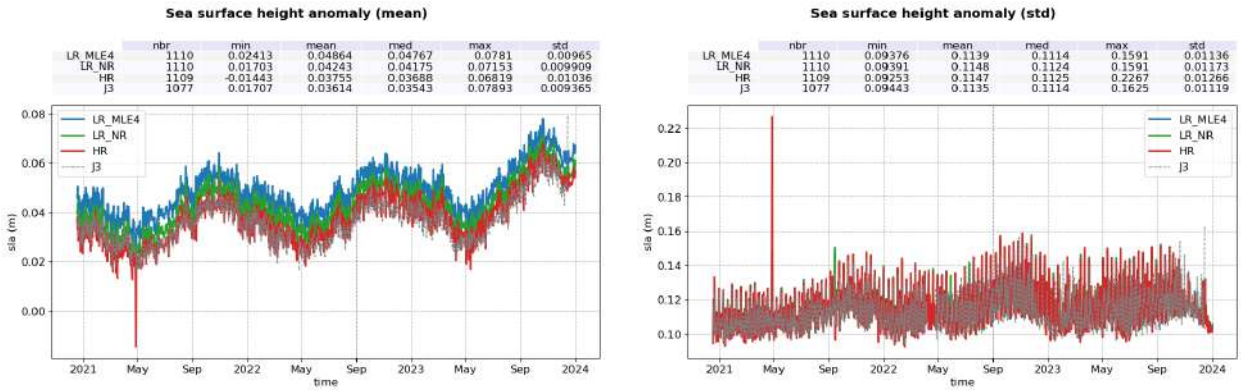

Figure 102: Mean (left) and standard deviation (right) SSHA by day for LR MLE4 (blue), LR NR (green), HR (red) and Jason-3 (black).

Figure 103 presents the monitoring of the SSHA computed with model WTC, both in mean (left panel), and standard deviation (right). The use of the model wet tropospheric correction has little impact on the SSHA mean (less than 0.5 mm for both Sentinel-6 MF LR and HR and 1 mm for Jason-3).
The standard deviation of the SSHA is slightly impacted as well, and increases of about 0.5 mm for all datasets when using the model WTC.

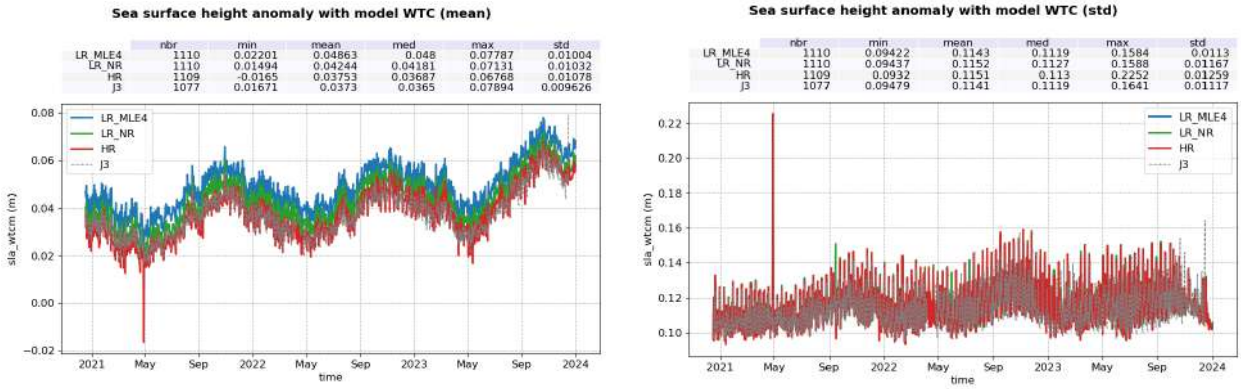

Figure 103: Mean (left) and standard deviation (right) SSHA with wet tropospheric correction from model by day for LR MLE4 (blue), LR NR (green), HR (red) and Jason-3 (black).

7.2. SSHA differences between LR MLE4 and NR

The NR - MLE4 SSHA differences monitoring on figure 104 shows an about 1.5mm jump at side B switch, resulting from range (section 5.3.) and ionosphere correction behaviours (section 5.8.). The corresponding map on figure 105 highlights a significant SWH correlation, with about -1.5 cm decrease between 0.5 and 8m-SWH. This behaviour is expected and is part of the improvement brought by the numerical retracker. Indeed, contrary to MLE4, numerical retracker outputs are not corrected by instrumental LUTs, which are applied function of SWH values. Numerical retracker retrievals are then less sensitive to any approximation in the LUT estimation. Analysis performed in the frame of Sentinel-6 MF commissioning activities have shown that part of the residual bias between Sentinel-6 MF LR MLE4 and Jason-3 can be attributed to

Sentinel-6 MF instrumental MLE4 LUT. Using numerical retracker strongly reduces the correlation to SWH in Sentinel-6 MF LR/Jason-3 SSHA bias.

The standard deviation of the SSHA difference is higher at low SWH which caused by the anomaly in negative SWH management in LR NR (see section 3.1.).

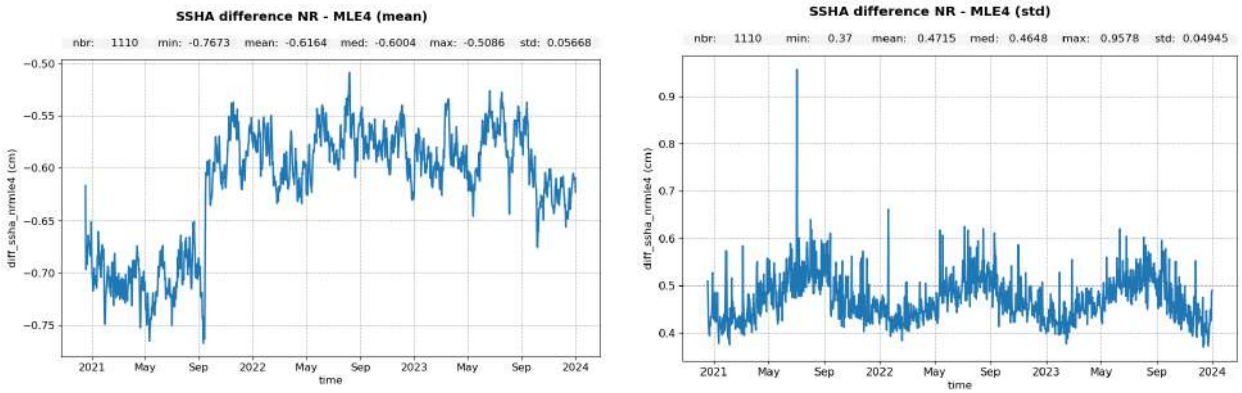

*Figure 104: Time monitoring of Sentinel-6 MF NR - MLE4 SSHA in meters, without the Caspian Sea. **Left**: mean per day, **Right**: standard deviation per day.*

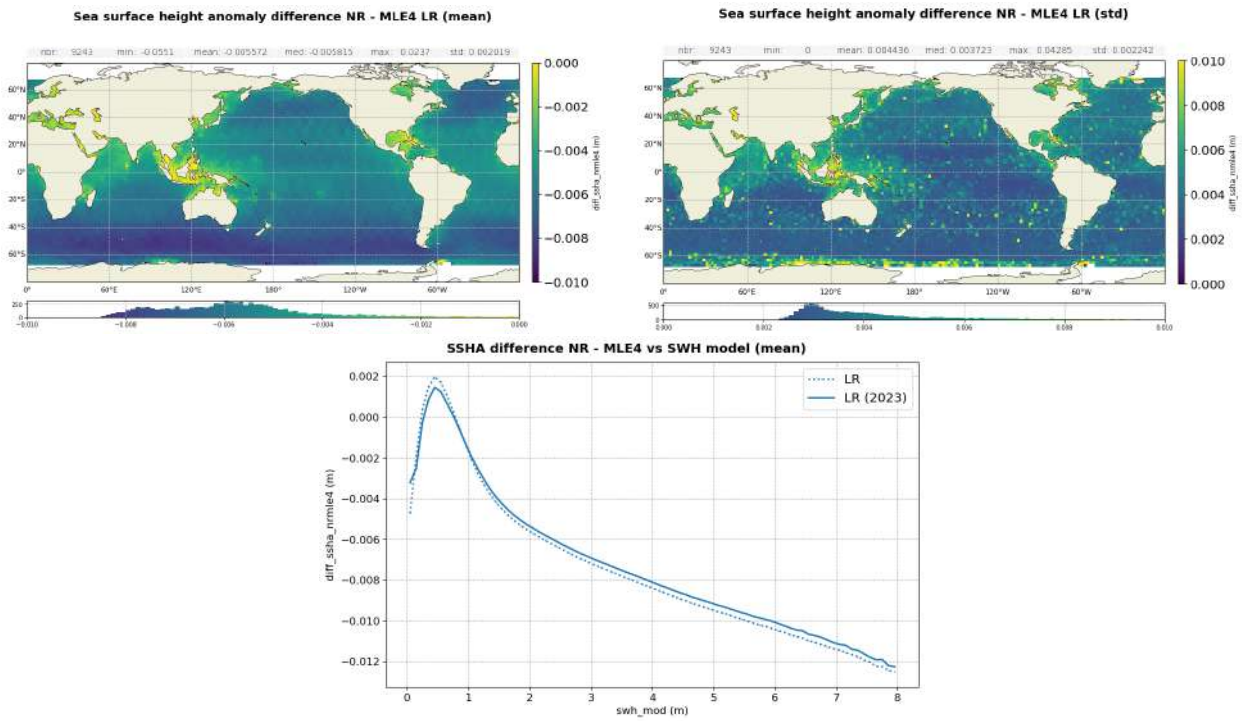

*Figure 105: Maps of mean (**left**) and standard deviation (**right**) of Sentinel-6 MF LR NR - MLE4 SSHA in meters, and its mean as a function of ERA 5 model SWH (**bottom**).*

The NR - MLE4 SSHA distributions are presented on figure 106 for side A (left panel) and side B (right panel). SSHA are consistent between both retrackings, with only a -7.0 mm bias on side A and -5.9 mm on side B.

7.3. SSHA differences between HR and LR

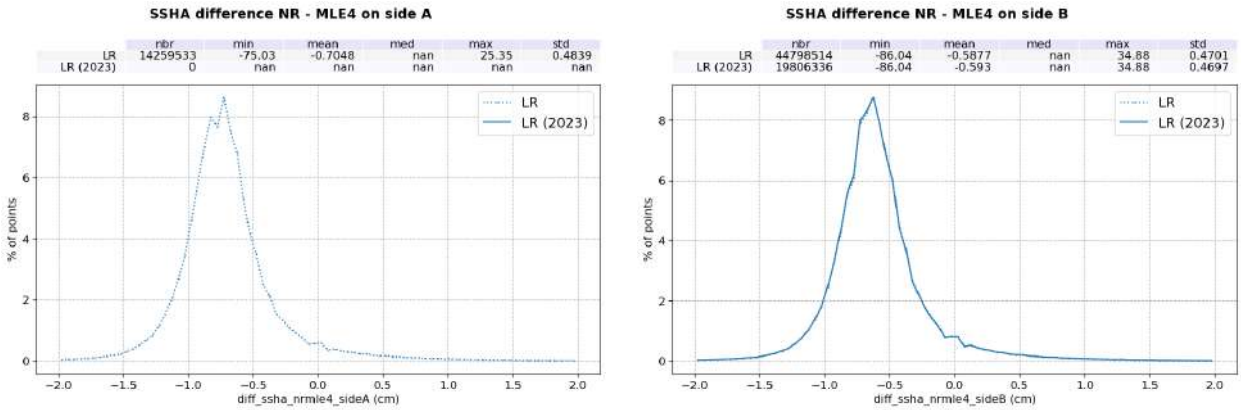

*Figure 106: Distributions of Sentinel-6 MF F08 NR - MLE4 SSHA difference for side A (**left**) and side B (**right**).*

Figure 107 presents the monitoring of the HR-LR SSHA differences. These differences are centred on -1.1 cm for LR MLE4 and -0.5 cm for LR NR. The absolute value decreases after the switch to side B (September 2021), with a drift consistent with the one observed on range (cf section 5.3.). This drift is caused by the evolution of the PTR shape and is reduced with LR NR that uses the in-flight PTR. Range walk correction in the HR processing, implemented with PB F09, will further reduce the drift.

The standard deviation of these differences (right panel) is centred on 2.5 cm with a yearly oscillation for both LR MLE4 and LR NR.

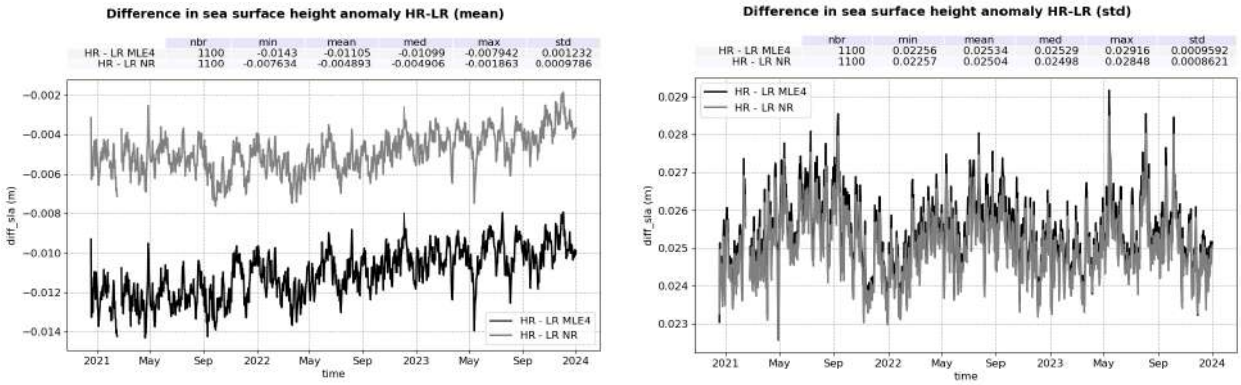

Figure 107: Mean (left) and standard deviation (right) SSHA HR-LR (MLE4 in black, NR in grey) difference by day.

The geographical distributions of both HR-LR SSHA differences are represented on figure 108. As expected from section 5.3., these differences are highly correlated with SWH and are mainly due to the absence of skewness parameter in the HR processing.

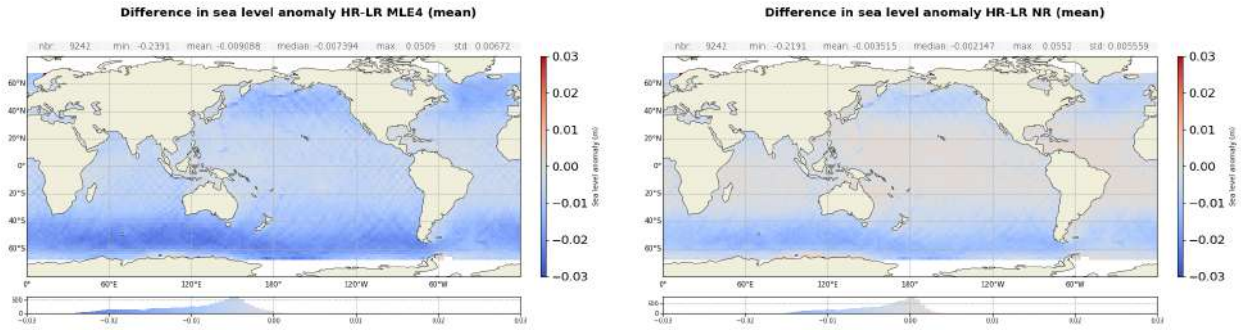

Figure 108: Maps of mean SSHA HR-LR MLE4 (left panel) and NR (right panel) difference in meters. Computed on year 2023.

7.4. SSHA yearly variations

Figures 109, 110 and 111 present the mean SSHA maps per year for 2021 to 2023 for Sentinel-6 MF LR MLE4, LR NR and HR respectively. In all cases, geographical distributions for year 2023 are different from prior years and are typical of El Nino phenomenon, with a slightly higher average.

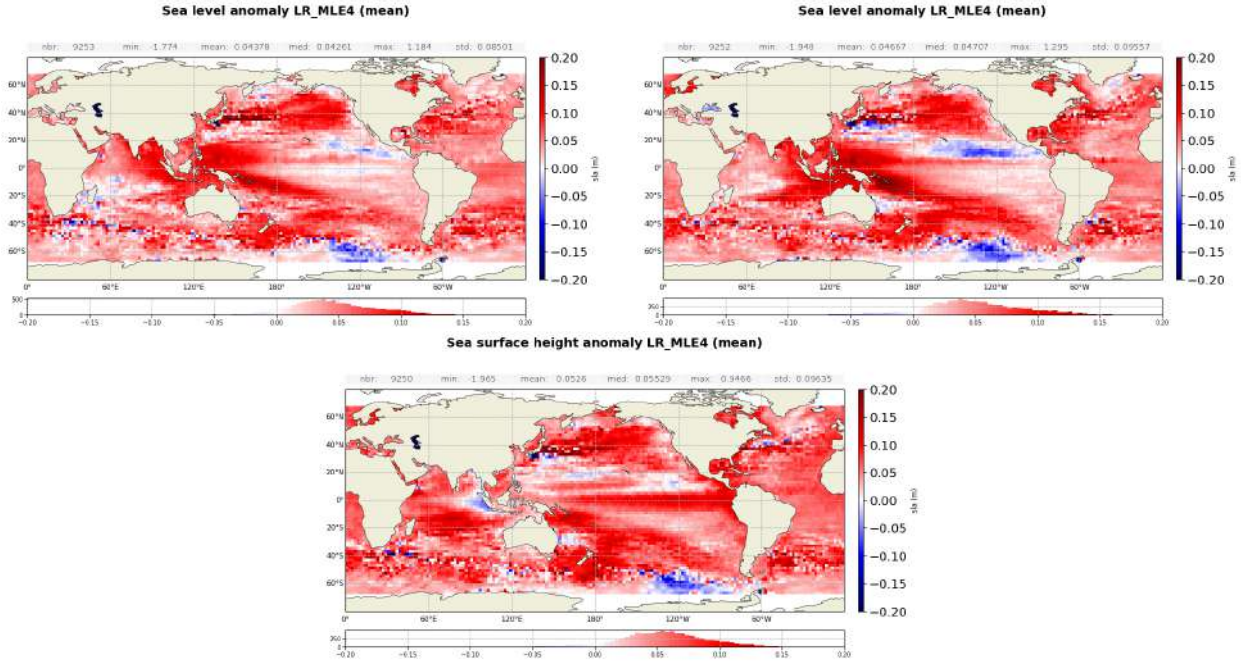

Figure 109: Maps of mean SSHA for LR MLE4 in meters for the year 2021 (top left), 2022 (top right) and 2023 (bottom).

Figures 112, 113 and 114 present the STD SSHA maps per year for 2021 to 2023 for Sentinel-6 MF LR MLE4, LR NR and HR respectively. No significant evolution is visible.

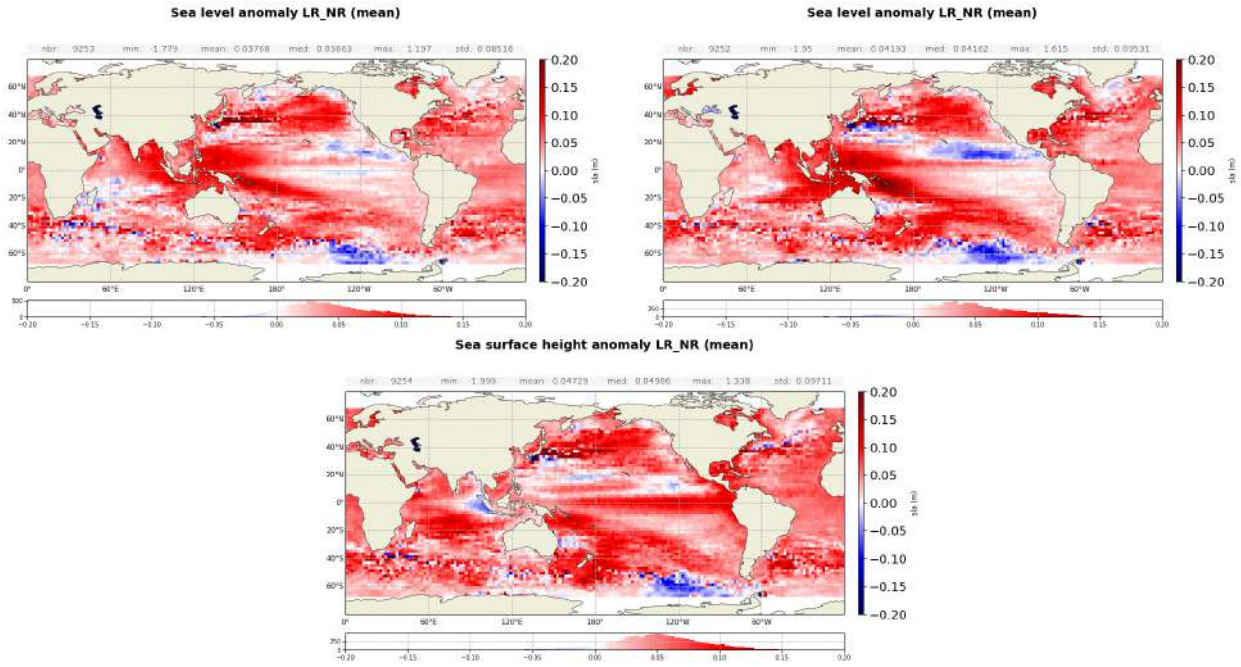

Figure 110: Maps of mean SSHA for LR NR in meters for the year 2021 (top left), 2022 (top right) and 2023 (bottom).

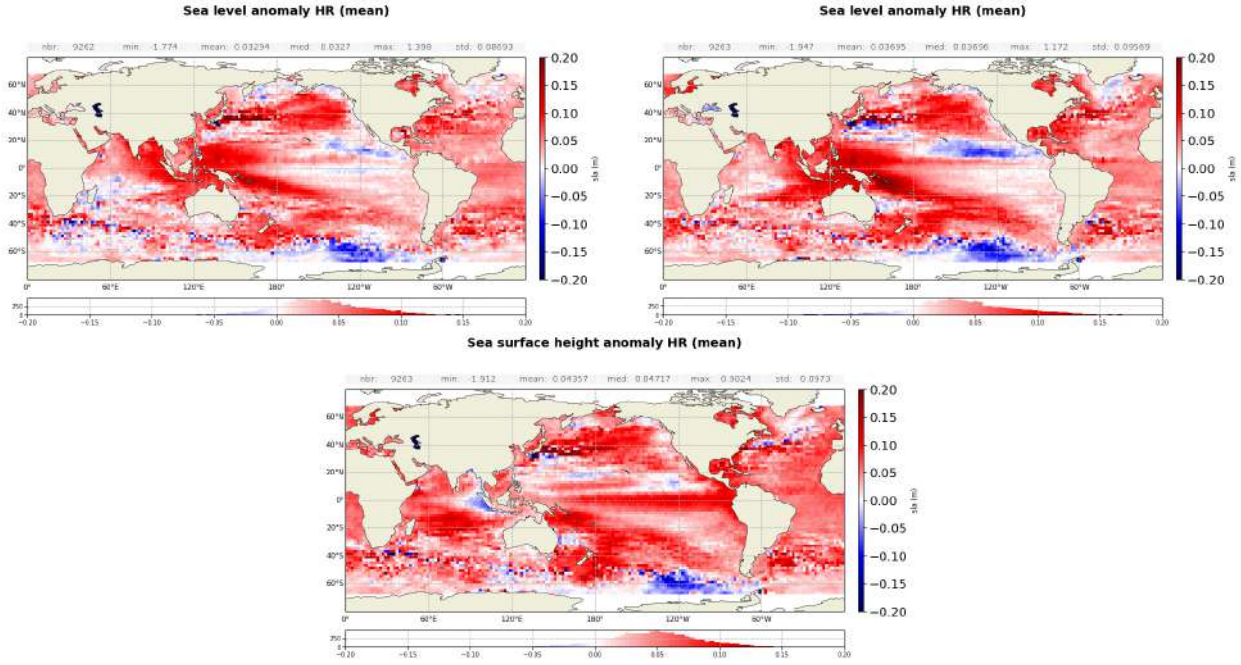

Figure 111: Maps of mean SSHA for HR in meters for the year 2021 (top left), 2022 (top right) and 2023 (bottom).

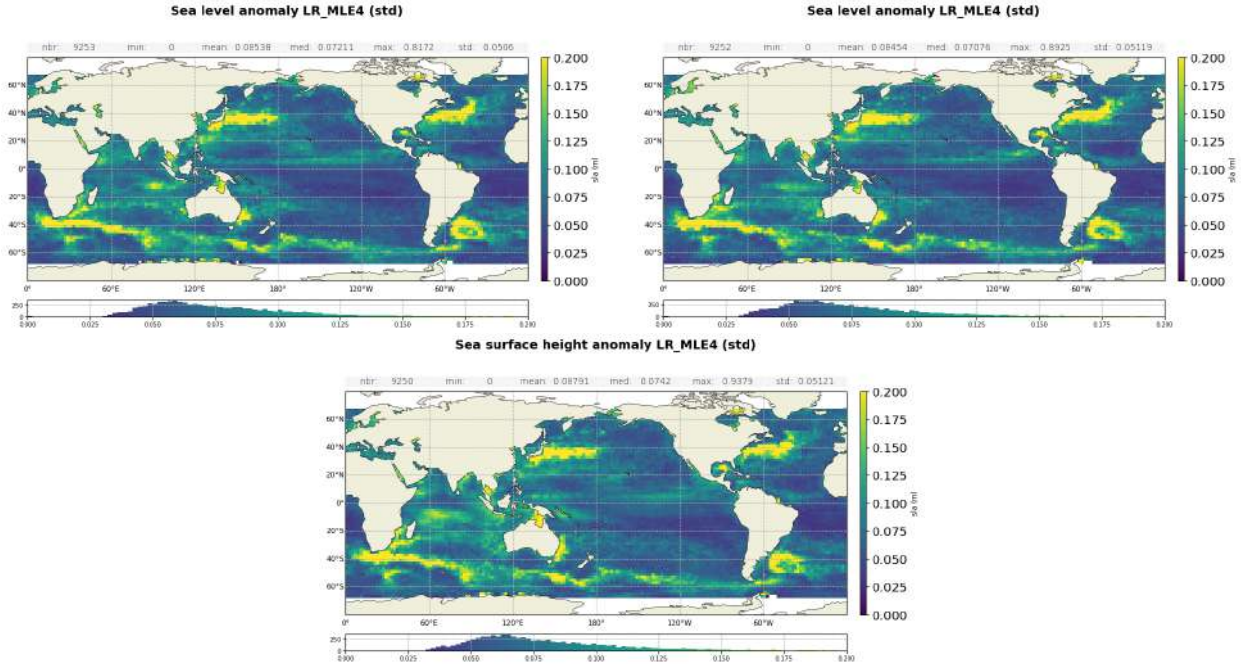

Figure 112: Maps of SSHA standard deviation for LR MLE4 in meters for the year 2021 (top left), 2022 (top right) and 2023 (bottom).

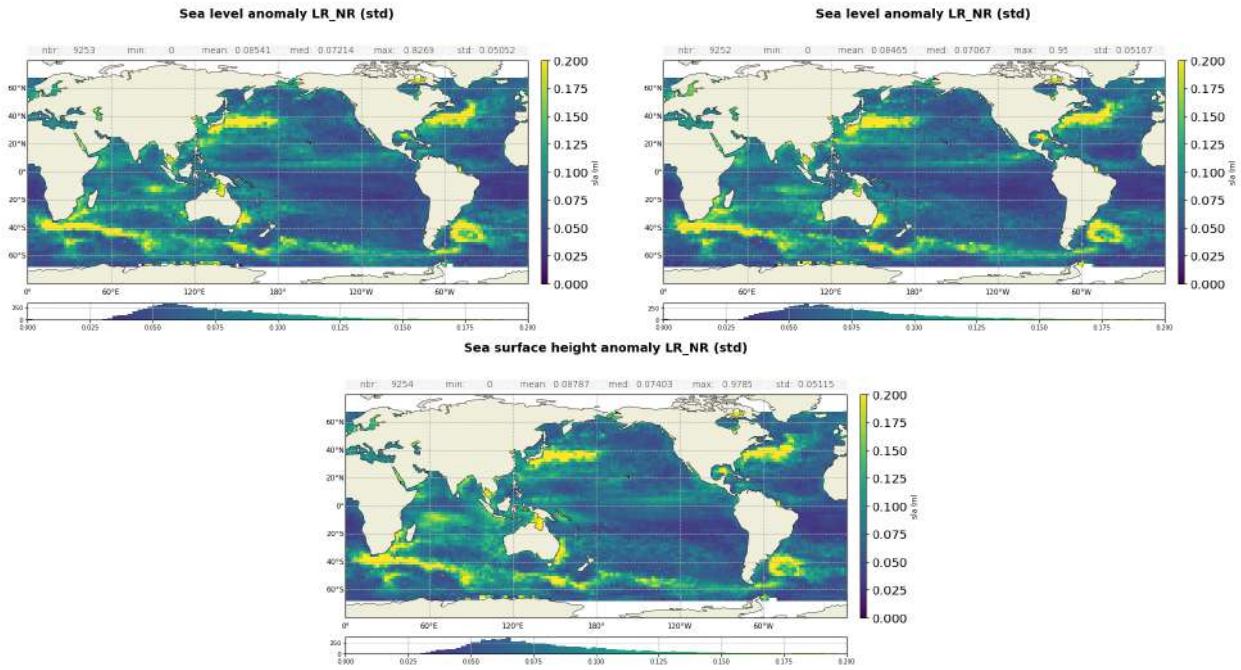

Figure 113: Maps of SSHA standard deviation for LR NR in meters for the year 2021 (top left), 2022 (top right) and 2023 (bottom).

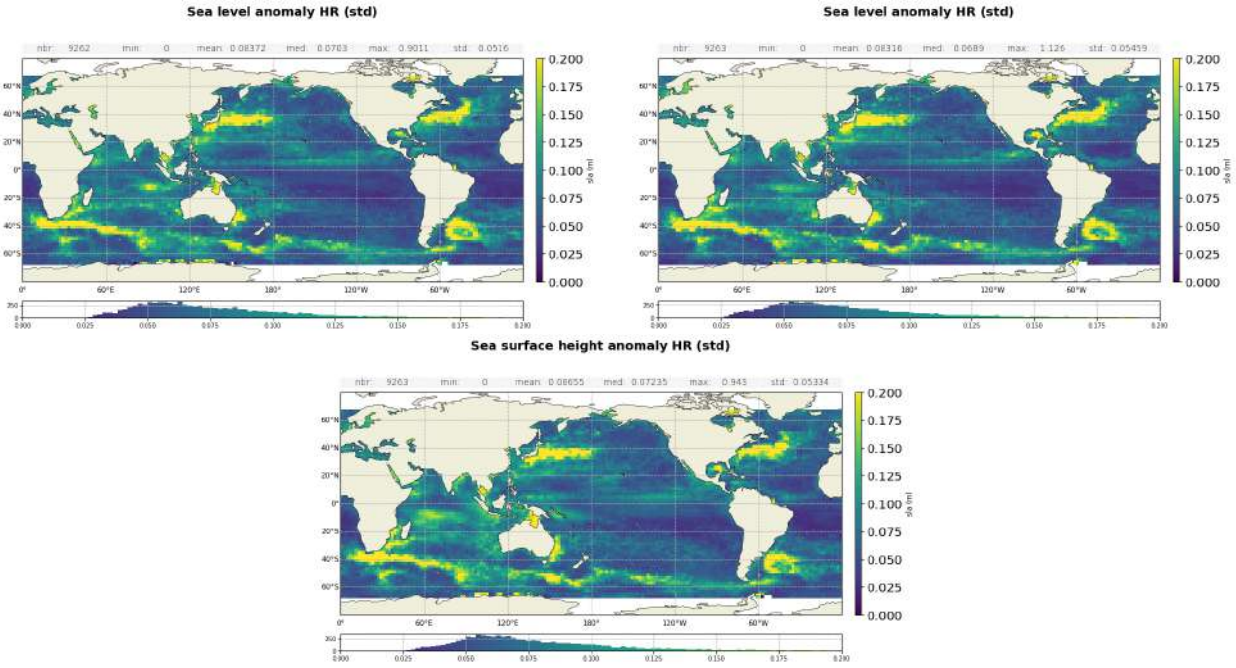

Figure 114: Maps of SSHA standard deviation for HR in meters for the year 2021 (top left), 2022 (top right) and 2023 (bottom).

8 Mean Sea Level trends

8.1. Computation of the Mean Sea Level

The Global Mean Sea Level (GMSL) is one of the most important indicators of the climate change. In the past two decades, sea level has been routinely measured from space using satellite altimetry techniques. Sentinel-6 MF satellite is taking over the responsibility as the reference mission to continue the long-term record of sea-surface height measurements. The role of Copernicus Sentinel-6 Michael Freilich is not only to extend the GMSL climate record, but also to monitor the changing height of the sea surface with greater precision than before.

Over the tandem phase of Sentinel-6 MF (till cycle 051), both Jason-3 and Sentinel-6 MF satellites flew on the same ground track, only 30s apart. They therefore measured the same ocean, allowing to calibrate Sentinel-6 MF. This allowed linking precisely the MSL time series of Jason-3 and Sentinel-6 MF. The uncertainty of the bias value between the two time series is less than 1 mm. The evolution of the ocean MSL can therefore be precisely observed on a continuous basis since 1993 thanks to the 5 reference missions: TOPEX/Poseidon, Jason-1 (from May 2002 to October 2008), Jason-2 (from October 2008 to May 2016), Jason-3 (from May 2016 to April 2022) and now Sentinel-6 MF (from April 2022 onwards).
Please note that the present GMSL analysis is performed using DT2021 L2P standards, which uses LR MLE4 data for S6-MF. In the upcoming DT2024, it will be updated to LR NR data.

Wet troposphere correction, inverse barometer correction, GIA (-0.3 mm/yr) are applied to calculate the MSL and the data series are linked together accurately thanks to the tandem flying phases. The following global biases are applied: 1.16 cm between T/P and Jason-1, 0.23 cm between Jason-1/Jason-2, -2.97 cm between Jason-2/Jason-3 and -0.21 cm for Jason-3/Sentinel-6 MF. The uncertainty relative to this Jason-3/Sentinel-6 MF global bias, which is exclusively computed on Sentinel-6 MF side B, is 0.2mm at 1 sigma.

An exhaustive overview of possible errors impacting the MSL evolution is given in [13]. Furthermore, annual and semi-annual signals are removed from the time series and a 2-month filter is applied. For more details about Mean Sea Level (MSL) estimation method, see the dedicated report on the MSL Aviso Website: http://www.aviso.altimetry.fr/msl. This report includes the description of the Mean Sea Level indicator, the comparisons between altimetry and tide gauges measurements, the comparisons between altimetry and ARGO+GRACE measurements and specific studies linked to MSL activities.

Though mean sea level trend is globally positive, it is inhomogeneously distributed over the ocean: locally, sea level rise or decline up to $\pm$10 mm/yr are observed as shown on the right panel of figure 115 (note that this map of regional MSL trends is estimated from multi-mission grids (Copernicus Climate Change Service products) in order to improve spatial resolution).

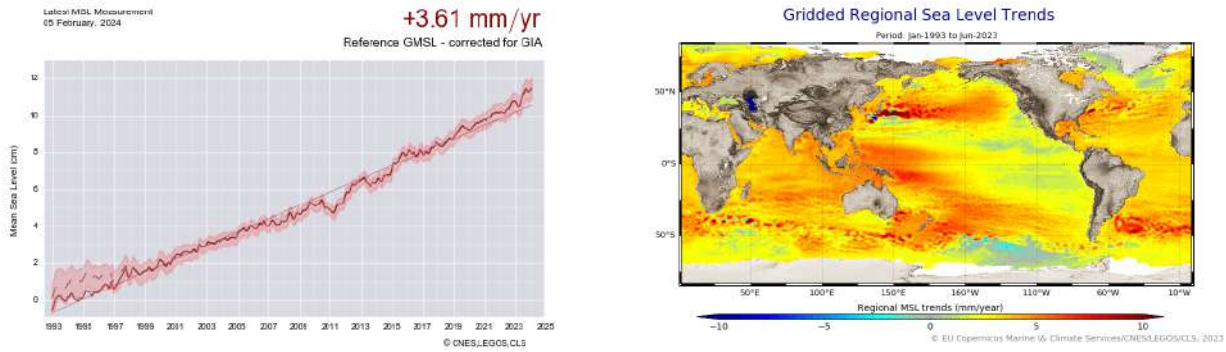

Figure 115: Global (left) and regional (right) MSL trends from 1993 onwards.

8.2. Comparison of LR MLE4, LR NR and HR GMSL

This section focusses on GMSL derived from Sentinel-6 MF from the switch to POS4-B to the end of 2023. The GMSL for LR (MLE4 and NR) and HR modes are plotted on figure 116, along with Jason-3 estimate over the same period. This GMSL is computed on a 2-months low-pass filtered data, after having removed the seasonal signals. Such computation is performed with an Ordinary Least Square (OLS) approach, using SSHA from L2 products as input. The details on the computation of the GMSL and its uncertainties are described in Guerou et al. (2022) [13].

Sentinel-6 MF LR MLE4 and LR NR show similar trends with slopes at 4.99 $\pm$ 1.23 mm/yr, 5.08 $\pm$ 1.23 mm/yr respectively. Over the period available here, the improvement brought by the numerical retracker in terms of long term stability cannot be demonstrated. It rather shows the stability of POS-4B retrievals. Over the same time period, Jason-3 GMSL trend is consistent with 5.39 $\pm$ 1.26 mm/yr. HR trend is higher, at 5.97 $\pm$ 1.23 mm/yr, which is probably the result of the absence of range walk correction (see below). These trends do not significantly change when using model wet tropospheric correction, as shown on the dashed curves of figure 116 and in table 9, suggesting a good stability of the radiometer-derived wet tropospheric correction. Uncertainties are given at the 1 sigma confidence level.

Please note that the side B GMSL presented here are computed on a small timescale (less than 28 months) and therefore are impacted by correlated noise leading to significant uncertainties.

Mission/mode	Trend with Rad WTC (mm/yr)	Trend with model WTC (mm/yr)
Sentinel-6 MF LR MLE4	4.99 $\pm$ 1.23	4.97 $\pm$ 1.22
Sentinel-6 MF LR NR	5.08 $\pm$ 1.23	5.05 $\pm$ 1.23
Sentinel-6 MF HR	5.97 $\pm$ 1.24	5.94 $\pm$ 1.23
Jason-3 MLE4	5.39 $\pm$ 1.26	5.34 $\pm$ 1.25

Table 9: GMSL trend values and corresponding 1 sigma uncertainties for Sentinel-6 MF LR, HR and Jason-3 (on the Sentinel-6 MF period), with AMR+HRMR and model wet tropospheric corrections. Computed over POS4-B period, i.e. from cycle 32 onwards.

Sentinel-6 MF GMSL are impacted by two known effects, **none of which are taken into account in the uncertainties computation**:

- the evolution of the PTR shape in the range direction. It impacts range (PTR dissymmetry) and SWH estimates (main lobe width) both in LR MLE4 and HR SAMOSA. Numerical retracker allows

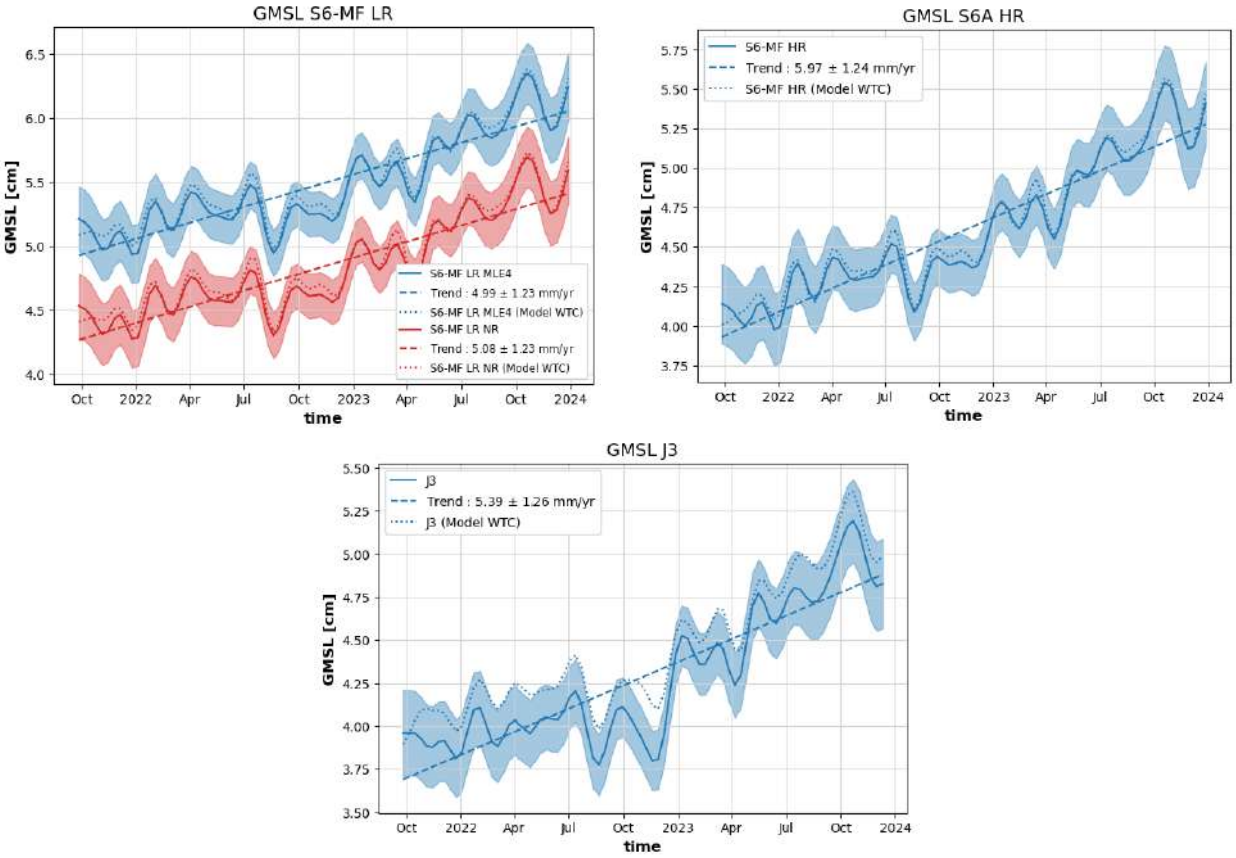

Figure 116: GMSL from Sentinel-6 MF LR data (top left), Sentinel-6 MF HR data (top right) and from Jason-3 GDR-F data with a 1.645 sigma confidence interval. Computed over Sentinel-6 MF POS4-B period, i.e. from cycle 32 onwards.

accounting for the PTR shape evolution thanks to the use of in-flight PTRs. HR NR is implemented in the PB F09 deployed in February 2024.

- the evolution of the PTR shape in the azimuth direction, impacting HR range only. It is corrected thanks to the range walk correction, that is available in PB F09. The impact of this correction has been estimated at 3.1 mm/yr, based on Dinardo 2022 study [10]. Please note that the Dinardo 2022 study only covers the first 9 months of side B, from September 2021 to June 2022, and that values may be different after the second half of 2022 because of an expected ongoing stabilization.

9 System Requirements

In this section, the system requirements are verified for reprocessed data, in LR MLE4 and NR and in HR.

9.1. LR

9.1.1. R-S-00260

Requirement	Status
For low-resolution ALT-NTC products, the standard deviation of the 1-second along-track averaged corrected low-resolution altimeter range measurements shall be less than 2.83 cm. Note: This requirement is based on the apportionment given in the table of the Sentinel-6 low-resolution altimetry error budget at the end of the document. Note: Like all performance requirements on the altimeter, unless specified otherwise, this specifies the maximum global RMS error over open ocean. Note: A goal is 1.73 cm.	Not addressed in this report

Table 10: R-S-00260

9.1.2. R-S-00270

Requirement	Status
For low-resolution ALT-NTC products, the noise of the 1-second along-track average of the low-resolution Ku-band altimeter range measurements shall be less than 1.5 cm at 2 m significant wave height. Note: the requirement is applicable after ground re-tracking. Note: The upper limit depends on SWH: 1.2 cm at 1 m SWH, 1.5 cm at 2 m SWH, 2.4 cm at 5 m SWH, and 3.2 cm at 8 m SWH. Note: A goal is 1.0 cm at 2 m SWH	**OK**

Table 11: R-S-00270

To estimate the noise of 1-second along-track average of the LR Ku-band altimeter range, we analyse "data_01/ku/range_ocean_rms" variable from LR products. It contains the standard deviation of 20 Hz measurements used for the compression to 1hz. To retrieve 1 Hz level of noise, this value is divided by the square root of the number of valid 20Hz measurements used to compute 1Hz range (the corresponding variable from LR products is "data_01/ku/range_ocean_numval").

The resulting 1 Hz level of noise averaged over the complete period is plotted function of SWH on figure 117, left panel. Noise levels are similar for MLE4 and NR except at very low SWH. As expected, Sentinel-6 MF LR noise level is well below Jason-3 level and below the system requirement (purple curve) over almost all the SWH spectrum. For 1 m wave, the level of noise is slightly above the note in the requirement with a value of 1.21 cm and an upper limit at 1.2 cm. Please note that the requirement itself, i.e. the 2m SWH limit, is met. Table 12 reports the level of noise for the stated SWH values.

This noise level is stable in time, as shown on the cyclic monitoring of figure 117, right panel.

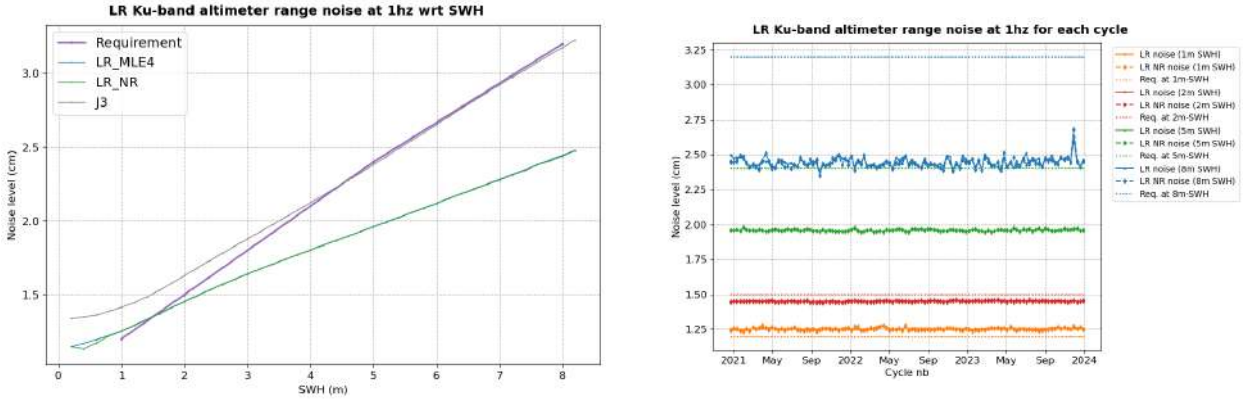

Figure 117: 1 Hz noise of LR Ku-band altimeter range. Left panel: noise function of SWH for Sentinel-6 MF LR MLE4 (blue for MLE4, green for NR) and Jason-3 (black); the purple line represents the requirement thresholds. Right panel : noise level computed for each cycle and at 1, 2, 5 and 8 m-wave (solid lines for MLE4, dashed lines for NR) and the corresponding requirement levels (dotted lines).

SWH	Requirement	Noise level MLE4	Noise level NR
1 m	**1.2 cm**	**1.25 cm**	**1.25 cm**
2 m	1.5 cm	1.46 cm	1.46 cm
5 m	2.4 cm	1.96 cm	1.96 cm
8 m	3.2 cm	2.44 cm	2.44 cm

Table 12: 1 Hz noise of LR Ku-band altimeter range at 1, 2, 5 and 8 m-wave.

9.1.3. R-S-00280

Requirement	Status
For low-resolution ALT-NTC products, the noise of the 1-second along-track average of the C-band altimeter range measurements shall be less than 5.7 cm at 2 m significant wave height. Note: the requirement is applicable after ground re-tracking. Note: The upper limit depends on SWH: 4.5 cm at 1 m SWH, 5.7 cm at 2 m SWH, 9.1 cm at 5 m SWH, and 12.0 cm at 8 m SWH	**OK**

Table 13: R-S-00280

Similarly to Ku-band, we analyse "data_01/c/range_ocean_rms" variable from LR products to estimate the noise of 1-second along-track average of the LR C-band altimeter range.

The resulting 1 Hz level of noise averaged over the complete period is plotted as a function of SWH on figure 118, left panel. Sentinel-6 MF LR noise level is and below the system requirement (purple curve) over all the SWH spectrum, except once again at 1m-SWH (4.6 cm for a limit of 4.5 cm). Please note that the requirement itself, i.e. the 2 m SWH limit, is met. Table 14 reports the level of noise for the stated SWH values.

This noise level is stable in time, as shown on the cyclic monitoring of figure 118, right panel.

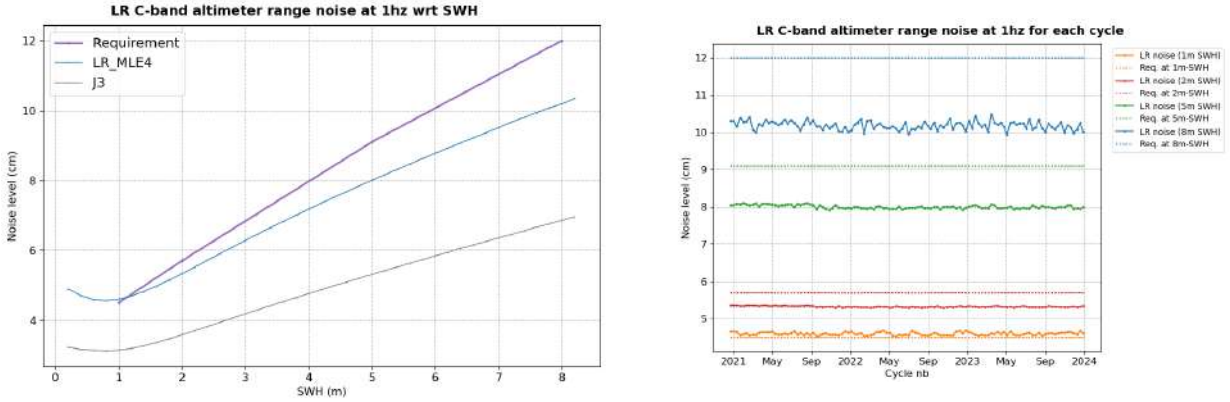

Figure 118: 1 Hz noise of LR C-band altimeter range. Left panel: noise function of SWH for Sentinel-6 MF LR and Jason-3; the purple line represents the requirement thresholds. Right panel : noise level computed for each cycle and at 1, 2, 5 and 8 m-wave (solid lines) and the corresponding requirement levels (dashed lines).

SWH	Requirement	Noise level
1 m	**4.5 cm**	**4.6 cm**
2 m	5.7 cm	5.3 cm
5 m	9.1 cm	8.0 cm
8 m	12 cm	10.3 cm

Table 14: 1 Hz noise of LR C-band altimeter range at 1, 2, 5 and 8 m-wave.

9.1.4. R-S-00290

Requirement	Status
For low-resolution ALT-NTC products, the contribution of the ionosphere correction error to the standard deviation of the 1-second along-track averaged corrected low-resolution altimeter range measurements shall be less than 0.5 cm. Note: Derived from C and Ku band and averaged over 200 km. Note: Like all performance requirements on the altimeter, unless specified otherwise, this specifies the maximum global RMS error over open ocean. Note: A goal is 0.3 cm	**OK**

Table 15: R-S-00290

To quantify the contribution of the ionosphere correction error to the standard deviation of 1 Hz corrected LR range, several metrics are checked.

A first estimation of filtered ionosphere correction error is performed by checking the noise between consecutive measurements. The results show a very low level of noise, compliant with requirements.

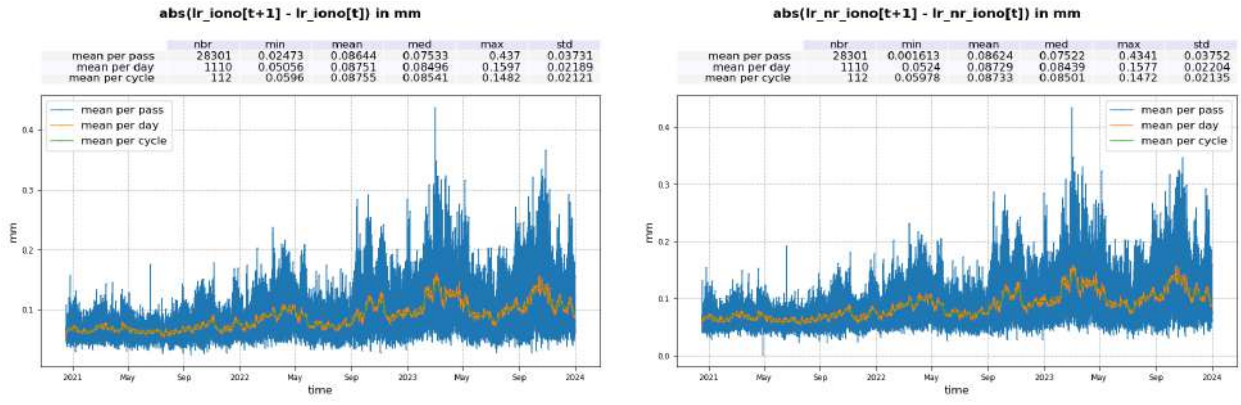

*Figure 119: Absolute value of consecutive filtered ionosphere correction measurement for MLE4 (**left**) and NR (**right**). Mean per pass (blue), mean per day (orange) and mean per cycle (green).*

Comparison to Jason-3 filtered ionosphere correction highlights a standard deviation ranging between 2 and 4.5 mm (figure 120) for both retrackings. And finally, comparison to ionosphere correction derived from

GIM model shows a standard deviation ranging between 3 mm and 1.5 cm (figure 121) for both retrackings. These values are all within requirement.

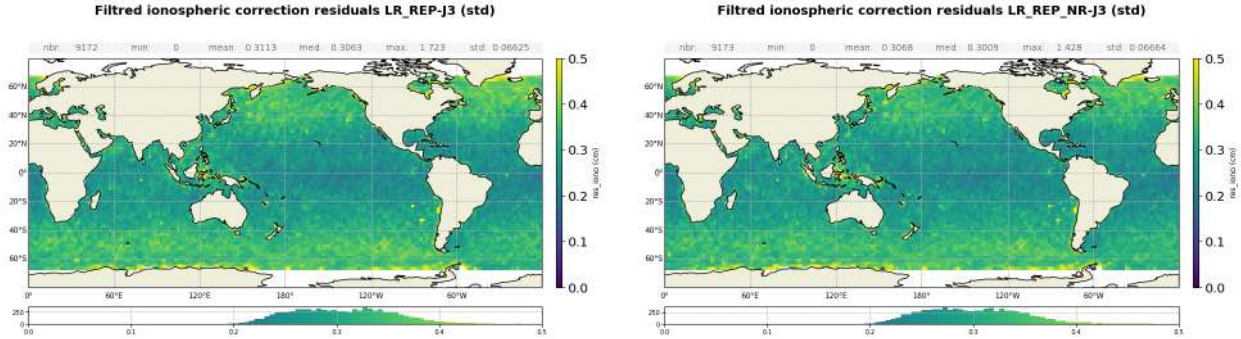

*Figure 120: Standard deviation gridded map of Altimeter Filtered Ionosphere correction Sentinel-6 MF-Jason-3 difference (cm) for MLE4 (**left**) and NR (**right**). Computed over the tandem phase.*

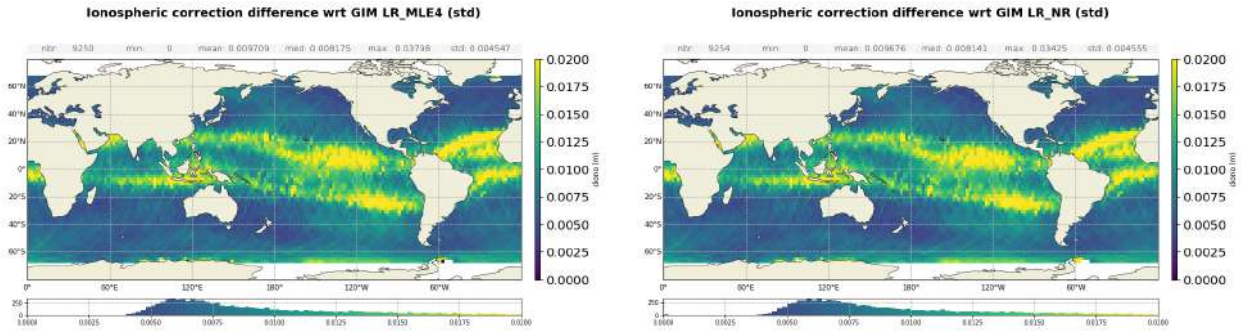

*Figure 121: Standard deviation gridded map of the difference between Altimeter Filtered Ionosphere correction and GIM model (cm) for MLE4 (**left**) and NR (**right**). Computed over year 2023.*

9.1.5. R-S-00300

Requirement	Status
For low-resolution ALT-NTC products, the contribution of the sea state bias error to the standard deviation of the 1-second along-track averaged corrected low-resolution altimeter range measurements shall be less than 2.0 cm. Note: Like all performance requirements on the altimeter, unless specified otherwise, this specifies the maximum global RMS error over open ocean. Note: A goal is 1.0 cm	**OK**

Table 16: R-S-00300

As for ionosphere correction, a first estimation of the SSB error is performed by checking the noise between consecutive measurements. The results show a low level of noise, below the cm (figure 122) for both LR retrackings.

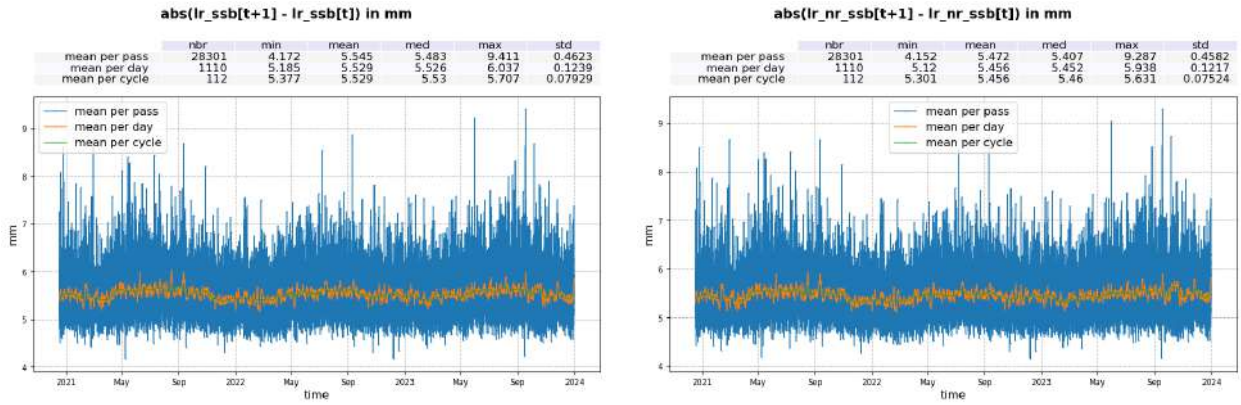

*Figure 122: Absolute value of consecutive LR sea state bias measurement for LR MLE4 (**left**) and NR (**right**). Mean per pass (blue), mean per day (orange) and mean per cycle (green).*

Comparison to Jason-3 SSB highlights a standard deviation ranging between 4.5 mm and 1.5 cm (figure 123) for both retrackings. These values are within requirement.

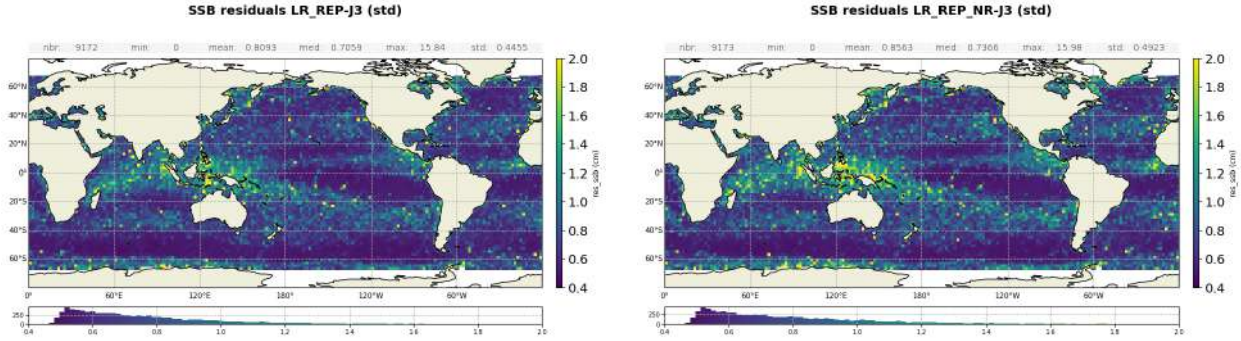

*Figure 123: Standard deviation gridded map of Ku-band SSB difference: Sentinel-6 MF LR minus Jason-3 computed over the complete tandem period for MLE4 (**left**) and NR (**right**).*

9.1.6. R-S-00310

Requirement	Status
For low-resolution ALT-NTC products, the contribution of the dry tropospheric correction error to the standard deviation of the 1-second along-track averaged corrected low-resolution altimeter range measurements shall be less than 0.7 cm. Note: this requirement applies to the model to be used to calculate the dry troposphere model. Note: Like all performance requirements on the altimeter, unless specified otherwise, this specifies the maximum global RMS error over open ocean. Note: A goal is 0.5 cm	**OK**

Table 17: R-S-00310

The dry troposphere correction model are identical between Jason-3 and Sentinel-6 MF products: same model and same estimation from model.

Analysis have shown that the two retrievals are indeed perfectly in line (see figure 124).

System requirement for Jason-3 dry troposphere correction is the same as Sentinel-6 MF present requirement, and it has been shown that Jason-3 dry troposphere correction is compliant.

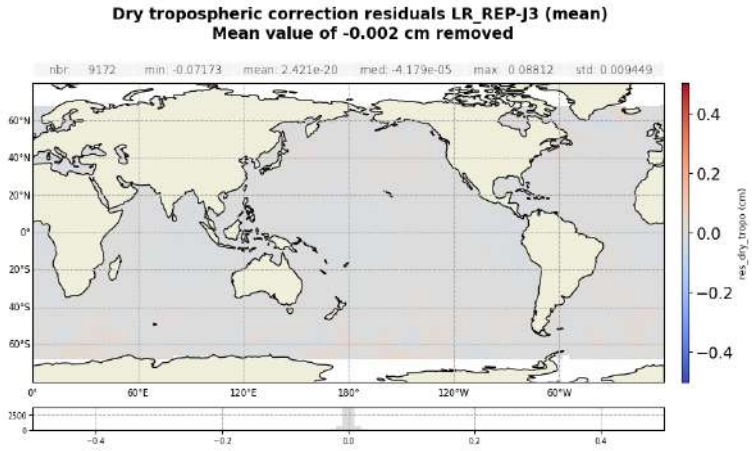

Figure 124: Mean gridded map of dry tropospheric correction difference: Sentinel-6 MF LR minus Jason-3. Computed over the tandem phase.

9.1.7. R-S-00320

Requirement	Status
For low-resolution ALT-NTC products, the contribution of the wet tropospheric correction error to the standard deviation of the 1-second along-track averaged corrected low-resolution altimeter range measurements shall be less than 1.0 cm. Note: Like all performance requirements on the altimeter, unless specified otherwise, this specifies the maximum global RMS error over open ocean. Note: A goal is 0.8 cm	**OK**

Table 18: R-S-00320

A first estimation of AMR-C WTC error is performed by checking the noise between consecutive measurements. The results show a very low level of noise, below 2 mm (figure 125).

Comparison to Jason-3 AMR WTC highlights a standard deviation below 8 mm (figure 126). These values are within requirement.

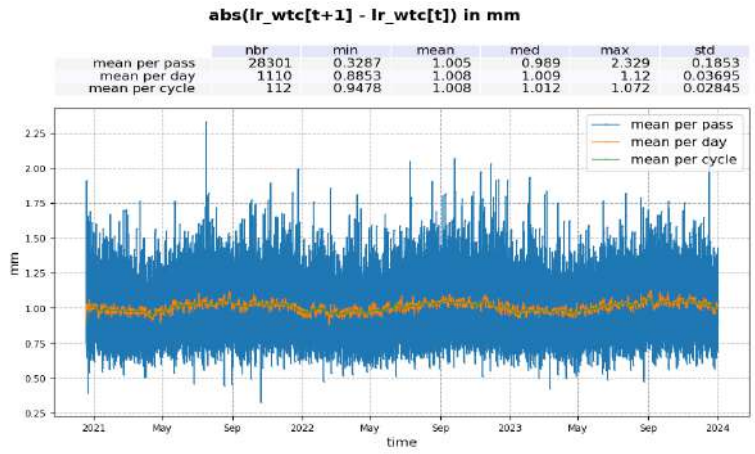

Figure 125: Absolute value of consecutive AMR-C WTC measurement in mm. Mean per pass (blue), mean per day (orange) and mean per cycle (green).

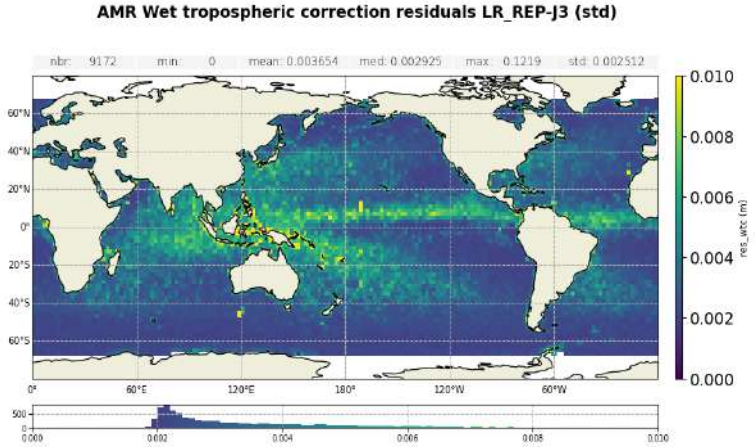

Figure 126: STD gridded map of AMR WTC difference: Sentinel-6 MF LR minus Jason-3, in m. Computed over the tandem phase.

9.1.8. R-S-00330

Requirement	Status
For low-resolution ALT-NTC products, the standard deviation of the determination of the radial component of the orbit shall be less than 1.5 cm. Note: This requirement is applicable to the orbital solution derived from the combined set of data from DORIS, GNSS-POD and LRA. Note: Orbit errors have a larger than 1000 km length scale, significantly different from the 1 Hz altimetry noise. Nevertheless, the orbit error is added in a RSS sense, presuming that the error is uncorrelated from cycle to cycle at the same location. Note: a goal is 1.0 cm	Not addressed in this report

Table 19: R-S-00330

9.1.9. R-S-00340

Requirement	Status
For low-resolution ALT-NTC products, the standard deviation of the 1-second along-track averaged corrected low-resolution measurements of sea surface height shall be less than 3.20 cm. Note: This requirement is based on the apportionment given in the table of the Sentinel-6 low-resolution altimetry error budget at the end of the document. Note: Like all performance requirements on the altimeter, unless specified otherwise, this specifies the maximum global RMS error over open ocean. Note: A goal is 1.99 cm	**OK**

Table 20: R-S-00340

To verify this requirement, the crossover analysis presented in section 6.2. is used. The standard deviation of corrected LR SSH difference is centred around 4.7 cm (see figure 91) in both MLE4 and NR. It means that the error is of 3.3 cm (standard deviation divided by $\sqrt{2}$). This value is slightly above requirement. However, looking at a region with low variability, for example the pacific patch, the error is of 2.25 cm in average. On a cyclic basis, this error is always below the requirement limit of 3.2 cm as shown on figure 127. The only exception is cycle 25 in the NR dataset.

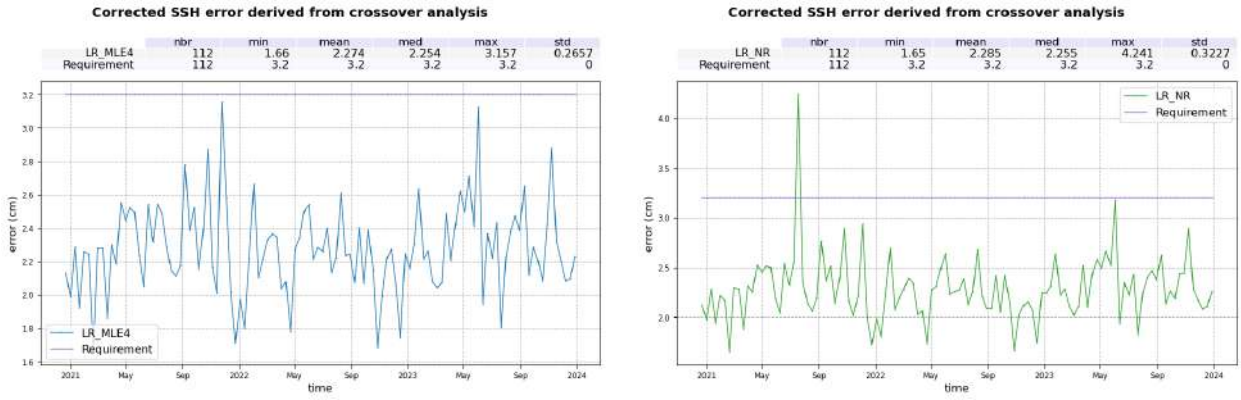

*Figure 127: Corrected LR SSH error derived from crossover analysis with a selection over Pacific patch (latitude in [-24.5°N; -3°N] and longitude in [220°E; 246°E]), in cm for MLE4 (**left**) and for NR (**right**). The error equals to the standard deviation of the SSH difference divided by $\sqrt{2}$. Computed on a cyclic basis.*

9.1.10. R-S-00350

Requirement	Status
For low-resolution ALT-NTC products, the uncertainty of 1-second along-track averaged low-resolution measurements of significant wave height in the range 0.5 to 8 m shall be less than 15 cm plus 5% of significant wave height. Note: This is based on the combination of noise and systematic error. Note: A goal is 10 cm plus 5% of significant wave height	**OK**

Table 21: R-S-00350

LR Ku-band SWH uncertainties are computed by adding the squares of the SWH noise and the SWH bias to model ERA-5 SWH, and then taking its square root. The results are plotted on figure 128. It shows a good consistency between the datasets, the difference being below requirement limit over the complete SWH spectrum.

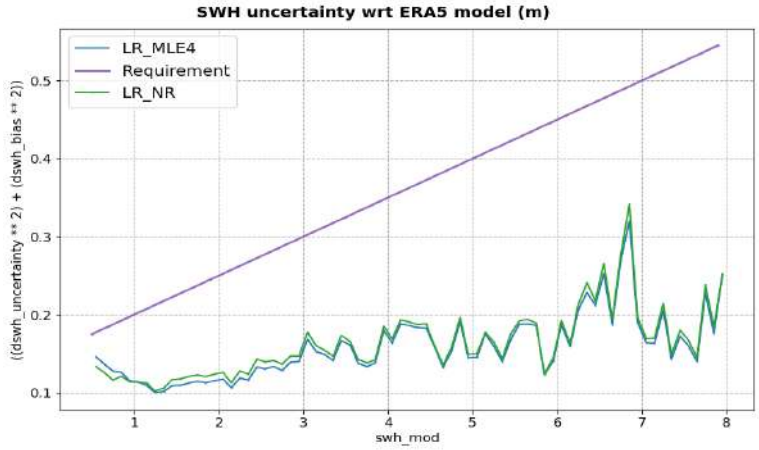

Figure 128: SWH difference between Sentinel-6 MF LR data and ERA-5 SWH, plotted function of ERA-5 SWH for MLE4 (red) and NR (green). Computed over Sentinel-6 MF cycle 110. Purple lines represent requirement limits. Results are identical for all cycles.

9.1.11. R-S-00355

Requirement	Status
For low-resolution ALT-NTC products, significant wave heights shall be provided up to at least 20 m. Note: The measurement performance under high sea state conditions will be determined during commissioning	**OK**

Table 22: R-S-00355

Figure 129 shows the maximum value per cycle of Sentinel-6 MF LR SWH. As expected, the values are above 20 m in MLE4, while they are at 20 m in NR.

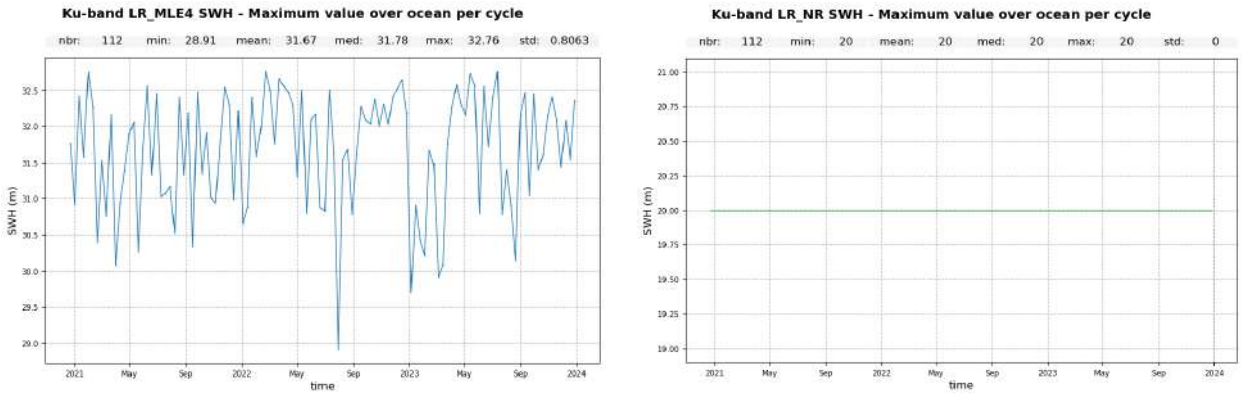

*Figure 129: Maximum value of Sentinel-6 MF LR SWH per cycle for MLE4 (**left**) and NR (**right**).*

9.1.12. R-S-00360

Requirement	Status
For low-resolution ALT-NTC products, the uncertainty of 1-second along-track averages of 10 meter wind speed over ocean surfaces, derived from low-resolution altimeter measurements, shall be better than 1.5 m/s for wind speeds in the range 3 m/s to 20 m/s. Note: Wind speed refers to the wind (not neutral wind) speed at a reference height of 10 meters above the sea surface. Note: This wind speed accuracy requirement translates to an accuracy requirement on the backscatter. Note: A goal is 1.0 m/s	**OK**

Table 23: R-S-00360

To verify the uncertainty of Sentinel-6 MF LR altimeter wind-speed, a comparison to model is performed. The model wind speed used is derived from U and V components provided in L2 product ("data_01/wind_speed_mod_ and "data_01/wind_speed_mod_v"). Difference between altimeter and model wind speed is plotted on figure 130 function of model wind speed. Values are within requirement.

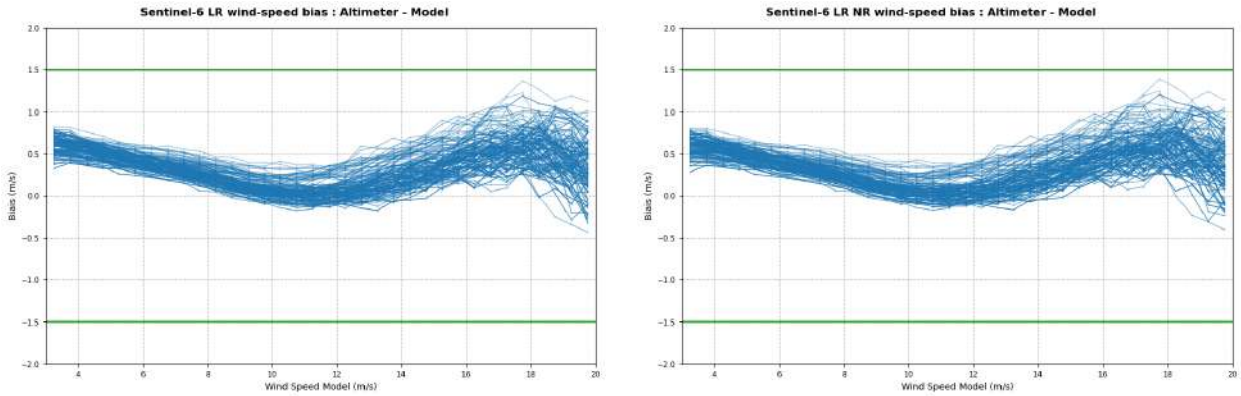

*Figure 130: Difference between Altimeter LR wind speed and model wind speed function of model wind speed, in m/s for MLE4 (**left**) and NR (**right**). Computed for all cycles (right, darker curves correspond to more recent cycles). Green lines represent requirement limits.*

9.1.13. R-S-00370

Requirement	Status
For low-resolution ALT-NTC products, the absolute accuracy of 1-second along-track averaged low-resolution measurements of normalized radar cross-section at Ku-band and vertical incidence, in the range 7 to 16 dB, shall be better than 0.3 dB. Note: This value (0.3 dB) is not the value at satellite level (1 dB), but it is achieved after external in-flight calibration to ensure coherence with other missions. In other words, 0.3 dB is the global value, what allows 1 dB at satellite level, to be compensated by the ground processing. Note: This requirement also sets limits on the accuracy of sigma0 attenuation correction to be supplied by the radiometer	Not addressed in this report

Table 24: R-S-00370

The absolute accuracy of the LR sigma0 is not addressed in this report as there is currently no facility available to measure it.

9.2. HR

9.2.1. R-S-00680

Requirement	Status
For high-resolution ALT-NTC products, the standard deviation of the 1-second along-track averaged corrected high-resolution altimeter range measurements shall be less than 2.53 cm. Note: This requirement is based on the apportionment given in the table of the Sentinel-6 high-resolution altimetry error budget at the end of the document. Note: Note: Like all performance requirements on the altimeter, unless specified otherwise, this specifies the maximum global RMS error over open ocean. Note: Note: A goal is 1.49 cm.	Not addressed in this report

Table 25: R-S-00680

9.2.2. R-S-00690

Requirement	Status
For high-resolution ALT-NTC products, the noise of the 1-second along-track average of the high-resolution Ku-band altimeter range measurements shall be less than 0.8 cm at 2 m significant wave height. Note: the requirement is applicable after ground re-tracking. Note: The upper limit depends on SWH: 0.7 cm at 1 m SWH, 0.8 cm at 2 m SWH, 1.3 cm at 5 m SWH, and 2.0 cm at 8 m SWH. Note: A goal is 0.5 cm at 2m SWH	**OK**

Table 26: R-S-00690

Similarly to LR, we analyse "data_01/ku/range_ocean_rms" variable from HR products to estimate the noise of 1-second along-track average of the HR Ku-band altimeter range.

The resulting 1 Hz level of noise averaged over the complete period is plotted function of SWH on figure 131, left panel. As expected, Sentinel-6 MF HR noise level is well below Jason-3 and Sentinel-3A levels. However, Sentinel-6 MF HR noise level is above the additional note in the requirement (purple curve) for 5 m and 8 m wave upper limits. Please note that the requirement itself, i.e. the 2 m SWH limit, is met. Table 27 reports the level of noise for the stated SWH values.

Please note that the use of a numerical retracking for HR in PB F09 improves noise levels.

This noise level is stable in time, as shown on the cyclic monitoring of figure 131, right panel.

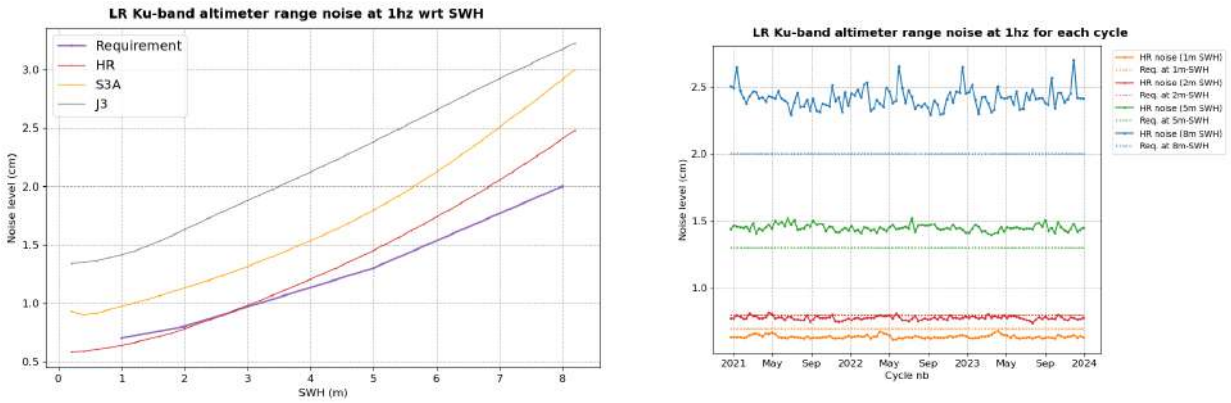

Figure 131: 1 Hz noise of HR Ku-band altimeter range, in cm. Left panel: noise function of SWH in m for Sentinel-6 MF HR and Jason-3; the purple line represents the requirement thresholds. Right panel : noise level computed for each cycle and at 1, 2, 5 and 8 m-wave (solid lines) and the corresponding requirement levels (dashed lines).

SWH	Requirement	Noise level
1 m	0.7 cm	0.64 cm
2 m	0.8 cm	0.77 cm
5 m	**1.3 cm**	**1.44 cm**
8 m	**2.0 cm**	**2.39 cm**

Table 27: 1 Hz noise of HR Ku-band altimeter range at 1, 2, 5 and 8 m-wave.

9.2.3. R-S-00700

Requirement	Status
For high-resolution ALT-NTC products, the contribution of the ionospheric correction error to the standard deviation of the 1-second along-track averaged corrected high-resolution altimeter range measurements shall be less than 0.5 cm. Note: Derived from C and Ku band and averaged over 200 km. Note: Like all performance requirements on the altimeter, unless specified otherwise, this specifies the maximum global RMS error over open ocean. Note: A goal is 0.3 cm	**OK, see section 9.1.4.**

Table 28: R-S-00700

9.2.4. R-S-00710

Requirement	Status
For high-resolution ALT-NTC products, the contribution of the sea state bias error to the standard deviation of the 1-second along-track averaged corrected high-resolution altimeter range measurements shall be less than 2.0 cm. Note: Since the sea state bias model will have to be determined for the altimeter data itself, the error can only be evaluated based on day-2 processing. Note: Like all performance requirements on the altimeter, unless specified otherwise, this specifies the maximum global RMS error over open ocean. Note: A goal is 1.0 cm	**OK**

Table 29: R-S-00710

As for LR data, a first estimation of HR SSB error is performed by checking the noise between consecutive measurements. The results show a low level of noise, below the cm (figure 132).

Comparison to Jason-3 SSB highlights a standard deviation ranging between 4.5 mm and 1.6 cm (figure 133). These values are within requirement.

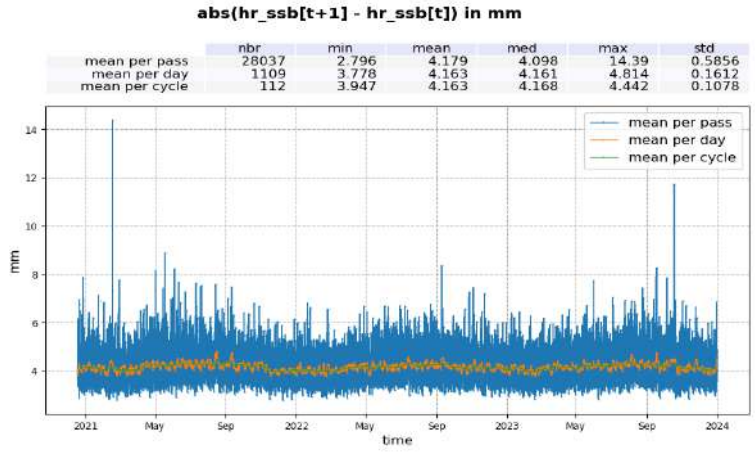

Figure 132: Absolute value of consecutive HR sea state bias measurement. Mean per pass (blue), mean per day (orange) and mean per cycle (green).

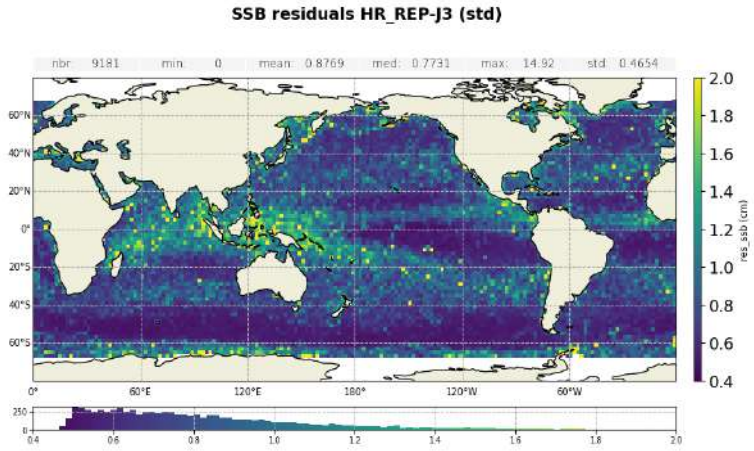

Figure 133: Standard deviation gridded map of Ku-band SSB difference: Sentinel-6 MF HR minus Jason-3 computed over the complete tandem period.

9.2.5. R-S-00720

Requirement	Status
For high-resolution ALT-NTC products, the contribution of the dry tropospheric correction error to the standard deviation of the 1-second along-track averaged corrected high-resolution altimeter range measurements shall be less than 0.7 cm. Note: this requirement applies to the model to be used to calculate the dry troposphere model. Note: Like all performance requirements on the altimeter, unless specified otherwise, this specifies the maximum global RMS error over open ocean. Note: A goal is 0.5 cm	**OK, see section 9.1.6.**

Table 30: R-S-00720

9.2.6. R-S-00730

Requirement	Status
For high-resolution ALT-NTC products, the contribution of the wet tropospheric correction error to the standard deviation of the 1-second along-track averaged corrected high-resolution altimeter range measurements shall be less than 1.0 cm. Note: Like all performance requirements on the altimeter, unless specified otherwise, this specifies the maximum global RMS error over open ocean. Note: A goal is 0.8 cm	**OK, see section 9.1.7.**

Table 31: R-S-00730

9.2.7. R-S-00740

Requirement	Status
For high-resolution ALT-NTC products, the standard deviation of the determination of the radial component of the orbit shall be less than 1.5 cm. Note: This requirement is applicable to the orbital solution derived from the combined set of data from DORIS, GNSS-POD and LRA. Note: Orbit errors have a larger than 1000 km length scale, significantly different from the 1 Hz altimetry noise. Nevertheless, the orbit error is added in a RSS sense, presuming that the error is uncorrelated from cycle to cycle at the same location. Note: A goal is 1.0 cm	Not addressed in this report

Table 32: R-S-00740

9.2.8. R-S-00750

Requirement	Status
For high-resolution ALT-NTC products, the standard deviation of the 1-second along-track averaged corrected high-resolution measurements of sea surface height shall be less than 2.94 cm. Note: This requirement is based on the apportionment given in the table of the Sentinel-6 high-resolution altimetry error budget at the end of the document. Note: Like all performance requirements on the altimeter, unless specified otherwise, this specifies the maximum global RMS error over open ocean. Note: A goal is 1.80 cm	**OK**

Table 33: R-S-00750

To verify this requirement, the crossover analysis presented in section 6.2. is used. The standard deviation of corrected HR SSH difference is centred around 4.5 cm (see figure 91). It means that the error is of 3.2 cm (standard deviation divided by $\sqrt{2}$). This value is slightly above requirement. However looking at a region with low variability, for example the pacific patch, the error is of 2.02 cm in average. On a cyclic basis, this error is always below the requirement limit of 3.2 cm as shown on figure 127, except for two cycles (19 and 24).

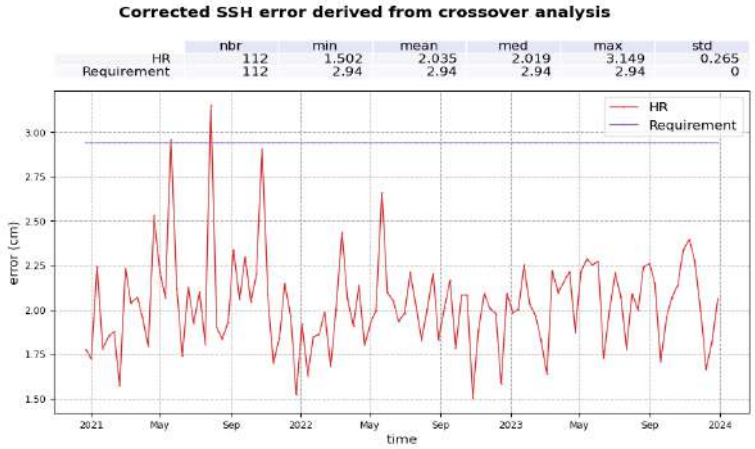

Figure 134: Corrected HR SSH error derived from crossover analysis with a selection over Pacific patch (latitude in [-24.5 °N; -3 °N] and longitude in [220 °E; 246 °E]), in cm. The error equals to the standard deviation of the SSH difference divided by $\sqrt{(2)}$. Computed on a cyclic basis.

9.2.9. R-S-00760

Requirement	Status
For high-resolution ALT-NTC products, the uncertainty of 1-second along-track averaged high-resolution measurements of significant wave height in the range 0.5 to 8 m shall be less than 15 cm plus 5% of significant wave height. Note: This is based on the combination of noise and systematic error. Note: A goal is 10 cm plus 5% of significant wave height	**NOK**

Table 34: R-S-00760

HR Ku-band SWH are compared to SWH derived from ERA-5 model on figure 135. Sentinel-6 MF HR SWH are not compliant with requirement. Please note that the use of a numerical retracking for HR in PB F09 improves the uncertainties.

Figure 135: SWH difference between Sentinel-6 MF HR data and ERA-5 SWH, plotted function of ERA-5 SWH. Computed over Sentinel-6 MF cycle 110. Green lines represent requirement limits. Results are identical for all cycles.

9.2.10. R-S-00765

Requirement	Status
For high-resolution ALT-NTC products, significant wave heights shall be provided up to at least 20 m. Note: The measurement performance under high sea state conditions will be determined during commissioning	**OK**

Table 35: R-S-00765

Figure 136 shows the maximum value per cycle of Sentinel-6 MF HR SWH. It equals to 20 m for all cycles, which is consistent with the requirement.

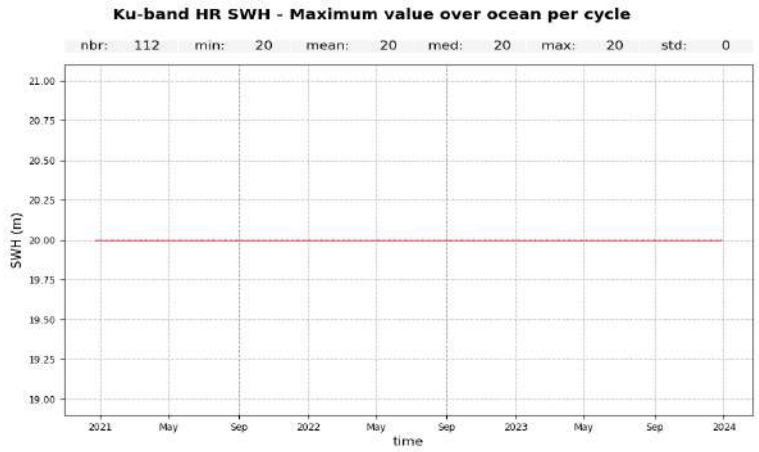

Figure 136: Maximum value of Sentinel-6 MF HR SWH per cycle.

9.2.11. R-S-00770

Requirement	Status
For high-resolution ALT-NTC products, the uncertainty of 1-second along-track averages of 10 meter wind speed over ocean surfaces, derived from high-resolution altimeter measurements, shall be better than 1.5 m/s for wind speeds in the range 3 m/s to 20 m/s. Note: Wind speed refers to the wind (not neutral wind) speed at a reference height of 10 meters above the sea surface. Note: This wind speed accuracy requirement translates to an accuracy requirement on the backscatter Note: A goal is 1.0 m/s	**OK**

Table 36: R-S-00770

As for LR, a comparison to model is performed to verify the uncertainty of Sentinel-6 MF HR altimeter wind-speed. Difference between altimeter and model wind speed is plotted on figure 137 function of model wind speed. Values are within requirement.

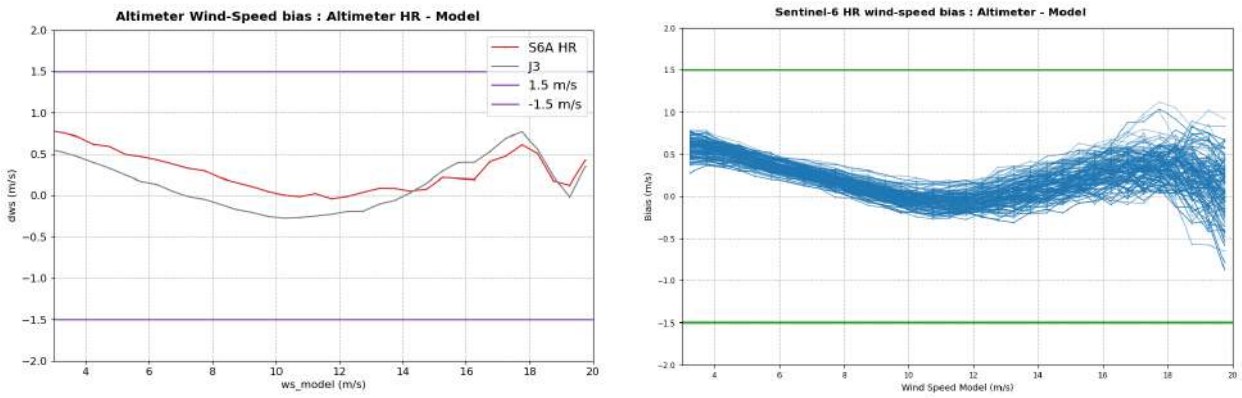

Figure 137: Difference between Altimeter HR wind speed and model wind speed function of model wind speed, in m/s. Computed over Sentinel-6 MF cycle 110 (left) and for all cycles (right, darker curves correspond to more recent cycles). Green lines represent requirement limits.

9.2.12. R-S-00780

Requirement	Status
For high-resolution ALT-NTC products, the absolute accuracy of 1-second along-track averaged high-resolution measurements of normalized radar cross-section at Ku-band and vertical incidence, in the range 7 to 16 dB, shall be better than 0.3 dB. Note: This value (0.3 dB) is not the value at satellite level (1 dB), but it is achieved after external in-flight calibration to ensure coherence with other missions. In other words, 0.3 dB is the global value, what allows 1 dB at satellite level, to be compensated by the ground processing. Note: This requirement also sets limits on the accuracy of sigma0 attenuation correction to be supplied by the radiometer	Not addressed in this report

Table 37: R-S-00780

The absolute accuracy of the HR sigma0 is not addressed in this report as there is currently no facility available to measure it.

10 Conclusions

Sentinel-6 MF was launched on November 21th, 2020 and reaches its operational orbit on December 17th 2020. From this date until April 7th, 2022, Jason-3 and Sentinel-6 MF were flying in tandem formation, with only 30 seconds delay, before Jason-3 was moved to the interleaved orbit. On April 7th 2022, Sentinel-6 MF became the reference mission in DUACS mission, taking on the responsibility to extend the global sea level record on the reference ground track started in 1992 by Topex/Poseidon and continued by the Jason's series.

In 2023, a new Numerical Retracking has been added in LR processings in Sentinel-6 MF data in PB F08, enabling the use of in-flight PTR, thus eliminating the need of instrumental LUT corrections. The entire time series have been reprocessed using this processing baseline. The calval assessment of this reprocessing is available online [4] and includes a detailed analysis of the Sentinel-6 MF/Jason-3 tandem phase. Most notably, it demonstrated the improvements brought by the Numerical Retracking in the consistency between Sentinel-6 MF and Jason-3 as well as in reducing dependencies of the range, ionospheric correction and SSHA residuals to SWH variations.

The main points of the present performance assessment are summarized below:

- Ocean data availability is excellent with a percentage above 99% in both LR and HR modes (in LMRC only mode in HR).
- Data quality is also very good with 11.8 %, 11.6 % and 10.3 % of measurements not consistent with altimeter and radiometer parameters threshold criterion in LR MLE4, LR NR and HR respectively.
- HR mode is impacted by the remaining effect of ocean vertical velocity. The next processing baseline F09 (deployed in February 2024) provides a correction for this effect. The absence of skewness parameter in the HR processing does not allow to properly compare HR range derived parameter to LR data or to Jason-3. Please note that in the F09 processing baseline, the HR numerical retracker uses the same skewness coefficient as in LR.
- At crossovers, Sentinel-6 MF shows very good performance with errors of 3.3 cm, 3.3 cm and 3.2 cm for LR MLE4, LR NR and HR respectively. Jason-3 standard deviation is similar to LR.
- At crossovers between Sentinel-6 MF and Jason-3, SSH performance presents excellent results with an SLA bias of about -1.7 cm, -1.1 cm and 0.1 cm for LR MLE4, LR NR and HR respectively.
- The time series is still to short to properly estimate the impact of NR on LR SSHA long term stability and MSL estimation. In HR, NR and range walk correction are implemented in the PB F09, improving the long term stability.

The compliance status to system requirements shows once again the excellent quality of Sentinel-6 MF data, especially for LR dataset. The only exception is due to the remaining impact of ocean vertical velocity on HR data, with HR SWH uncertainty above requirement (R-S-00760), that are corrected by the PB F09.

11 References

References

[1] Sentinel-6A user handbook available at https://eumetsatspace.atlassian.net/wiki/spaces/SEN6/overview

[2] 2022 Annual Report of Sentinel-6 MF validation and cross calibration activities available at : https://user.eumetsat.int/s3/eup-strapi-media/S6_A_2022_annual_report_v1_2_2a133d5f61.pdf

[3] Product notice for Sentinel-6 MF Processing Baseline F06 available at : https://www.eumetsat.int/media/50743

[4] Sentinel-6 MF F08 Reprocessing Calval Assessment available at : https://user.eumetsat.int/s3/eup-strapi-media/S6_A_F08_Reprocessing_Calval_Assessment_v2_1_c6273b0e23.pdf

[5] Emeline Cadier, Bastien Courcol, Pierre Prandi, Victor Quet, Thomas Moreau, Claire Maraldi, François Bignalet-Cazalet, Salvatore Dinardo, Cristina Martin-Puig, Craig Donlon : Assessment of Sentinel-6MF low resolution numerical retracker over ocean: continuity on reference orbit and improvements, Advances in Space Research, Volume 75, Issue 1, 1 January 2025, Pages 30-52

[6] Raynal et al, Lessons learned from Sentinel SARM missions in preparation of Jason-CS. Oral Presentation, Ocean Surface Topography Science Team Meeting 2019, Chicago

[7] Jason-3 product handbook available at https://www.aviso.altimetry.fr/fileadmin/documents/data/tools/hdbk_j3.pdf

[8] Brown G.S., “The average impulse response of a rough surface and its application”, IEEE Transactions on Antenna and Propagation, Vol. AP 25, N1, pp. 67-74, Jan. 1977.

[9] Thibaut, P. O.Z. Zanif´e, J.P. Dumont, J. Dorandeu, N. Picot, and P. Vincent, 2002. Data editing: The MQE criterion. Paper presented at the Jason-1 and TOPEX/Poseidon Science Working Team Meeting, NewOrleans (USA), 21-23 October.

[10] Dinardo S. poster, Sentinel 6 MF Poseidon 4 main results from the first year of mission from the S6PP LRM and UF SAR chain , OSTST 2022

[11] Changes in ECMWF model, web page: https://www.ecmwf.int/en/forecasts/documentation-and-support/changes-ecmwf-model

[12] Boy F., Callahan P., Desjonqueres J. D., Egido A., Smith W. H. F., Fornari M., Martin-Puig C. (2022): High-Level Instrument Processing Summary for Jason 3 and Sentinel-6 Michael Freilich Tandem Phase. Oral Presentation, Ocean Surface Topography Science Team Meeting(Virtual). Available on-line at https://ostst.aviso.altimetry.fr/fileadmin/user_upload/OSTST2022/presentations/01-Jason3andSentinel-6MFTandemPhaseInstrumentProcessing_20220321.pdf

[13] Guérou, A., Meyssignac, B., Prandi, P., Ablain, M., Ribes, A., and Bignalet-Cazalet, F.: Current observed global mean sea level rise and acceleration estimated from satellite altimetry and the associated uncertainty, EGUsphere [preprint], https://doi.org/10.5194/egusphere-2022-330, 2022.

[14] Nencioli Francesco, Roinard Hélène, Bignalet-Cazalet Francois. 2021. Filtering ionospheric correction from altimetry dual-frequencies solutions. DOI 10.24400/527896/a02- 2021.001. Availableathttps://www.aviso.altimetry.fr/fileadmin/documents/data/tools/NT-Nencioli_FilteredIonosphericCorrection.pdf

[15] Obligis, E., L. Eymard, M. Ablain, B. Picard, J.F. Legeais, Y. Faugere and N. Picot, 2010. The wet tropospheric correction for altimetry missions: A mean sea level issue. Oral presentation at OSTST meeting, Lisbon, Portugal. Available at http://www.aviso.oceanobs.com/fileadmin/documents/OSTST/2010/oral/19_Tuesday/OBLIGIS.pdf.

[16] Sentinel-6 ALT Level 2 Product Generation Specification available at https://www.eumetsat.int/media/48266

[17] Michaël Ablain, Benoît Meyssignac, Lionel Zawadzki, Rémi Jugier, Aurélien Ribes, Giorgio Spada, Jerôme Benveniste, Anny Cazenave, and Nicolas Picot : Uncertainty in satellite estimates of global mean sea-level changes, trend and acceleration ESSD, 11, 1189–1202, 2019

[18] Collard, F., 2005. "Algorithmes de vent et période moyenne des vagues jason à base de réseaux de neurones." Boost Technologies, BO-021-CLS-0407-RF, 33 pp.